POLYCYCLIC AROMATIC HYDROCARBONS: PARTITIONING TO LAKE MICHIGAN SEDIMENT

By

Leif Krag Rowles

A Thesis

Submitted to
Michigan State University
in partial fulfillment of the requirements
for the degree of

MASTER OF SCIENCE

Department of Civil and Environmental Engineering

1994

ABSTRACT

POLYCYCLIC AROMATIC HYDROCARBONS: PARTITIONING TO LAKE MICHIGAN SEDIMENT

By

Leif Krag Rowles

Experimental batch absorption studies were completed to evaluate the apparent solid phase organic carbon partitioning coefficient of four PAH compounds to Lake Michigan Sediment. The experiments were conducted over a range of solid concentrations to study the concept of a solid effect. Additionally, partitioning coefficients for phenanthrene and benzo-a-pyrene were determined for the aqueous phase distribution in terms of "free" and "bound" by using the reverse phase and the fluorescence quenching techniques which have been developed by other researchers.

Data obtained for benzo-a-pyrene using both a constant and varying solid technique suggested that heterogeneous sorption was occurring. This data was calibrated to the Solute Complexation Model developed by Voice, 1985. A non-linear parameter estimation technique was attempted to estimate both the aqueous "free" and "bound" solid phase sorption coefficients which are conceptualized in the model.

TABLE OF CONTENTS

TABLE OF CONTENTS (continued)

TABLE OF CONTENTS (continued)

LIST OF TABLES

Appendices

LIST OF FIGURES

List of Figures (continued)

Appendices

List of Symbols:

$1/n$	=	Freundlich Sorption Intensity
C_s	=	Concentration in solid
C_{sb}	=	"bound" concentration in the solid
C_{sf}	=	"free" concentration in the solid
C_w	=	Concentration in water
C_{wb}	=	"bound" concentration in the water
C_{wf}	=	"free" concentration in the water
DOC	=	Dissolved organic carbon
F	=	Fluorescence in presence of quencher
F_o	=	Fluorescence in absence of quencher
f_{oc}	=	fraction of organic carbon
HOC	=	Hydrophobic Organic Contaminant
K	=	Freundlich Sorption Capacity
K_1	=	"free" compound partitioning coefficient
K_2	=	"bound" compound partitioning coefficient
K_{doc}	=	Partitioning coefficient to dissolved organic carbon
K_{oc}	=	Organic carbon partitioning coefficient
K_{ow}	=	octanol water partition coefficient

List of Symbols (continued)

K_p	=	Apparent partitioning coefficient
o	=	Quantum yield of PAH-DOM complex
PAH	=	Polycyclic Aromatic Hydrocarbon
TOC	=	Total organic carbon
$[PAH]_{bound}$	=	DOM Bound PAH in solution
$[PAH]_{free}$	=	Free PAH in solution
$[PAH]_{total}$	=	Total PAH in solution

Introduction

This thesis develops methods for evaluating the partitioning of phenanthrene, fluoranthene, pyrene, and benzo-a-pyrene between solid and aqueous phases. Measurements of the partitioning of polycyclic aromatic hydrocarbons to sediments are made using batch sorption experiments. Additionally, phenanthrene and benzo-a-pyrene partitioning to dissolved organic carbon is measured using fluorescence quenching and reverse phase techniques. The results are evaluated under equilibrium partitioning assumptions and partitioning coefficients are calculated in terms of the solid phase organic carbon and the aqueous phase dissolved organic carbon. Finally, the solute complexation model (Voice 1983) is used to evaluate the data obtained for benzo-a-pyrene partitioning to Lake Michigan Sediments.

The objectives are as follows:

1. To measure the partitioning of phenanthrene, fluoranthene, pyrene, and benzo-a-pyrene to Lake Michigan Sediments in laboratory batch sorption studies.

2. To measure the partitioning of phenanthrene and benzo-a-pyrene to dissolved organic carbon from Lake Michigan Sediments using fluorescence quenching and reverse phase techniques.

3. To evaluate a correction technique which has been used for the "particle concentration effect" and to apply the Solute Complexation Model (Voice 1983) to benzo-a-pyrene sorption data.

Polycyclic Aromatic Hydrocarbons (PAH's) were the chosen compounds to evaluate partitioning to Lake Michigan sediments from offshore Muskegon. PAH's are one class of hydrophobic organic contaminants (HOC's) which are of environmental concern. They are formed from the incomplete oxidation of fossil fuels, and are present as byproducts of the petrochemical industry. Wood treating, oil recycling, and incineration facilities have been the source of PAH contamination for many sites across the US. (Booth and Jacobson 1992). Many of the PAH's are known or suspected carcinogens and mutagens and have been shown to bioaccumulate when exposure occurs in environmental systems (Giesy 1986).

Because PAH's are nonpolar and characterized as hydrophobic organic compounds (HOC's, operationally, Log $K_{ow} > 10^3$, Voice 1983), they are present in water systems in trace quantities. Sorption dominates PAH fate in sediments and soils. (Karickhoff 1981) developed the following expression to predict K_{oc} values for PAH's:

$$K_{oc} = 4.9 \times 10^{-7} * K_{ow}^{1.00}$$

Selected solubility data and octanol water partitioning coefficients for a range of PAH compounds are included in Figure 1.

Figure 1.1
Polycylic Aromatic Hydrocarbon Properties

		Molecular Weight (1)	Solubility (mg/l) (2)	Log Kow (2)
Napthalene	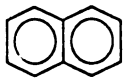	128.19	30	3.37
Fluorene	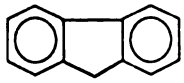	166.23	1.9 @ 25 C	4.18
Phenanthrene	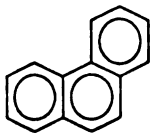	178.24	0.816 @ 21 C	4.46
Anthracene	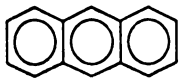	178.24	1.29 @ 25 C	4.45
Pyrene	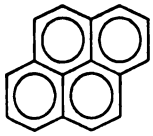	202.26	0.16 @ 26 C	4.88
Fluoranthene	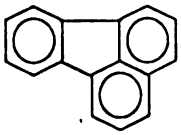	202.26	0.265 @ 25 C	5.22
Chrysene	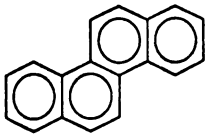	228.3	0.006 @ 25 C	5.91
3-4 benzopyrene	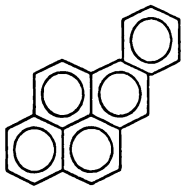	252.32	0.003	6.50

(1) Handbook of Environmental Data on Organic Chemicals
(2) McKay, 1980

Chapter I: Theory and Background

1.1 Introduction

The fate of chemicals once they are released into the environment is very complex. Many mechanisms exist which describe how a chemical will interact with environment. For hydrophobic organic chemicals (HOC's) which have a distaste for water (or more appropriately, for which water has a distaste) sorption to sediment and soils is a primary fate process.

The following chapter is a review of hydrophobic sorption and literature partitioning data from contaminants which undergo hydrophobic sorption. The chapter describes the relationship between observed partitioning and solid concentration and presents the dissolved/particle-bound/dissolved organic carbon bound system for hydrophobic contaminants. Additionally, this chapter presents the solute complexation model as a possible description of the distribution of hydrophobic compounds among the dissolved/particle-bound/dissolved organic carbon bound system.

1.2 Hydrophobic Sorption and Evaluation of Partitioning Data

Hydrophobic sorption is a mechanism which is driven by the incompatibility of nonpolar compounds and water (Stumm, 1988). It has been described by some researchers as an entropically driven dissolution reaction (Voice, 1983). Sorption of a hydrophobic

contaminant is favorable because of the increase in entropy which occurs when the tetrahedral ordering of water molecules around molecules of the contaminant in solution is broken (Voice, 1983). The bonding force of hydrophobic chemicals is due to amplified van Der Waals interactions as well as the thermodynamic gradient driving the molecules out of solution and on to the sorptive surface (Voice, 1982). Other researchers reason that the mechanism of hydrophobic sorption is really a partitioning process similar to dissolution. In environmental systems, soil organic matter acts as a solvent which is more compatible with the hydrophobic compound than water (Chiou, et. al., 1977, 1983).

Partitioning, as it is used in our study, is the distribution of a hydrophobic contaminant among solid and liquid phases. Partitioning relates to solute as well as sorbent properties, and for HOC's, the degree of sorption is related to the compound hydrophobicity in terms of the octanol/water partitioning coefficient (K_{ow}) and the fraction of organic carbon (f_{oc}) on the sorbent. Total organic carbon content appears to be the major factor in determining a solid's sorptive potential, while the octanol-water partition coefficient is the best known indicator of the extent to which a compound will sorb (Briggs, 1973; Voice, 1983).

Many correlations have been developed to describe HOC partitioning in relation to K_{ow} and f_{oc} (Means 1980, Swarzenbach and Westall 1983, Karickoff 1981). Swarzenbach 1983, correlated

polycyclic aromatic hydrocarbon (PAH) sorption to several different sorbents using the following expression:

$$\text{Log } K_p = a*\text{Log } K_{ow} + \text{Log } f_{oc} + b$$

Where the coefficients a and b vary for different solute/sorbent systems, f_{oc} denotes sorbent organic carbon fraction, and K_{ow} is the octanol/water partitioning coefficient.

A sorption isotherm is a way of describing graphically, the distribution of a compound between the aqueous and absorbed phases. A typical experiment would involve spiking varying amounts of a compound into equivalent volumes of water and sorbent. Alternately, the amount of sorbent could be varied and the amount of compound kept constant. After equilibrium is reached, the amount of compound sorbed and the amount of compound in solution is measured. The data is then plotted as amount sorbed vs. amount in solution. Models are used to describe this relationship by fitting the data to mathematical equations. Early studies noted that the absorption isotherm, was linear at solute concentrations less than 50 % of the aqueous solubility. Karickoff (1983), identified that at pollutant concentrations common to aquatic systems, (low ppm or less), the assumption of linearity would be expected. He reasoned that constant aqueous phase activity coefficients would be expected unless pollutant levels approached solubility limits.

The simplest isotherm model which describes absorption data is that of linear adsorption or constant partitioning:

$$C_s = K_p * C_w$$

In the linear absorption isotherm, C_s defines the concentration in the soil or sediment, C_w defines the concentration in the water, and K_p defines the distribution between the water and sediment. Although linear partitioning may be convenient due to its mathematical simplicity, caution is recommended, since it may not be applicable over large ranges of solute and sorbent concentrations.

The Freundlich isotherm is an alternate way to describe sorption data:

$$C_s = K * C_w^{1/n}$$

It is often used for heterogeneous systems such as soils and sediments to describe partitioning data which exhibit an exponential mathematical form (Voice, 1983). The exponential form of the Freundlich equation allows it to be linearized on a logarithmic scale, and therefore it is useful to describe partitioning data from large ranges of solute and sorbent concentrations. K can generally be thought of as sorption capacity, while 1/n is a measure of sorption intensity (Voice and Weber, 1985).

In the Freundlich equation, linear partitioning occurs when n=1 and it is often observed for sorption studies involving soils and sediments at low solution concentrations (Karickoff, 1979). Using the logarithmic form of the Freundlich equation,

$$\text{Log } C_s = \text{Log } K + 1/n * \text{Log } C_w$$

the Freundlich sorption capacity parameter, K, can be determined by extrapolating the plot of log C_s vs. log C_w to C_w=1 (Log C_w = 0). The sorption intensity parameter, 1/n, can also be determined by the slope of the plot.

In order to compare partitioning among different soils and sediments, the observed partition coefficient, K_p, can be normalized to the fraction of organic carbon, f_{oc}:

$$K_{oc} = K_p / f_{oc}$$

Lambert (1968) demonstrated that this term normalized the linear partition coefficient for a wide range of soils with different organic carbon contents.

1.3 The Relationship Between Observed Partitioning and Solids Concentration

One of the difficulties in the evaluation and prediction of hydrophobic sorption arises as a consequence of the "particle

concentration effect". The relationship of solids concentration to observed partitioning in laboratory studies has been well established (Voice 1983, O'Connor and Connolly 1980). It is noted that apparent partitioning coefficients for HOC's which have been normalized to the fraction of organic carbon, f_{oc}, decrease with increased solids concentration. The effect is present in data from partitioning experiments which use a varying solids to solution ratio. Partition coefficients have been observed to increase as much as an order of magnitude for every order of magnitude decrease in solids concentration. Voice, 1983, noted that this observation is in conflict with the predictions of many partitioning models and appears to contradict fundamental thermodynamic principles.

Although linearized partitioning may be applicable over relatively small ranges of sorbent concentrations in partitioning studies, many researchers have noted that the observed K_{oc} values decrease at high solid concentration for many solute/sorbent systems (O'Connor and Connoly 1980, Voice 1983). This observation is often noted even in apparently linear sorption isotherms. Reasons for this apparent anomaly have been developed by many researchers:

1. Equilibrium has not been achieved, (Karichoff, 1984)
2. Binding to dissolved organic matter has not been corrected for in the calculation of K_p (Gschwend and Wu,1985, Hoke and Giesy, 1992 prepublication)

3. The system is not a true two-phase system, rather it includes additional compartments that are not measured independently in the isotherm procedure (Voice, 1985).
4. Competitive sorption between pollutant and an implicit adsorbate initially on the sorbent (Curl and Keoleian, 1984).
5. Presence of both reversible and resistant components (Di Toro, 1986)

These developments are the subject of on-going research, and irrefutable descriptions of the relationship between observed partitioning and solids concentration are not available.

In actual environmental systems, little data is available to study the affect that increasing f_{oc} or the "particle concentration effect" has on observed partitioning. However, a field study conducted by Hoke and Giesy (1992 prepublication) on the Grand Calumet provided a range of sediment f_{oc}'s and partitioning data for HOC's. The DOC in Hoke's experiments was derived from centrifuging wet sediments sampled from the Grand Calumet and filtering the supernatant. The DOC was defined as pore water within the study.

Our reduction of Hoke's data shows that the value of the partitioning coefficient for all of the PAH compounds decreased over the range of sediment f_{oc} which was sampled (Figures 1.1 and 1.2). At the very least, these data suggest that measured Koc values may

Figure 1.1: Grand Calumet River Data: PAH's, Koc vs foc

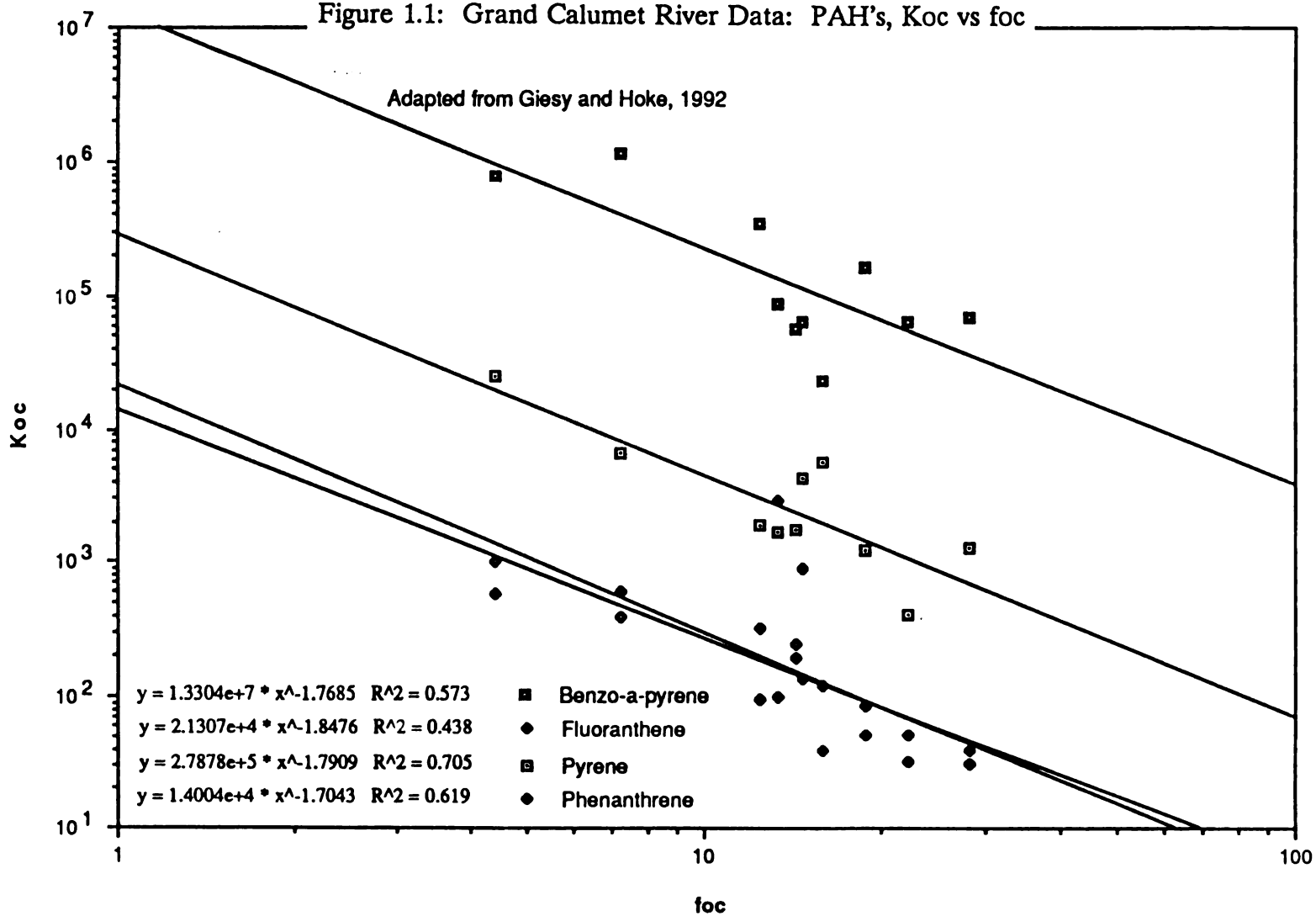

Figure 1.2: Grand Calumet River Data: PAH's, Koc vs foc

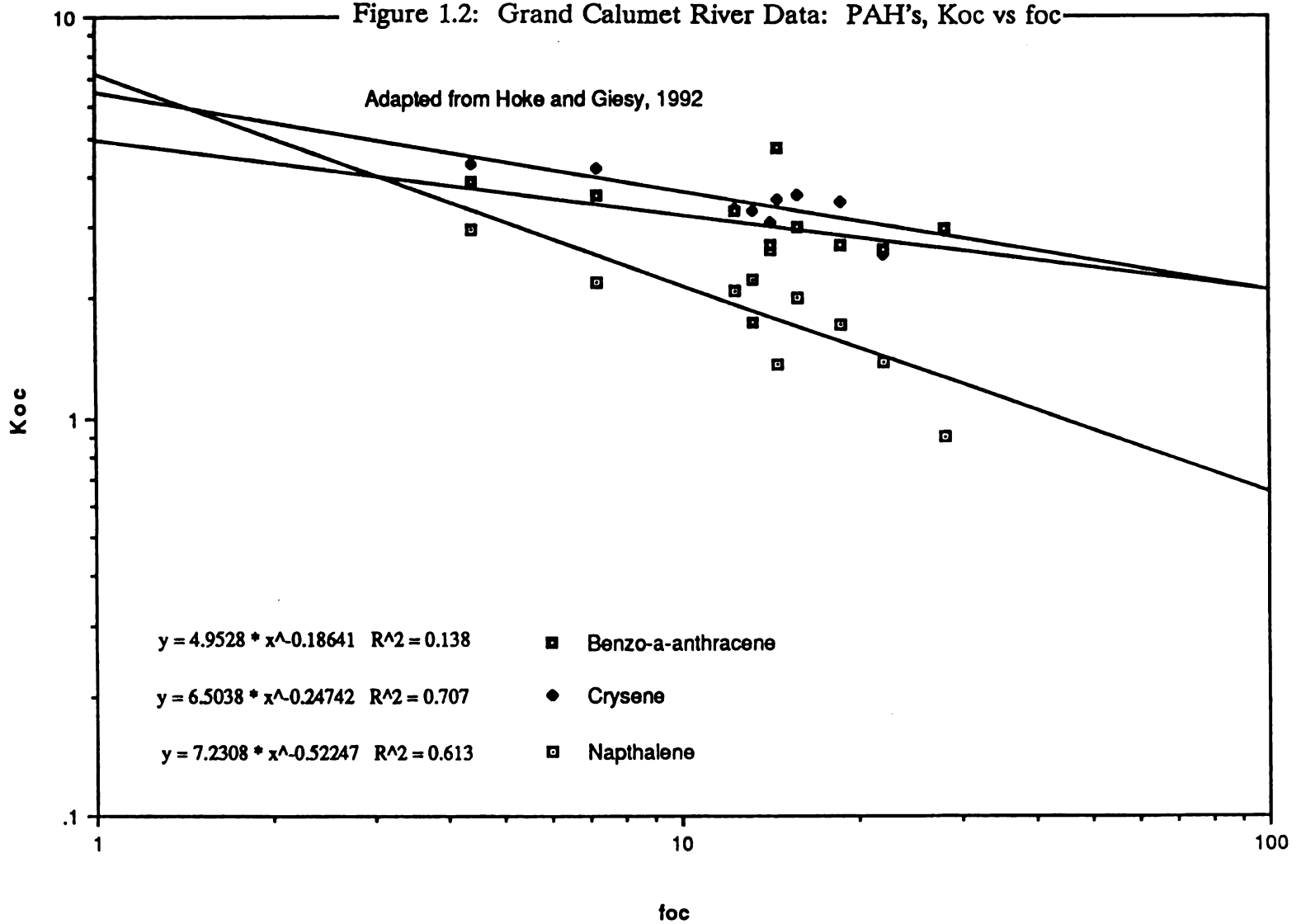

not be linearly correlated to sorbent oc%. Other factors are present including sorbent and solute heterogeneities--a conclusion which was hypothesized by Voice 1985.

Additionally, further reductions of the data from Hoke's study were completed to evaluate the DOC to f_{oc} ratio. It was hypothesized that the DOC may by a function of f_{oc}, since as the organic carbon within the sediment increased, the organic carbon in the dissolved state is expected to increase. As indicated in figure 1.3, DOC shows little relationship to increasing f_{oc}. This may be an indication that the dissolution of sediment organic material within the Grand Calumet has reached a limiting value even at low f_{oc}.

The data reduction from Hoke's study simply indicate the site specific nature of field K_{oc} evaluations regardless of using a coefficient normalized to organic carbon content. Complications include the fact that sediments in the Grand Calumet contain high levels of grease and oil, and composition is specific to sampling location. However, they demonstrate that in environmental systems, K_p adjusted for f_{oc} and corrected for aqueous phase DOM to eliminate the effect of binding to DOM, does not describe fully the partitioning relationship to oc% and DOM. And, although details regarding the exact nature of these relationships are not available as yet, they demonstrate the need for further lab studies.

Figure 1.3: Grand Calumet DOC vs foc

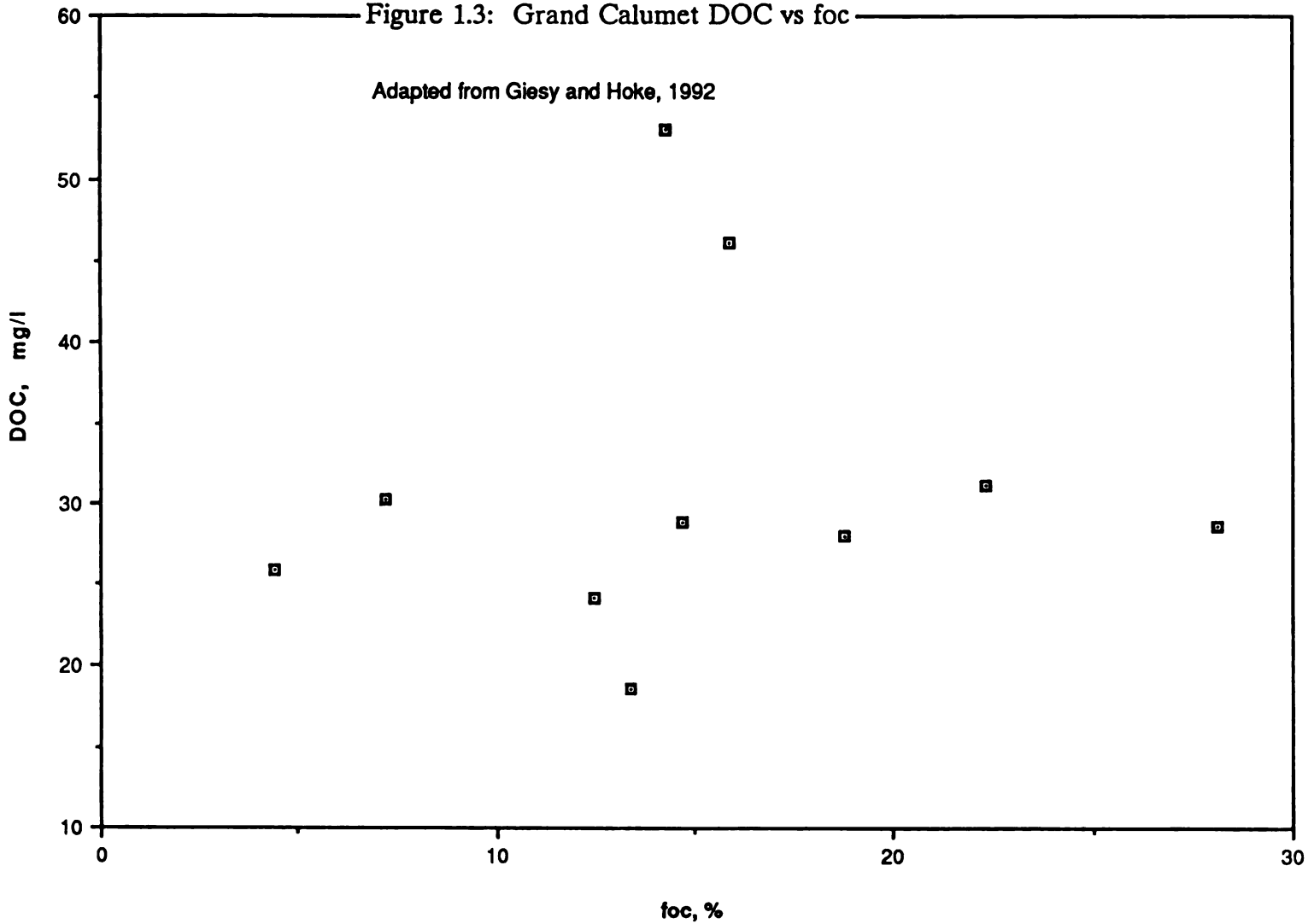

1.4 Three Phase Modeling

Much of the current research which addresses the distribution of HOC's within environmental systems relies on the concept of a three phase system. Pertinent environmental systems which correspond to a three phase model include partitioning of HOC's from contaminated sediments into the water column (Voice, 1983; Eadie, 1990) and partitioning between sediments and pore water (Hoke and Giesy, 1992). Additionally, the movement of HOC's within contaminated aquifers is described by retardation factors which relate to solid phase sorption and desorption. Organic colloidal material has been shown to facilitate transport by binding with hydrophobic contaminants in experimental soil columns and field studies (McCarthy, 1989; McGee, 1991).

The following conceptual schematic shows compartments which may be considered in environmental systems. Actual interactions between each compartment are conceptualized differently by different researchers. It is generally felt that the free fraction of environmental contaminants are significant in that they are bioavailable and can enter the food chain (McCarthy, 1985; Giesy, 1983).

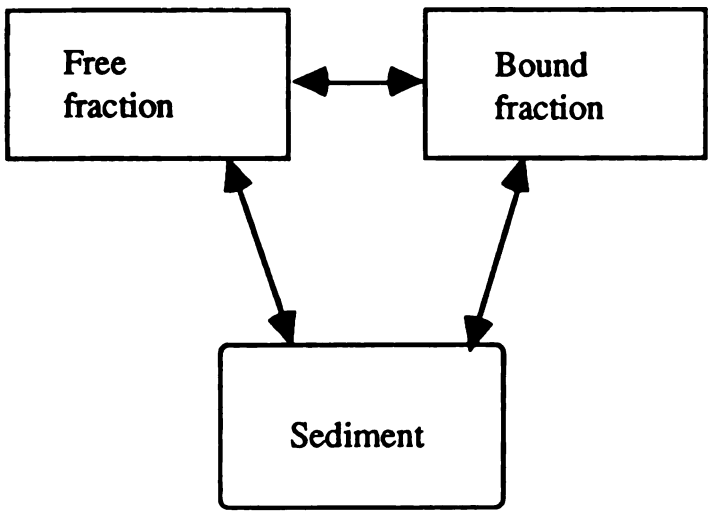

1.5 Equilibrium Partitioning

By conceptualizing environmental systems as boxes where the distribution of HOC's is defined by partitioning coefficients, exposure and fate analysis can be simplified. Equilibrium partitioning is a concept which has been proposed to estimate biouptake from various compartments in environmental systems (DiToro, 1991) Its success depends on the following assumptions:

1. Equilibrium is achieved
2. Kinetics are rapid in all phases
3. Only "Free" compound is bioavailable

The first and second assumptions are related in that rapid kinetics will permit equilibrium to be reached quickly. However, as

noted by some researchers (DiToro, 1986; Karickoff, 1983), sorption kinetics can be slow and true equilibrium is not rapidly attained. The third assumption has been tested by many researchers. McCarthy 1985, found that biouptake of PAH's in bluegills was reduced when the PAH's were bound to dissolved humic material. Giesy 1983, found that in some cases the bioavailability was reduced for PAH's bound to humics. Although the assumption of equilibrium partitioning is reasonably achieved under controlled experimental conditions, it is not feasible to suggest that the assumptions are met in environmental systems at all times. None-the-less, partitioning models provide a basis for extrapolating measured data to real systems.

1.6 Solute Complexation Model

A model was developed by Voice, 1985, to describe three phase partitioning. The model conceptualizes a phase transfer of HOC binding material from organic solids and a distribution of the aqueous phase between "free" and "bound" constituents. A schematic of the model system is shown in figure 1.4. Concentrations of HOC's within each compartment can be predicted by using equilibrium partitioning.

The aqueous HOC species within Voice's model are defined by a partition coefficient between the dissolved organic carbon (DOC) and water. Each constituent in the liquid phase is in turn distributed to the solid phase by distinct partition coefficients, K_1 and K_2. The

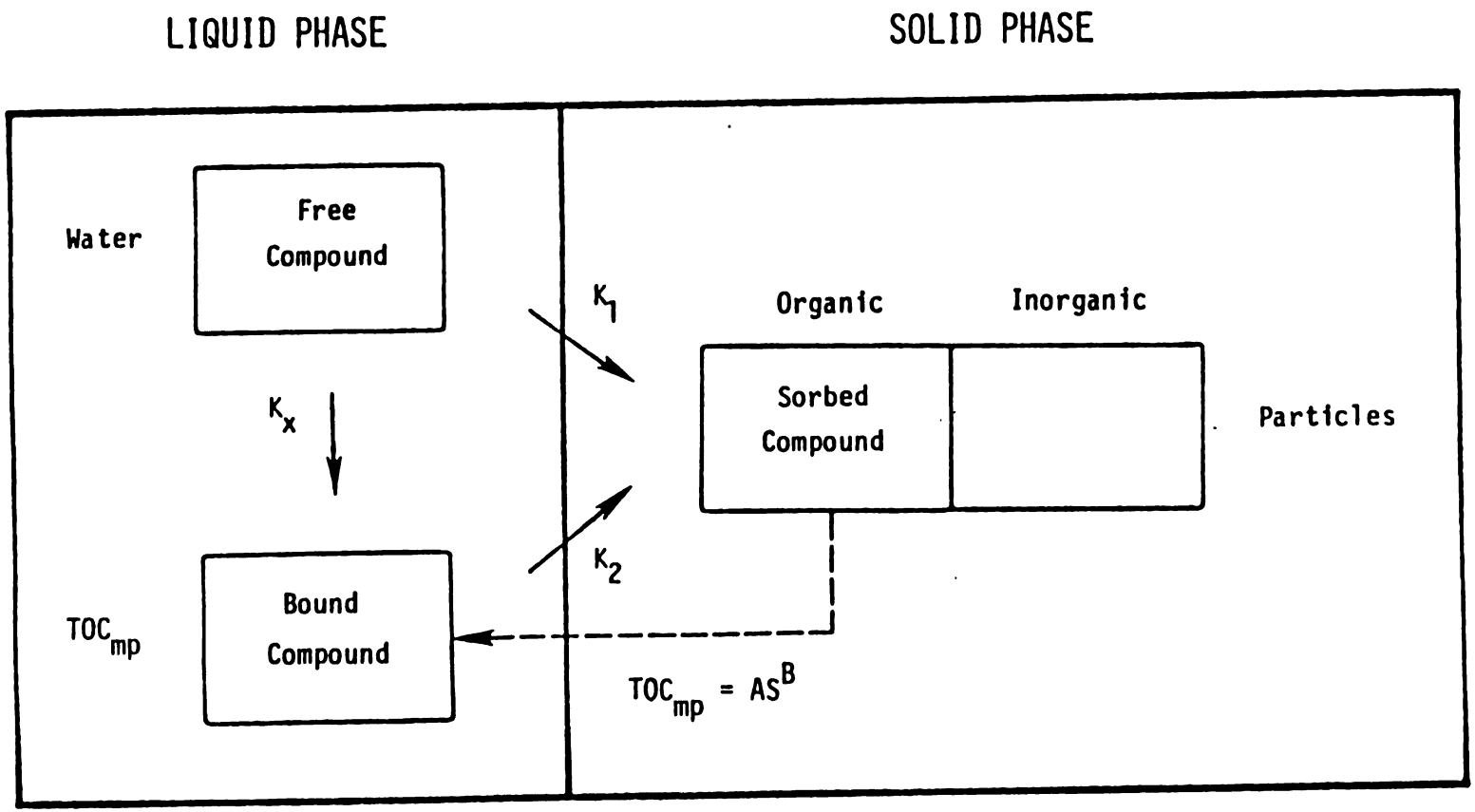

Figure 1.4: Schematic of Solute Complexation Model

overall partition coefficient or apparent K_p determined experimentally is then defined as:

$$K_p = (C_{sf} + C_{sb})/(C_{wf} + C_{wb})$$

Where, C_{sf} = mass fraction of free compound in solid

C_{sb} = mass fraction of bound compound in solid

C_{wf} = mass fraction of free compound in solution

C_{wb} = mass fraction of bound compound in solution

Although Voice did not propose a distinction between C_{sf} and C_{sb}, we have developed it in this way since K_1 and K_2 are equilibrium coefficients. Voice proposed that the observed decrease in the partitioning coefficient with changes in solids concentration be attributed to transfer of a sorbing, or solute binding material from the solid to the liquid phases. The amount of the binding material released to solution would increase with increasing solids, resulting in values of Koc which decrease as a logarithmic function of solids concentration. In order to evaluate the amount of a contaminant at equilibrium within each phase, the solid phase partitioning coefficient as well as the free/bound distribution within the aqueous phase must be measured.

The solute complexation approach also incorporates solute heterogeneity in its development by allowing for different equilibrium sorption coefficients for the "bound" and "free" phase in solution. Figure 1.5, adapted from Voice, shows a hypothetical chart

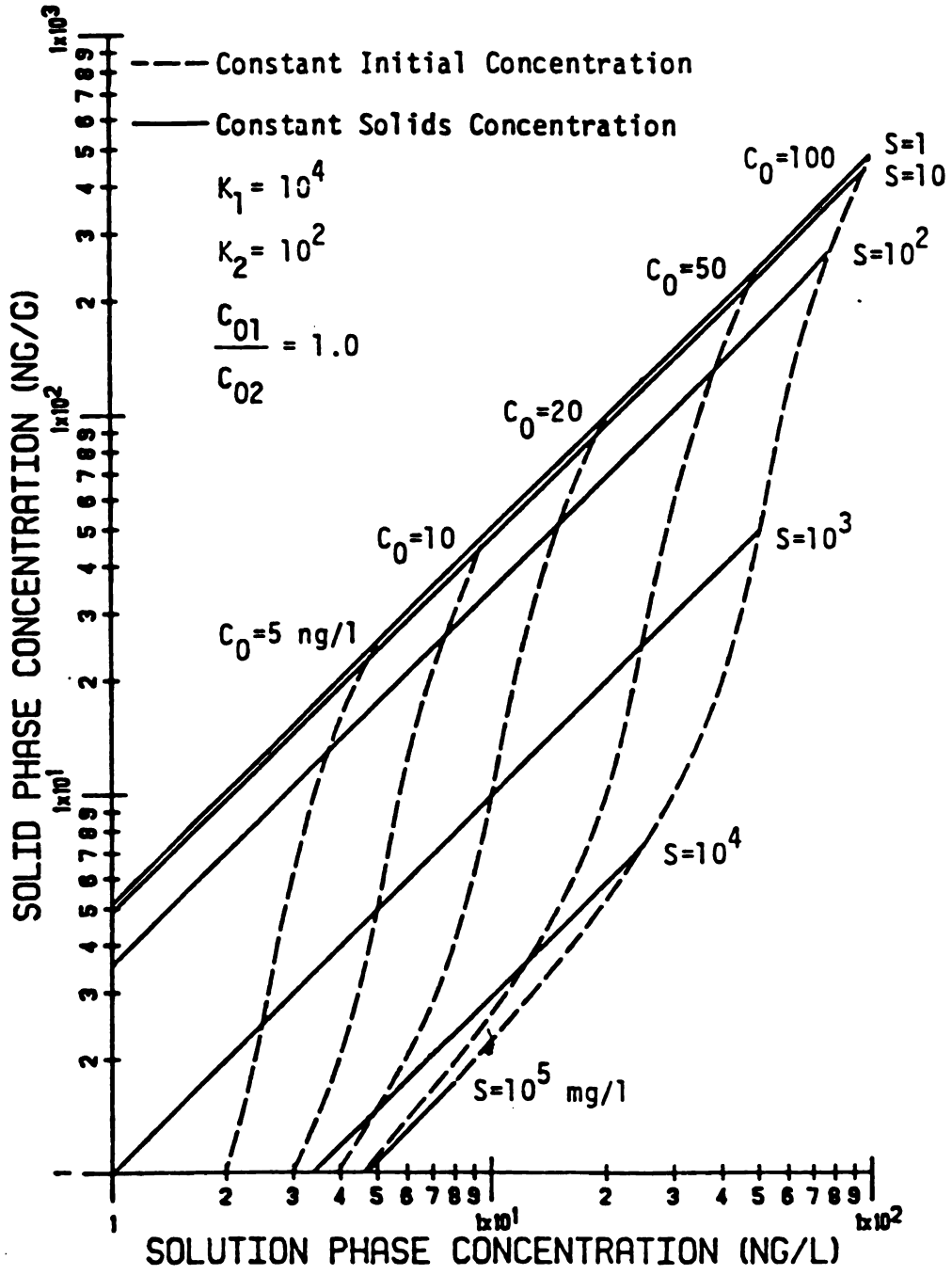

Figure 1.5: Effect of Isotherm Procedure for Heterogeneous Solute

indicating the effect of the isotherm procedure on observed partitioning for a heterogeneous solute. The curves represent a system with two compounds having partition coefficients of 10^4 and 10^2. Each initially comprises 50 % of the mixture. The curves are developed assuming both the constant and varying solids experimental techniques. As can be seen, the varying procedures result in different isotherms. The constant sediment isotherm is linear while the constant concentration isotherm is non-linear even on the log-log plot. Voice (1983), experimented with humic and fulvic acid sorption to activated carbon and showed data trends similar to the hypothesized heterogeneous solute curves. He interpreted the results as examples of heterogeneous solute sorption.

Several researchers have experimented with systems consisting of an inorganic surfaces coated with humic and fulvic acids to simulate natural organic coated aquifer material (Murphy, 1990; Slautman, 1992). Slautman found that the PAH binding properties of humic and fulvic acids were reduced when the organic material itself was bound to a synthetic solid. K_{oc} values for anthracene which were obtained by Murphy, decreased with increasing foc for both peat humic acid and Suwannee humic acid. The sorption enhancement due to coated humics was not linear and the anthracene sorption was most dramatically increased for low f_{oc}'s. Murphy attributed his results to heterogeneities in the sorbent phase due to alternate configurations of the humics or size exclusion in sites available for HOC's with increasing f_{oc}. The possibility of phase transfer or solute heterogeneities, however, was not considered.

The models developed by Voice and the abundance of data showing a decrease in K_{oc} with increasing sorbent in terms of both foc and solids concentration, suggest that solute complexation is a plausible explanation of observed and natural conditions. This is not to say that sorbent heterogeneities do not play a role in sorption phenomena, however, the decreases in K_{oc} with increasing foc or solids concentration observed in our study and seen in several published experiments is not described adequately by sorbent conditions alone.

Chapter II: PAH sorption Experiments

2.1 Introduction

The objective of the following chapter is to measure PAH sorption to Lake Michigan Sediments in laboratory batch partitioning experiments. The degree of sorption is described as a partitioning coefficient K_p defined as follows:

$$K_p = C_s/C_w$$

Where C_s is the concentration of the PAH in the sediment and C_w is the concentration of the PAH in water. Lambert (1966, 1967, 1968) and Karickoff (1983) found that the observed partition coefficient K_p remained essentially constant over a wide variety of soils and sediments when it was normalized to the percent organic carbon. The partition coefficient is normalized to the organic carbon content of the sediment by dividing Kp by % organic carbon. The organic carbon partition coefficient is then defined as:

$$Koc = C_s/(C_w * \%TOC)$$

Batch isotherm experiments have the advantage of being relatively simple to study PAH sorption over a range of compound concentrations and sediment concentrations. Within this thesis, PAH partitioning over a range of sediment concentrations from 500 to

40,000 mg/l and PAH concentrations at ng/l levels is measured in batch experiments.

The solid to water ratio has been shown to play an important role in the evaluation of partition coefficients. The absorption isotherm can be obtained by two experimental methods. The first involves keeping the solid to solution ratio constant and varying the initial amount of solute, while the second involves varying the solid to solution ratio and keeping the initial solute concentration constant. The effect of this change in experimental technique on Koc is evaluated in this Chapter for phenanthrene and benzo-a-pyrene.

Absorption data is modeled by plotting an isotherm. The isotherm is a graph of the solution equilibrium concentration vs. the solid phase equilibrium concentration. Many models are available for fitting absorption data, however, the Freundlich model can be used for large ranges of solid and solution concentrations and for this reason it is used to model the PAH sorption data found in our study. The Freundlich Equation is defined as follows:

$$C_s = K*C_w^{1/n}$$

Where, C_s is the equilibrium solid phase concentration

C_w is the equilibrium solution phase concentration

K and 1/n are fitting constants

The following objectives will be met in this chapter:

1. To develop an experimental procedure for PAH batch sorption studies.

2, To establish the relationship between solids concentration and the partitioning of phenanthrene, fluoranthrene, pyrene, and benzo-a-pyrene.

3. To determine whether correcting the apparent water concentration for the amount of PAH bound to aqueous organic matter as total organic carbon is adequate to eliminate the dependence that partitioning has on solids concentration.

4. To establish any differences in using a constant and varying sediment batch sorption technique for phenanthrene and benzo-a-pyrene.

2.2 Materials and Methods

2.2.1 Sediment Sampling

Sediment samples were obtained on May 30, 1991 from four locations offshore Lake Michigan at Muskegon harbor. NOAA (National Oceanic and Atmospheric Administration) provided transport and equipment for the sampling trip. A Ponar sampler was lowered at each location shown on attached figure 2.1 and a grab sample was collected. The top 1 inch layer of the sediment sample exhibiting dark, organic color was retained for laboratory experiments.

The sediment samples were processed by sifting wet through a 200 mesh screen. They were subsequently centrifuged at 5000 rpm for 1 hour to remove residual water and freeze dried at - 40 °C for 12 hours. The dry material was pulverized in a mortar and stored at room temperature for experimentation. An evaluation of the organic carbon content was completed by the Standard Methods, 1990, solids determination. Additional samples were tested for TOC by the Michigan State University Crop and Soil Science laboratory.

Because of the turbulence at the entrance of Muskegon Harbor, most of the silty organic material was scoured at the shallower sampling points. This was evident by the organic carbon percentages as well as visually within each sample. Testing of PAH binding was only conducted on the samples collected at 100 and 75 meter depths,

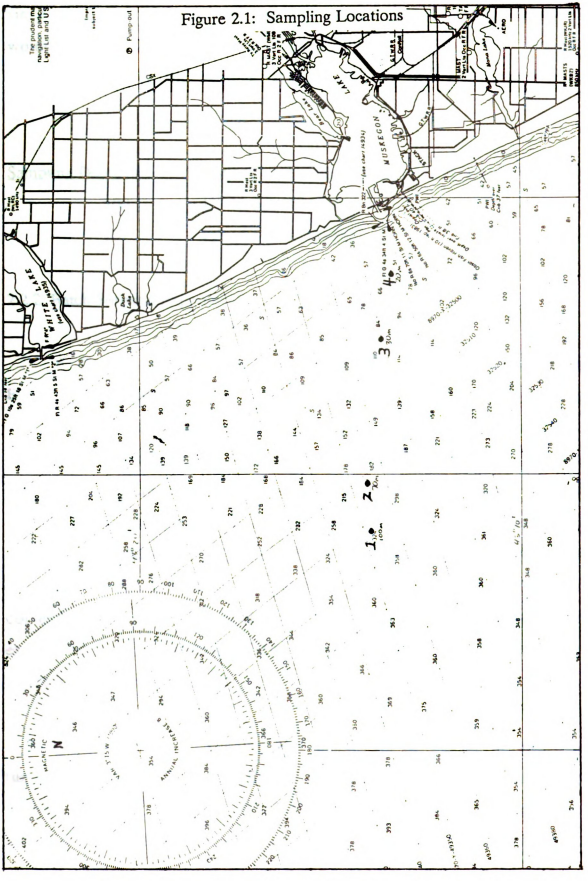

Figure 2.1: Sampling Locations

since they had the highest organic carbon fractions and therefore would exhibit the greatest binding effects for PAH's. The organic carbon content of the samples along with the station location is as follows:

Sampling Depth (m)	Station Location (lat., long.)	% organic C
100	43°-13.89', 86°-13.23'	5.6
70	43°-14.11', 86°-30.56'	4.8

2.2.2 Batch Sorption Experiments

A flow diagram of the procedure which was used is shown in Figure 2.2. Initially, Corex brand #4664, 25 ml centrifuge tubes were spiked with radiolabelled PAH standards prepared in acetonitrile. The radiolabelled PAH's obtained from Sigma chemical were purified by using reversed-phase high pressure liquid chromatography (HPLC). An example of the fraction chromatogram is shown in figure 2.3. The instrument specifications which were used for this procedure are included in Appendix II. Only the fraction corresponding to the peak at 9 minutes was retained for experimentation. Selected information regarding the ^{14}C labelled PAH's is included as Table 2.1.

After the carrier solvent was permitted to evaporate under a fume hood, about 25 g of purified water (deionized, carbon filtered, reverse osmosis) with 0.02% NaN3 as an antibacterial agent was added to each tube. Known quantities of the freeze-dried sediments

Figure 2.2: Procedure Flow Chart

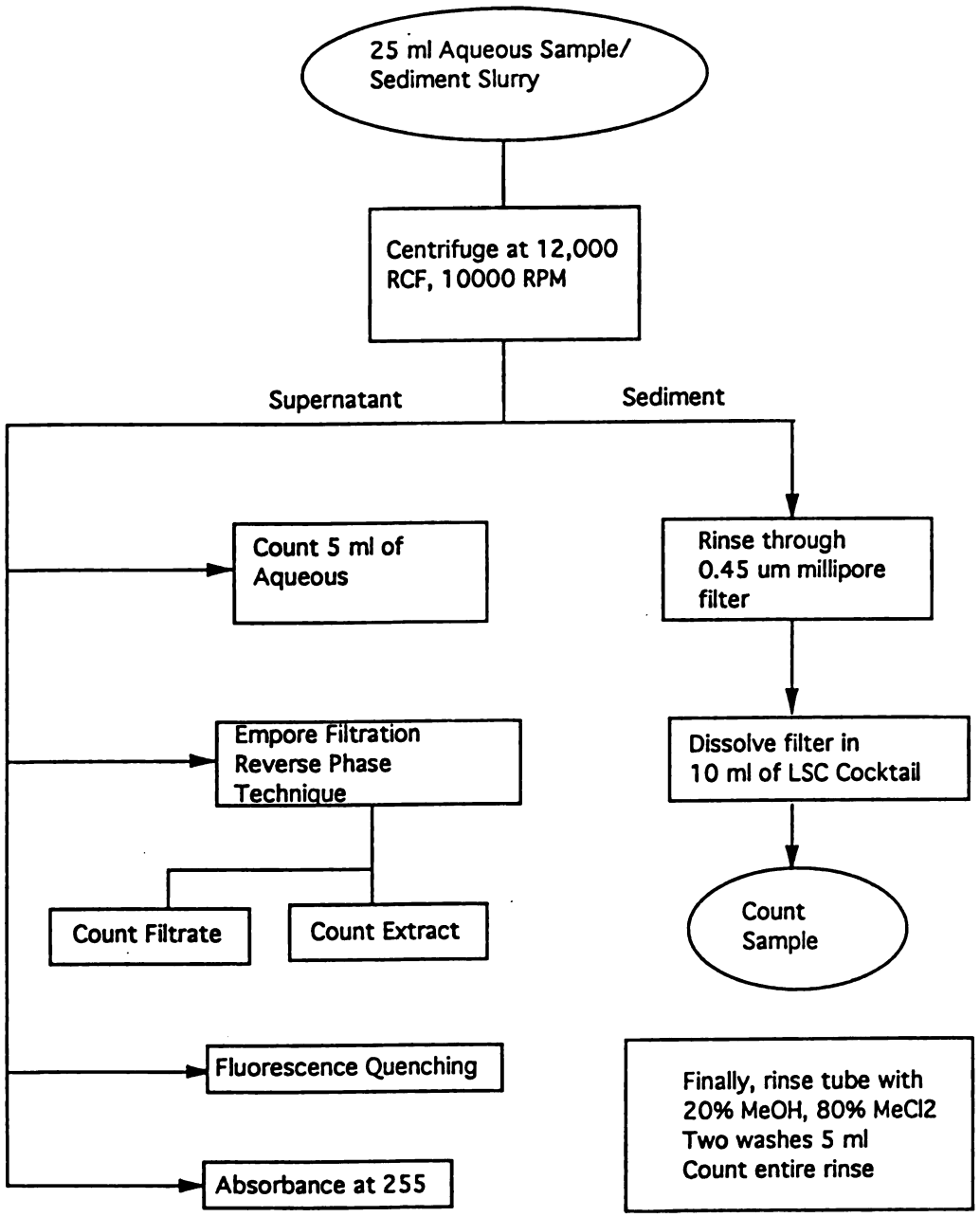

Figure 2.3: Radiolabelled Compound Purification

Integration time 15.00 min
Peak width 1.30 min
Peak sensitivity 2.0%
Minimum area 3000

----Area percent report----

RT	Area	Area%	Peak Name
7.764	3053	0.058	
9.908	5066905	96.935	
11.173	65093	1.245	
12.584	6367	0.122	
13.355	85716	1.640	

9 Peaks integrated

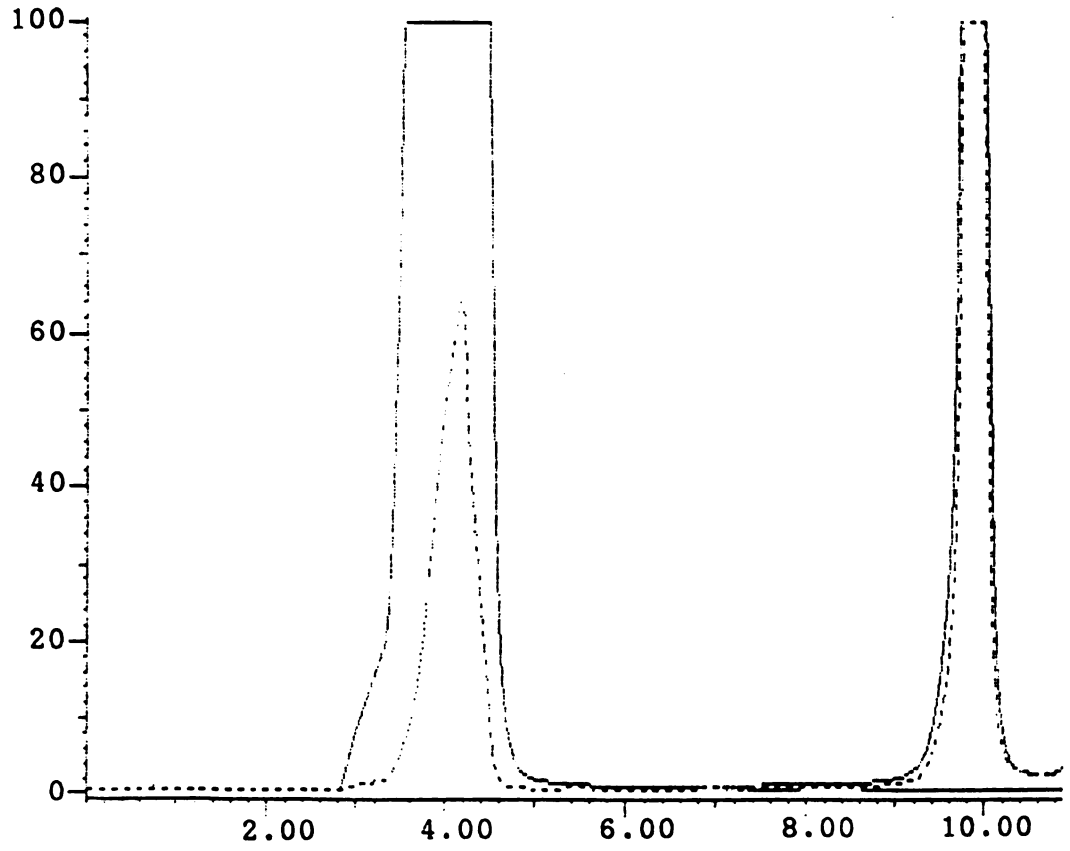

—Analysis Channel A, 50.1 mVFS
—Overlay Channel A, Min = -0.1 Max = 50.0
---Overlay Channel B, Min = 0.0 Max = 0.1

Table 2.1: Radiolabelled PAH Data

	Phen	Flrntn	Pyrene	BAP
Product #	31,528-1	F6147	P4185	B9776
Lot #	049F9271	061H0151	061H0152	080H9216
Molecular Weight	178.2	202.3	202.2	252.3
Purity*	>98%	98%	98%	>98%
Activity, mCi/mmol	13.1	55	55	16.2
Concentration, mCi/ml	---	1	0.56	1
Solvent	---	Benzene	Benzene	Toluene

* determined by radiochromatography

were added to each centrifuge tube. The tubes were then covered with opaque adapters and permitted to equilibrate for 24 hours on a wrist action shaker to allow dissolution and absorption equilibration of the PAH spike with the sediment.

A kinetic experiment was initially conducted using pyrene as a model compound. Pyrene was chosen because it has an intermediate hydrophobicity in the range of compounds which we studied. A series of batch systems spiked with pyrene were permitted to equilibrate over increments of one hour. After this time the same procedure was followed as previously described. The majority of the pyrene, approximately 90 %, was absorbed in 2 to 4 hours, reaching an apparent equilibrium over an extended period (Figure 2.4). Voice (1983) found in his experiments that an equilibration time of 4 to 6 hours was necessary. Karickoff (1980), hypothesized that sorption kinetics were described by a short and long term coefficient, the latter limited by diffusion into the soil matrix. For the purposes of this study, equilibrium was operationally defined at 24 hours.

Each tube provided a point for the absorption isotherms at varying sediment concentrations and constant initial spike for the varying solids isotherms. A range of sediment concentrations from about 500 mg/l to 40,000 mg/l was studied. For the constant solids isotherm procedure, equal amounts of sediments were used in each tube and the concentration of PAH was varied. After the 24-hour equilibration time, the tubes were centrifuged at 12,000 RCF, (10,000 RPM) for 2 hours to separate solid and liquid phases. Five grams of

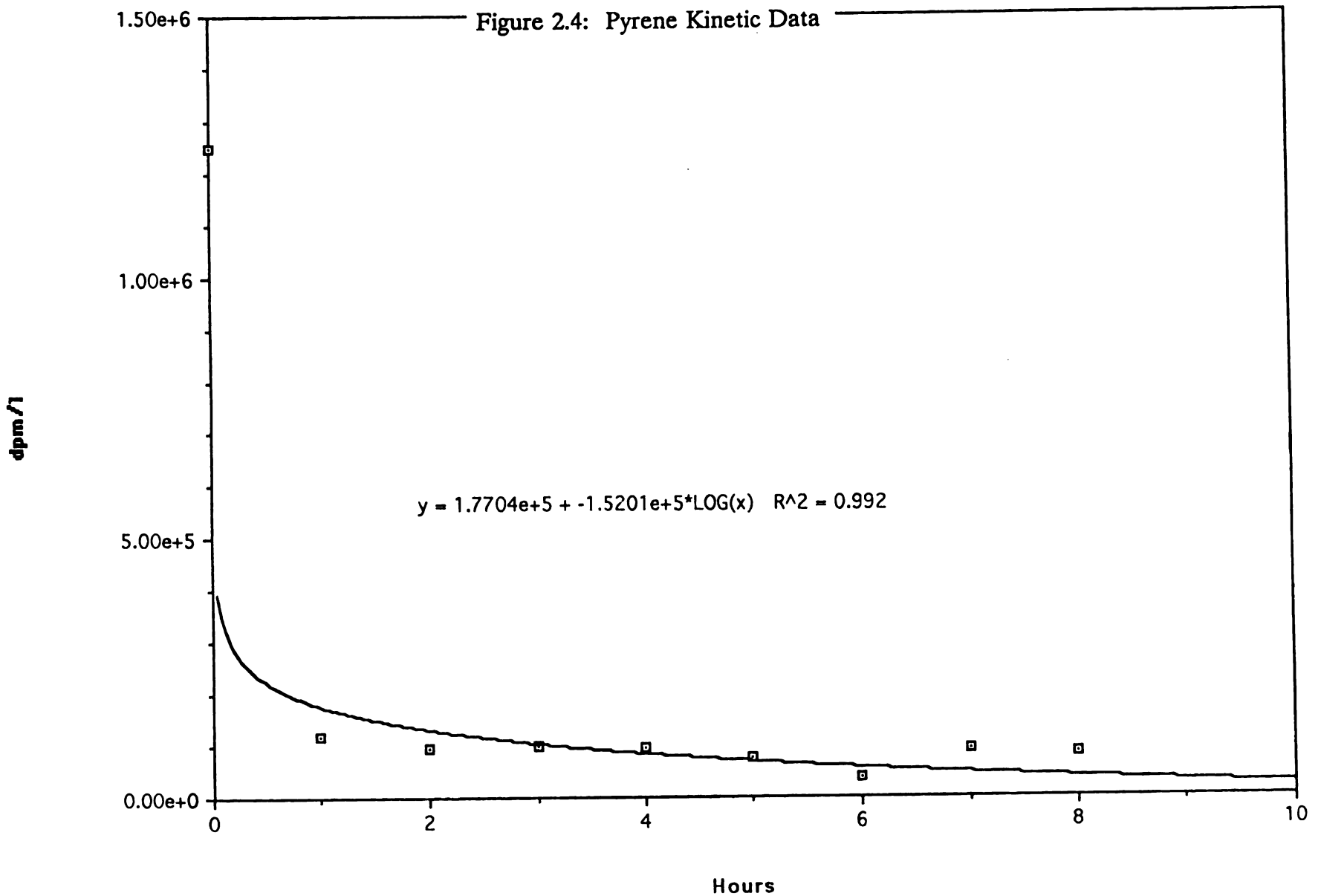

Figure 2.4: Pyrene Kinetic Data

the supernatant was drawn off the top of each tube and counted with 10 ml of LSC cocktail for 10 minutes. Three counts were taken for each sample and average values are reported. The instrument specifications which were used for this experiment are included in Appendix II.

The remainder of the supernatant in the phenanthrene and benzo-a-pyrene experiments was used for reverse phase separation and fluorescence quenching procedures. These techniques were described in detail in Chapter III. After separating the supernatant, the residual solids in each tube were flushed with DI water through Millipore 0.45 um filters. The filters with retained solids were then dissolved in 10 ml of LSC cocktail. The vials were shaken vigorously--2 to 3 minutes and allowed to set for 12 hours. Subsequently, each vial was analyzed on the Beckman LSC counter for 10 minutes to determine ^{14}C activity. The centrifuge tubes were then rinsed with 10 ml of $MeCL_2$ (in two 5 ml washes) to remove glass sorbed PAH. The entire rinse was combined with 5 ml of cocktail and counted for 10 minutes.

Tables 2.2 through 2.6 show the data which was generated using the batch isotherm procedure. The tables are spreadsheets of the calculation of solid concentration, PAH water concentration, and PAH concentration. Additionally, the PAH sediment concentration is adjusted based on the recovery efficiency. This calculation is possible in the procedure since the total initial activity of the spike is known and the glassware sorbed concentration, water concentration

Table 2.2: Phenanthrene Partitioning Data

Sample #	Sediment, g	Water, g	Sed, mg/l	Spike, dpm	Abs @ 255	g for lsc	Aqueous 5 ml, DPM	Aqueous 5 ml, DPM/l	ml MeCl2	Sediments DPM	Sonication of Sediments DPM/kg	Glassware Sorption	Material Balance % Recovery	Adjusted Sediment DPM/kg	Foc Adjusted Kp	Koc w/ Glassware Sorption Corr.
1	0.076	25.42	2989.77	1000000	0.12	5.05	3.84E+04	7.60E+03	6.03	758856	9.98E+09	1032	95.47	1.05E+10	2.63E+04	2.75E+04
2	0.0715	25.15	2842.94	1200000	0.113	5.09	4.70E+04	9.23E+03	6	889929	1.24E+10	1564	93.83	1.33E+10	2.70E+04	2.88E+04
3	0.0729	25.34	2876.87	1400000	0.134	5.14	5.46E+04	1.06E+04	6.43	1064309	1.46E+10	784	95.3	1.53E+10	2.75E+04	2.88E+04
4	0.075	25.4	2952.76	1600000	0.112	5.19	7.61E+04	1.47E+04	5.92	1120312	1.49E+10	1453	93.51	1.60E+10	2.04E+04	2.18E+04
5	0.0721	25.24	2856.58	1800000	0.146	5.22	8.00E+04	1.53E+04	6.01	1278387	1.77E+10	1462	92.72	1.91E+10	2.31E+04	2.50E+04
6	0.005	26.31	190.04	1000000	0.054	5.02	1.39E+05	2.77E+04	6.31	262518	5.25E+10	1440	99.43	5.28E+10	3.79E+04	3.82E+04
7	0.015	25.34	591.95	1000000	0.085	4.99	9.28E+04	1.86E+04	6.02	427984	2.85E+10	15238	93.74	3.04E+10	3.07E+04	3.27E+04
8	0.0359	25.59	1402.89	1000000	0.088	5.01	6.85E+04	1.37E+04	5.29	599246	1.67E+10	1990	95.45	1.75E+10	2.44E+04	2.56E+04
9	0.1452	25.6	5671.88	1000000	0.113	5.24	2.76E+04	5.26E+03	5.56	778947	5.36E+09	387	91.46	5.87E+09	2.04E+04	2.23E+04
10	0.4567	25.45	17944.99	1000000	0.217	5.21	8.32E+03	1.60E+03	6	827963	1.81E+09	101	86.88	2.09E+09	2.27E+04	2.61E+04
11	0.8221	25.08	32779.11	1000000	0.33	5.02	5.04E+03	1.00E+03	6.01	760744	9.25E+08	546	78.73	1.18E+09	1.84E+04	2.34E+04

Table 2.3: Fluoranthene Partitioning Data

Sample #	Sediment, g	Water, g	Sed, mg/l	Spike, dpm	Abs @ 255	g for lsc	Aqueous 5 ml, DPM	Aqueous 5 ml, DPM/l	ml MeCl2	Sediment DPM	Sonication of Sediments DPM/kg	Glassware Sorption	Material Balance % Recovery	Adjusted Sediment DPM/kg	Foc Adjected Kp	Koc w/ Glassware Sorption Corr.
1	0	25.28	0	4500	0.008	5.04	540	1.07E+05	4.96	79.2	#DIV/0!	239.52	#DIV/0!	#DIV/0!	#DIV/0!	#NUM!
2	0.0077	25.24	308	4500	0.016	5.1	211	4.14E+04	4.97	776.76	3.04E+08	92.34	75.30	4.04E+08	1.95E+05	1.88E+05
3	0.0164	25.26	656	4500	0.025	5.08	81	1.59E+04	4.98	1261.68	2.32E+08	35.62	93.40	2.48E+08	3.11E+05	3.08E+05
4	0.0307	25.25	1228	4500	0.043	5.05	76	1.50E+04	4.99	1250.26	1.22E+08	33.60	91.96	1.33E+08	1.77E+05	1.75E+05
5	0.0538	25.04	2152	4500	0.064	5.31	59	1.11E+04	5.02	1401.22	7.78E+07	24.60	99.23	7.84E+07	1.41E+05	1.40E+05
6	0.1139	25.16	4556	4500	0.129	5.01	40	7.98E+03	5.03	1354.16	3.55E+07	17.76	94.20	3.76E+07	9.43E+04	9.39E+04
7	0.1729	25.62	6916	4500	0.161	5.09	32	6.29E+03	5	1330.03	2.31E+07	14.24	92.25	2.50E+07	7.96E+04	7.93E+04
8	0.2769	25.31	11076	4500	0.21	5.03	29	5.77E+03	4.99	1269.11	1.38E+07	12.90	88.02	1.57E+07	5.43E+04	5.41E+04
9	0.4481	25.46	17924	4500	0.266	5.05	28	5.54E+03	5.02	1077.68	7.19E+06	12.48	74.70	9.62E+06	3.47E+04	3.46E+04
10	0.6506	25.23	26024	4500	0.339	5.02	27	5.38E+03	5	730.28	3.37E+06	12.00	51.70	6.51E+06	2.42E+04	2.41E+04
11	0.9964	25.3	39856	4500	0.428	5.02	25	4.98E+03	5.01	512.98	1.54E+06	11.14	36.93	4.17E+06	1.68E+04	1.66E+04
12	0.0057	25.14	228	4500	0.026	5.02	201	4.00E+04	4.99	1053.4	5.56E+08	89.01	92.74	5.99E+08	2.99E+05	2.91E+05

Table 2.4: Pyrene Partitioning Data

Sample #	Sediment, g	Water, g	Sed, mg/l	Spike, dpm	Abs @ 255	g for lsc	Aqueous 5 ml, DPM	Aqueous 5 ml, DPM/l	(20 ml total) ml MeCl2	Sediment DPM	Sonication of Sediments DPM/kg	Glassware Sorption	Material Balance % Recovery	Adjusted Sediment DPM/kg	Foc Adjusted Kp	Koc w/ Glassware Sorption Corr.
1	0.0138	25.04	551.12	24000	0.024	5.4	1054.11	195205.556	10	8962	1.30E+09	355.95	95.05	1.37E+09	1.40E+05	1.37E+05
2	0.031	25.61	1210.46	24000	0.035	5.5	557.6	101381.818	10	10433	6.73E+08	189.08	97.76	6.89E+08	1.36E+05	1.35E+05
3	0.041	25.66	1597.82	24000	0.04	5.54	411	74187.7256	10	8933	4.36E+08	138.63	82.37	5.29E+08	1.43E+05	1.42E+05
4	0.06	25.51	2352.02	24000	0.064	5.38	289	53717.4721	10	9032	3.01E+08	99.79	80.98	3.72E+08	1.38E+05	1.38E+05
5	0.0863	25.46	3389.63	24000		5.19	110	21194.605	10	7363	1.71E+08	39.30	63.61	2.68E+08	2.53E+05	2.52E+05
6	0.1574	26.11	6028.34	24000	0.113	5.22	107	20498.0843	10		0.00E+00	38.98		#NUM!	#NUM!	#DIV/0!
7	0.1946	25.16	7734.50	24000	0.135	5.02	71.91	14324.7012	10	4803	4.94E+07	26.25	41.53	1.19E+08	1.66E+05	1.66E+05
8	0.2756	25.43	10837.59	24000	0.173	5.31	61.1	11506.5913	10		0.00E+00	21.31		#NUM!	#NUM!	#DIV/0!
9	0.3351	25.42	13182.53	24000	0.201	5.31	54.14	10195.8569	10	4811	2.87E+07	18.87	41.17	6.97E+07	1.37E+05	1.37E+05
10	0.4764	25.33	18807.74	24000	0.254	5.05	44.14	8740.59406	10	6573	2.76E+07	16.12	55.70	4.95E+07	1.13E+05	1.13E+05
11	0.6933	25.39	27306.03	24000	0.324	5.17	37.66	7284.33269	10	3175	9.16E+06	13.47	27.23	3.36E+07	9.24E+04	9.22E+04
12	0	25.59	0.00	24000	0.001	5.13	4366	851072.125	10	793	#DIV/0!	1586.00	97.35	#DIV/0!	#DIV/0!	#NUM!

Table 2.5: Benzo-a-pyrene Partitioning Data

	Benzo-a-pyrene absorption data												Material	Adjusted		Koc w/
					Aqueous						Glassware	Glassware	Balance	Sediment	Foc Adjusted	Glassware
Sample #	Sediment, g	Water, g	Sed, mg/l	Spike, DPM	dpm, 5 ml	ml counted	Aqueous, dpm/l	ml MeCl2	Sediment DPM	DPM/kg Sed	sorption	sorption	% Recovery	DPM/kg	Kp	Sorption Corr
1	0.086	25.06	3431.76	3.72E+04	55.44	5	1.11E+04	5.19	11119	3.74E+08	1.27E+04	1.97E+01	87.03	4.29E+08	774462.956	468988.87
2	0.0077	25.22	305.31	3.72E+04	67.13	5.1	1.32E+04	5.3	11714	4.31E+09	1.53E+04	1.76E+00	89.90	4.79E+09	7277056.72	3908127.15
3	0.1909	25.19	7578.40	3.72E+04	64.56	5.07	1.27E+04	5.29	11774	1.75E+08	1.48E+04	4.36E+01	90.50	1.93E+08	303528.455	169331.257
4	0.409	25.65	15945.42	3.72E+04	41.68	5.09	8.19E+03	4.99	10862	7.98E+07	9.53E+03	9.35E+01	88.22	9.05E+07	221021.63	156515.334
5	0.0308	25.27	1218.84	3.72E+04	63.76	5.06	1.26E+04	5.03	12144	1.18E+09	1.46E+04	7.04E+00	98.08	1.20E+09	1902709.43	1136802.71
6	0.3044	25.41	11979.54	3.72E+04	35.73	5.03	7.10E+03	5.9	12642	1.06E+08	8.17E+03	6.96E+01	86.78	1.22E+08	342594.019	255518.135
7	0.6625	25	26500.00	3.72E+04	28.65	5	5.73E+03	5.4	11137	4.67E+07	6.55E+03	1.51E+02	83.45	5.60E+07	195314.982	153959.356
8	0.725	25.29	28667.46	3.72E+04	27.08	5.02	5.39E+03	5.2	8046	3.20E+07	6.19E+03	1.66E+02	62.68	5.11E+07	189357.84	138844.726
9	0.815	25.56	31885.76	3.72E+04	36.17	5.01	7.22E+03	5.2	8216	2.91E+07	8.27E+03	1.86E+02	64.12	4.54E+07	125637.465	81798.5838
10	0.9448	25.5	37050.98	3.72E+04	25.47	5.06	5.03E+03	5.41	8734	2.56E+07	5.82E+03	2.16E+02	65.36	3.92E+07	155816.392	118347.139
11	0	25.23	0.00	3.72E+04	145.2	5.04	2.88E+04	5.01	11088	#DIV/0!	3.32E+04	0.00E+00	91.07	#DIV/0!		#DIV/0!

Table 2.6: Benzo-a-pyrene Partitioning Data

								DPM/l	LSC dissolution			Material	Adjusted	Koc W/
							Aqueous	aqueous	Sediments	Sediments	Glassware	Balance	Sediment	Glassware
Sample #	Sediment, g	Water, g	Sed, mg/l	Spike, dpm	Abs @ 255	g for lsc	5 ml, DPM		DPM	DPM/kg	Sorption	% Recovery	DPM/kg	Sorption Corr.
1	0.037	25.3	1462.45059	190000	0.05	5.2	1524	2.93E+05	1.01E+05	2.73E+09	5.81E+04	87.68	3.12E+09	2.13E+05
2	0.0828	25.03	3308.03036	190000	0.081	5.07	1017	2.01E+05	1.06E+05	1.28E+09	4.68E+04	83.09	1.54E+09	1.54E+05
3	0.1824	25.14	7255.36993	190000	0.161	5.29	1009	1.91E+05	1.11E+05	6.09E+08	3.36E+04	78.69	7.74E+08	8.12E+04
4	0.3347	25.12	13324.0446	190000	0.229	5.21	854	1.64E+05	1.18E+05	3.52E+08	2.32E+04	76.46	4.61E+08	5.62E+04
5	0.6415	25.05	25608.7824	190000	0.348	5.2	512	9.85E+04	1.11E+05	1.72E+08	1.10E+04	65.28	2.64E+08	5.36E+04
6	0.2519	25.1	10035.8566	190000	0.195	5.23	780	1.49E+05	1.04E+05	4.13E+08	3.65E+04	75.91	5.44E+08	7.29E+04
7	0.2547	25.79	9875.9209	380000	0.187	5.3	1581	2.98E+05	2.03E+05	7.97E+08	7.97E+04	76.45	1.04E+09	6.99E+04
8	0.2509	25.49	9843.07572	570000	0.19	5.05	2216	4.39E+05	2.84E+05	1.13E+09	1.57E+05	79.28	1.43E+09	6.50E+04
9	0.2521	25.02	10075.9392	760000	0.171	5.15	2388	4.64E+05	3.64E+05	1.45E+09	1.94E+05	74.92	1.93E+09	8.32E+04
10	0.2513	25.25	9952.47525	950000	0.19	5.65	4701	8.32E+05	3.85E+05	1.53E+09	3.17E+05	76.16	2.01E+09	4.84E+04
11	0.2513	25.36	9909.30599	1140000	0.182	5.08	4904	9.65E+05	5.44E+05	2.16E+09	2.81E+05	74.55	2.90E+09	6.02E+04
12	0.1026	25.01	4102.35906	190000	0.105	5.23	872	1.67E+05	1.17E+05	1.14E+09	3.76E+04	83.49	1.36E+09	1.64E+05
13	0.1018	25.34	4017.36385	380000	0.105	5.08	1672	3.29E+05	1.71E+05	1.68E+09	1.18E+05	78.20	2.15E+09	1.30E+05
14	0.1035	25.02	4136.69065	570000	0.099	5.14	2611	5.08E+05	2.43E+05	2.35E+09	2.03E+05	80.41	2.92E+09	1.15E+05
15	0.1016	25.34	4009.47119	760000	0.106	5	3139	6.28E+05	3.58E+05	3.53E+09	2.36E+05	80.25	4.40E+09	1.40E+05
16	0.1009	25.42	3969.3155	950000	0.123	5.4	3770	6.98E+05	3.68E+05	3.65E+09	3.26E+05	74.98	4.87E+09	1.39E+05
17	0.5198	25.13	20684.4409	190000	0.312	5.05	687	1.36E+05	1.01E+05	1.94E+08	1.51E+04	62.97	3.09E+08	4.54E+04
18	0.5115	24.99	20468.1873	570000	0.295	5.21	2283	4.38E+05	2.88E+05	5.62E+08	1.09E+05	71.52	7.86E+08	3.59E+04
19	0.5082	25.16	20198.7281	1140000	0.305	5.37	4119	7.67E+05	4.76E+05	9.37E+08	3.36E+05	72.94	1.28E+09	3.35E+04

and sediment concentration are measured. If these three measured quantities did not equal the total initial spike, the sediment concentration was increased correspondingly. The material balance recovery then indicates the sediment extraction procedure. Appendix 4 includes a key to tables 2.2 through 2.6 which explains how the column calculations were made.

2.3 Results and Discussion: Solid Phase Sorption

In some cases, the aqueous phase measurement of PAH was close to background levels. In order to test whether the data was significantly above background, an hypothesis test was completed under the following assumptions:

1. H_o: u< or = 0
2. H_a: u>0
3. Test Statistic: Student t, t = (x-u)/(s/sqrt n)
4. Alpha = 0.05
5. Critical value @ n=3, 2 degrees of freedom
6. Reject H_o if computed t> or = 2.92

Based on this test, only one data point was not significantly greater than a background of 0 dpm. The results are included in Table 2.7. The data on background counts is included in Appendix five. Since the data points were background corrected, the hypothesis test compared the data to zero.

Table 2.7: Confidence in Benzo-a-pyrene Activity Measurements

Statistics for Benzo-a-pyrene Counts,								
Water concentrations were the lowest so they had the greatest chance for not being above background								
							95% confidence	
Activity, dpm/min		St. Dev.		T=(x-u)/(s/sqrt n)			x>u, t>2.92	
10.15		10.335		1.70104651			No	
55.44		4.725		20.3227295			Yes	
67.13		4.295		27.0716113			Yes	
64.56		4.38		25.5299544			Yes	
41.68		5.435		13.2827742			Yes	
63.76		4.405		25.0705016			Yes	
35.73		5.86		10.5607808			Yes	
28.65		6.535		7.59345916			Yes	
27.08		6.73		6.96938126			Yes	
36.17		5.84		10.7274448			Yes	
25.47		6.935		6.36125942			Yes	
145.18		2.925		85.9689355			Yes	

Figure 2.5 is an example of the K_{oc} values which were obtained for the varying sediment isotherm procedure. As shown, the K_{oc} value for fluoranthene exhibited a logarithmic decrease with increasing sediment concentrations. The results observed are similar to the work completed by Voice (1983) for several solutes using Lake Michigan sediment as the binding phase. Generally, a one order decrease in the partitioning coefficient is observed with a two order increase in solids concentration. Voice, 1983, noted that at very high solids concentrations, the K_{oc} appears to reach a limiting value. This is not apparent in the range of concentrations that were used in this study. Use of the Freundlich isotherm model, although appropriate for fitting the PAH sorption data, would not be appropriate for identifying a limiting K_{oc} value because of the exponential form of the equation.

For the procedure which we used, it was necessary to identify solid phase recoveries and correct the data for extraction inefficiencies. Figure 2.6 is an example of the recovery which was obtained for fluoranthene. It is a plot of the material balance % recovery vs. sediment concentration. The values also appear in table 2.3. Generally, the recoveries decreased with increasing solids in the system. Karickhoff (1980), observed that the ease of extraction of the sorbed phase was dependent on the equilibration time. Longer equilibration times resulted in reduced recoveries. These observations led to the conclusion that sorption continued over time from the surface of the soil into the soil matrix. It is suspected in our study that decreasing extraction efficiency related to the increase in

Figure 2.5: K_{oc} vs Sediment Concentration: Fluoranthene

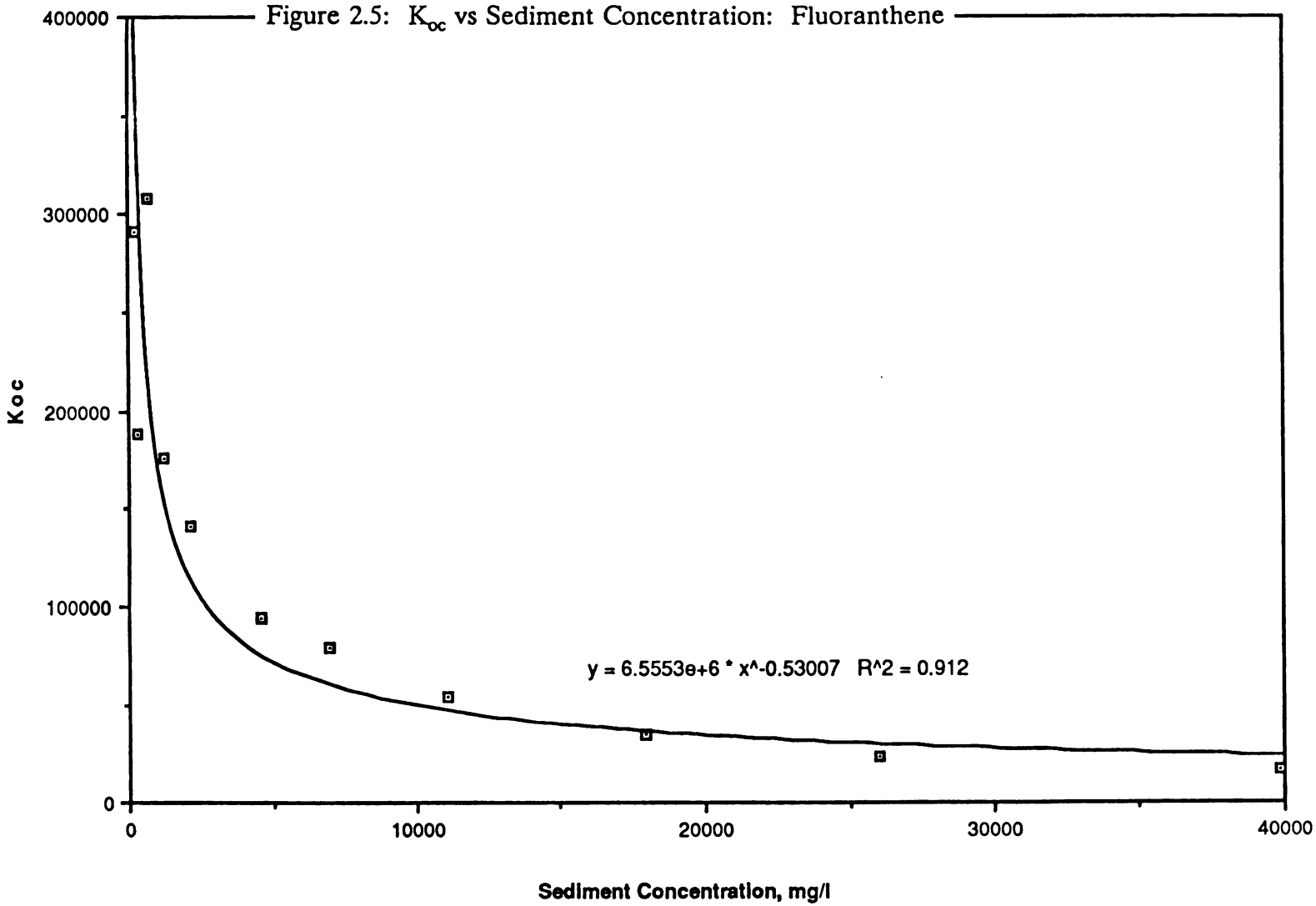

Figure 2.6: Recovery of Fluoranthene from Sediment

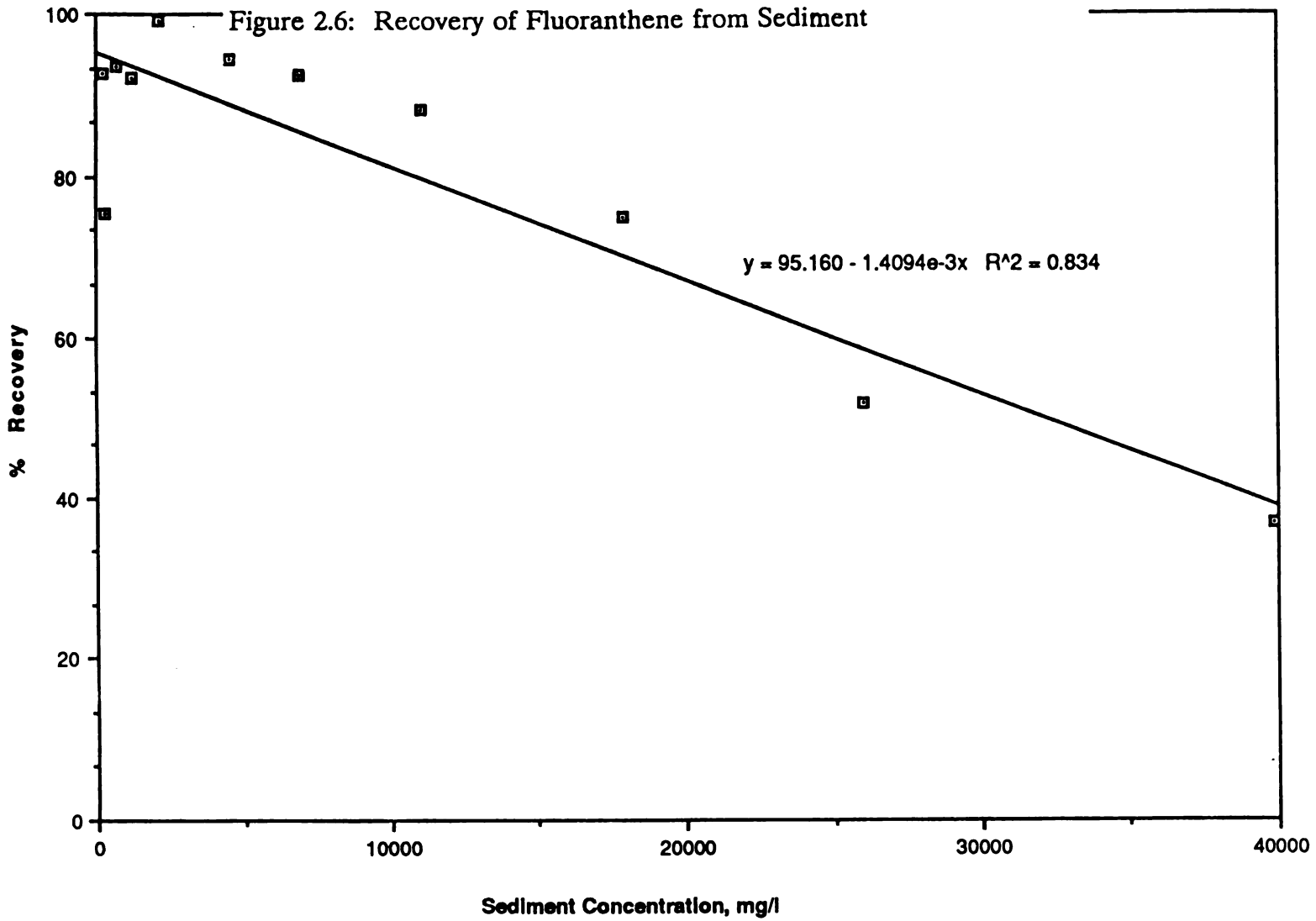

organic material which was available to bind the pollutants more tightly.

As noted, the observed dependency of K_{oc} on the solids concentration may be the result of binding to solution phase DOM. Several researchers have suggested the use of a corrected apparent K_{oc} which can be determined from calculations similar to the following equation (Hoke and Giesy 1992, Gschwend and Wu 1985):

$$\text{Corrected } K_{oc} = C_s/(C_w - K_{doc}*C_w*DOC)$$

Where K_{doc} = partitioning coefficient to DOC

DOC = Dissolved Organic Carbon

The intent of the correction is to make a distinction between the "free" and "bound" forms of the HOC. The measurement of C_w does not make this distinction. The measured value is the total HOC in the water. By assuming that $K_{doc} = K_{oc}$, the value of the "bound" contaminant in solution can be estimated and subtracted from the measure total to obtain "free" HOC.

In order to assess this correction for use with our data, we applied it to the apparent partitioning data for fluoranthene. K_{doc} was assumed to equal K_{oc} which is defined as a function of K_{ow} from the approximation (Lake 1990):

$$\text{Log}_{10} K_{oc} = 0.00028 + 0.983*\text{Log}_{10} K_{oc}$$

As shown in Figure 2.7, the K_{oc} values are increased as expected due to the correction which was applied to the measured aqueous phase concentration. However, the decrease in K_{oc} which is observed over the range of solid concentrations is still present in the corrected values. The correction equations which were implemented by Hoke (1992) do not correct for the solid concentration effect which was observed in this study.

Figure 2.8 shows varying solid partitioning coefficients for all of the PAH compounds which were used in our study. As indicated in the figure, the decrease in apparent K_{oc} with increasing solid concentration is observed for each PAH compound. Generally, the effect is the greatest for the compounds of higher hydrophobicity. This is apparent in the slope determined by logarithmic regression for each series of data. It increases (negatively) for the more hydrophobic compounds.

Considering the hypothesis suggested by Voice (1983), these results are expected since DOC binding would be the greatest for increasing hydrophobicity. In our data set, benzo-a-pyrene, as expected, exhibited the greatest decrease in K_{oc} over the experimental range of solid concentrations. Voice (1983) conceptualized a solute complexation model to describe these observations. The model relied on two major occurrences:

1. Phase transfer of solute complexing material (DOC) from solids to the aqueous phase.

Figure 2.7: Fluoranthene Sorption Data

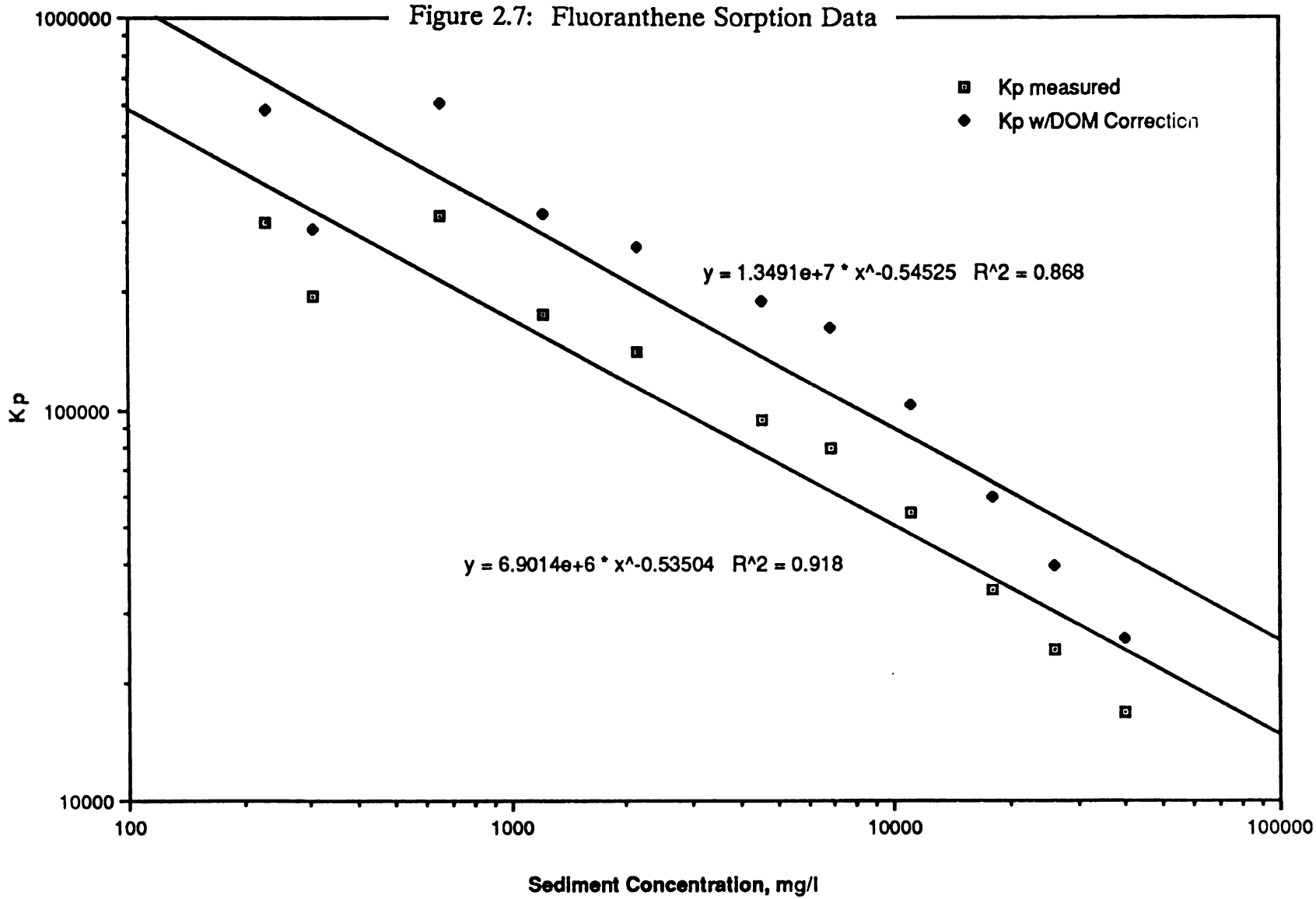

Figure 2.8: PAH Sorption Data

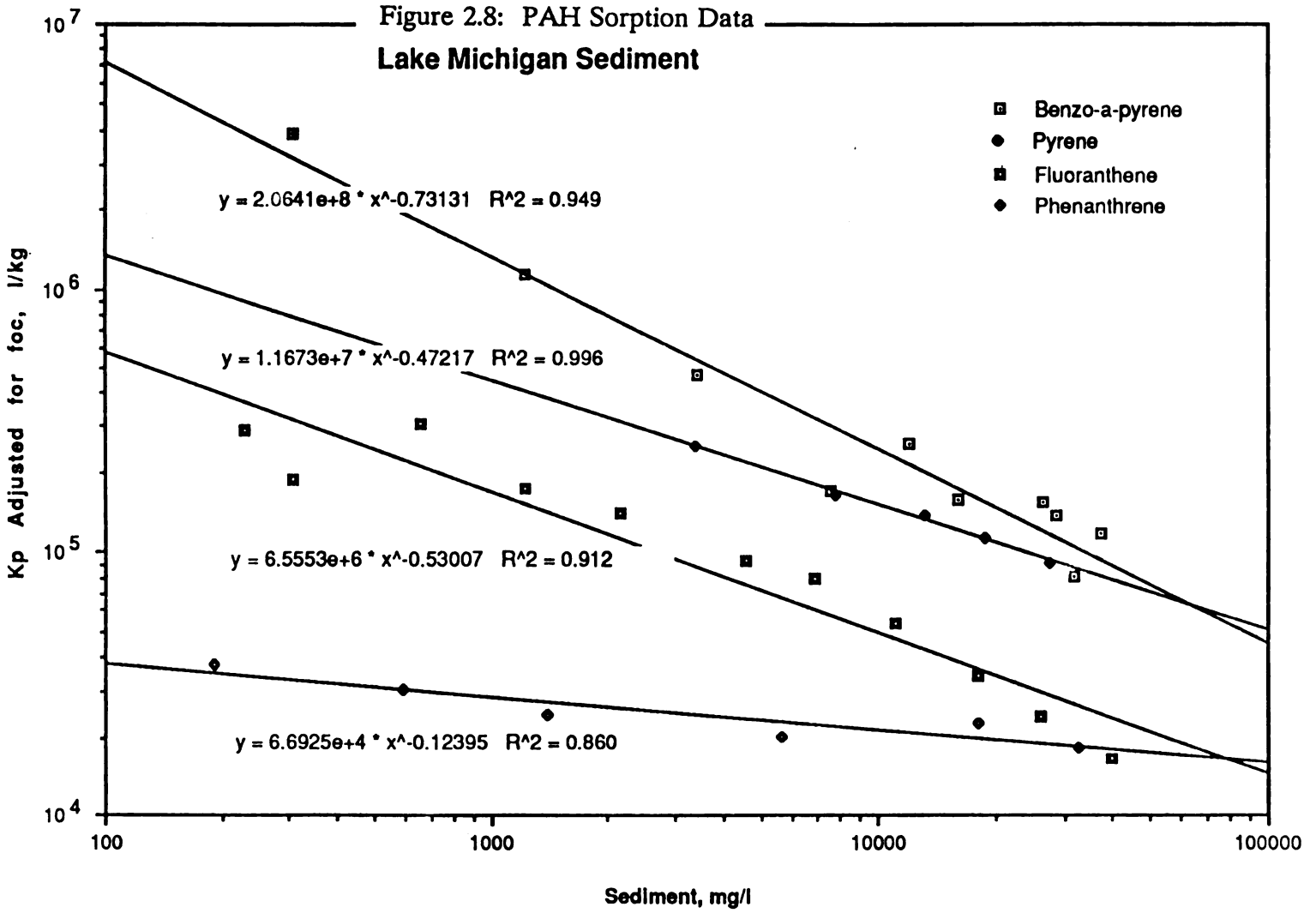

2. Heterogeneous solute in the aqueous phase made up of "free" and "DOC-bound" constituents.

Under these hypotheses, a sorption isotherm resulting from constant and varying solids techniques would produce a graph similar to the hypothetical plot shown in Figure 2.9. Data showing the absorption of humic and fulvic acids (Voice 1983) on activated carbon indicated behavior similar to that shown in Figure 2.9. It was suggested that these results are examples of heterogeneous solute absorption where the analytical technique does not distinguish between the various components in solution.

In order to assess the suggestion of heterogeneous solute sorption, varying and constant sediment isotherms were constructed for phenanthrene and benzo-a-pyrene to model both relatively low and high hydrophobicity compounds. The Freundlich isotherm was used to model the data. Figure 2.10 shows the results obtained using phenanthrene. As indicated, separate logarithmic regressions on the constant and varying solids data did yield different slopes, however

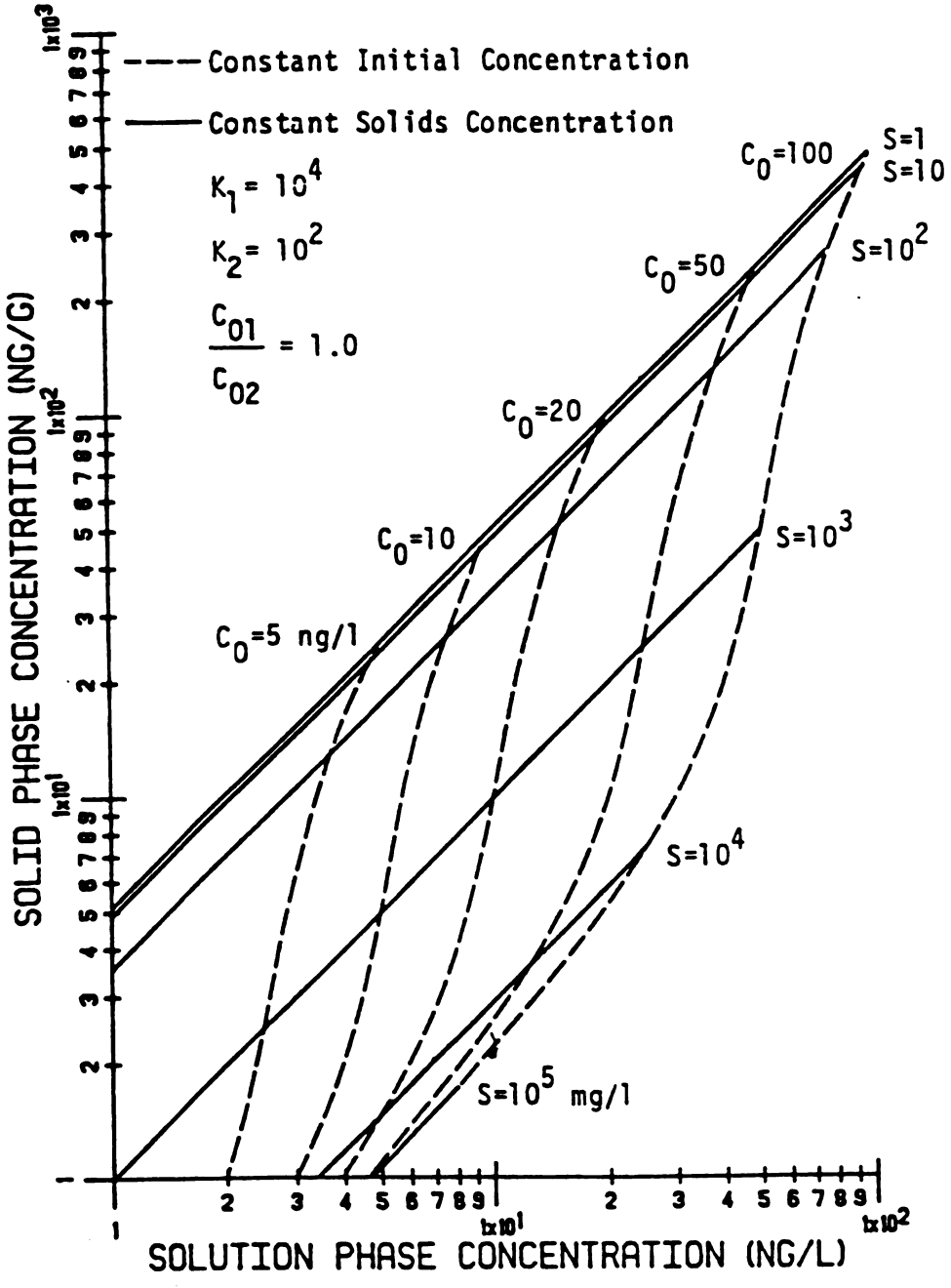

Figure 2.9: Effect of Isotherm Procedure on Observed Partitioning for a Heterogeneous Solute

Figure 2.10: Phenanthrene Absorption Isotherm

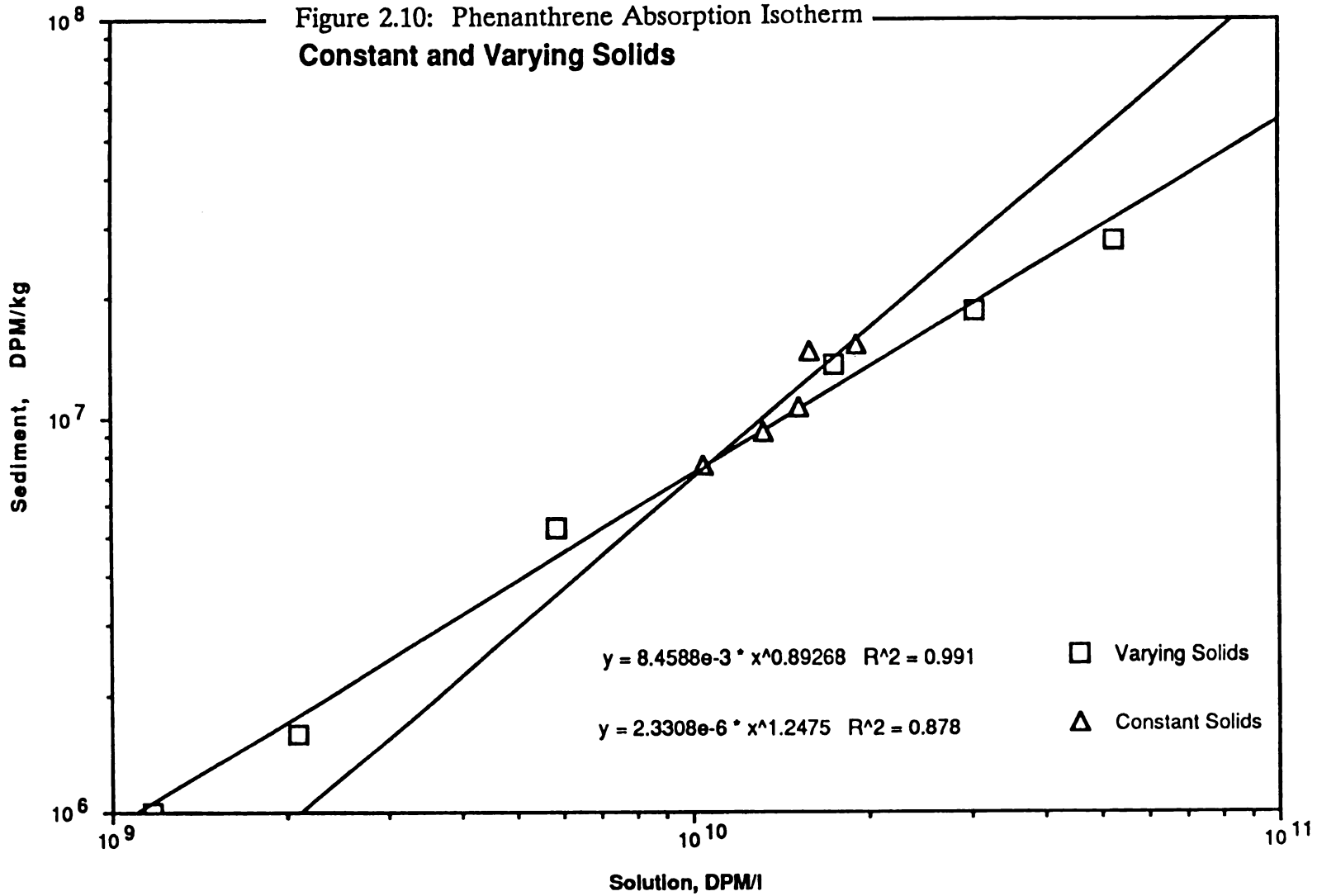

the difference in the results was not as evident as the difference observed using benzo-a-pyrene. For phenanthrene which is less hydrophobic than benzo-a-pyrene, the data may suggest that little binding occurred in the solution phase, thus there is little difference in the constant and varying sediment concentration isotherms.

Figure 2.11 shows the results obtained using benzo-a-pyrene. As indicated, the isotherms obtained using the constant and varying solid techniques were strikingly different. The BAP experiment incorporated three constant solids isotherms including 4,000, 10,000, and 20,000 mg/l solids concentrations and two varying solids isotherms in which different initial concentrations were spiked. The constant solids isotherms are parallel on a C_s vs C_w plot. Additionally, the Freundlich sorption intensity coefficient for constant solid data is less than 1. Logarithmic regressions on the varying solids isotherms, however result in Freundlich intensity constants greater than 1, consistent with Voice's (1983) results.

The general form of the data shown in Figure 2.11 is consistent with results obtained for humic and fulvic acid sorption to organic carbon using the varying sorbent and varying initial concentration techniques (Voice, 1983). Simple linear partitioning would have modeled the data as a straight line and the slope would be used to predict the partition coefficient. However, as noted by Voice and paralleled in this study, our results suggest that a full description of the data requires at least one additional variable, C_0 or S, to describe equilibrium conditions. Additionally, extrapolation of data from

Figure 2.11: Benzo-a-pyrene Absorption Isotherm

Constant and Varying Sediment Isotherms

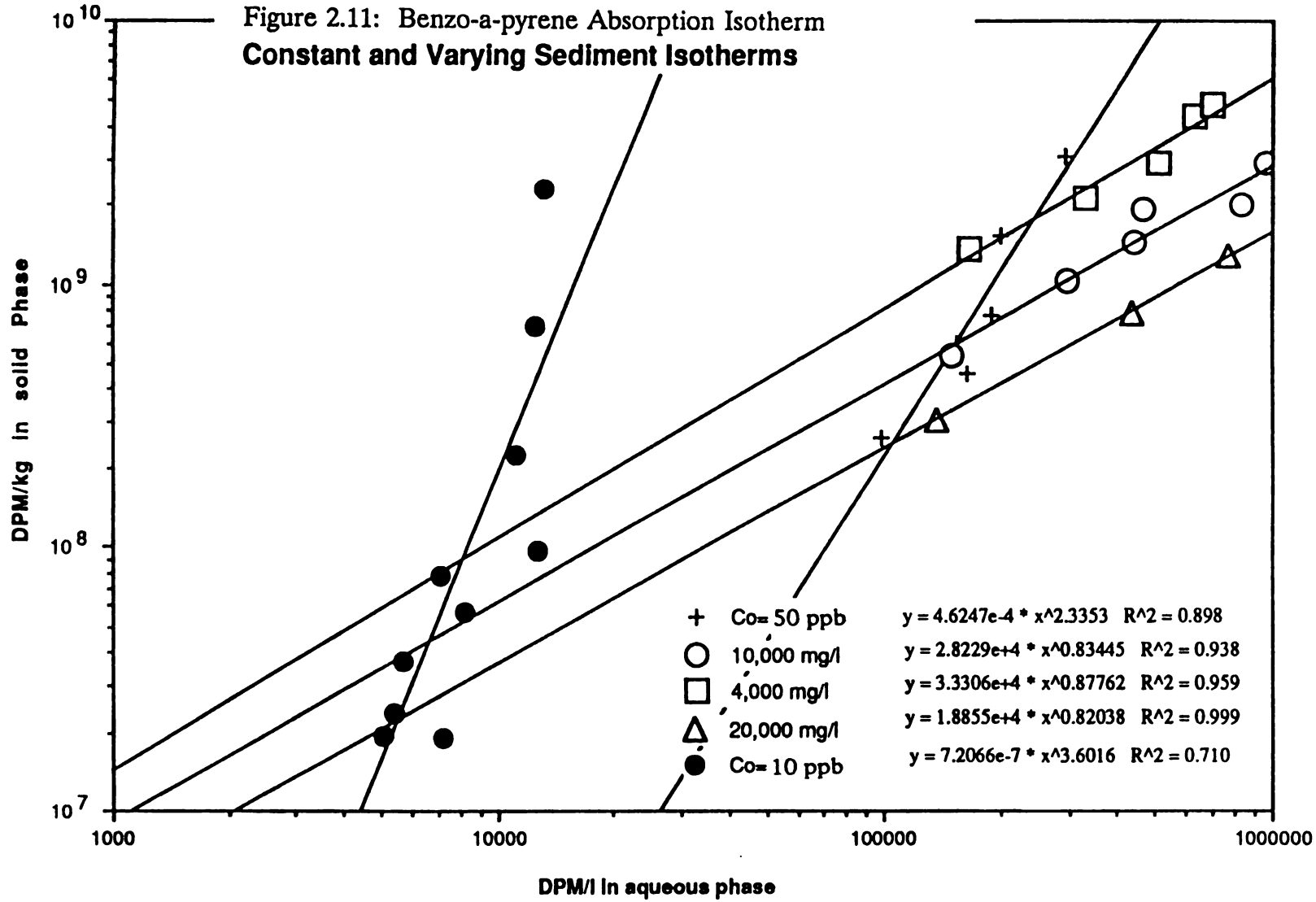

experimental to field conditions without designating experimental design conditions is questionable.

2.4 Conclusions: PAH Sorption Experiments

The relationship between solid concentration and K_{oc} is evident in figures 2.5 and 2.8. As the concentration of solids in the system increases, the partitioning coefficient K_{oc} decreases exponentially. For the range of PAH's studied, the effect is increased for the more hydrophobic compounds. The following summary identifies the Range of K_{oc} values which were found for each PAH studied.

PAH	Log K_{oc} Range	Solids concentration, (mg/l)
Phenanthrene	4.3 - 4.6	190 - 33,000
Fluoranthrene	4.2 - 5.5	228 - 40,000
Pyrene	5.0 - 5.4	551 - 27,306
Benzo-a-pyrene	4.5 - 6.6	305 - 37,051

By varying the conditions needed in the batch sorption studies by using a constant and varying solids technique, the data produced considerably different isotherms for benzo-a-pyrene. The effect was not as readily apparent in the phenanthrene data. For BAP the following data summarizes the Freundlich parameters which described BAP sorption.

Solid Concentration, (mg/l)	Freundlich, K	Freundlich, 1/n
4,000	3.33e4	0.88
10,000	2.82e4	0.83
20,000	1.89e4	0.82
Initial PAH Spike, (ppb)		
10	7.21e-7	3.60
50	4.62e-4	2.34

As previously noted, the Freundlich K is an indicator of the amount of absorption while 1/n is an indicator of absorption intensity. For the varying solids technique, 1/n remained relatively unchanged while the Freundlich K decreased with increasing solids. for the constant solids technique, K increased while n decreased with increasing initial BAP spike.

The significance of this data is that simple predictions of BAP concentration in one phase of the system, either solid or water, by knowing the partition coefficient should be used with caution since, the results depend on isotherm procedure. Additionally, as noted by Figure 2.7, correcting the observed partition coefficient value by using a technique similar to Gschwend and Wu's or Hoke and Giesy may not be adequate for data which is generated by techniques similar to ours.

Chapter 3: Measurement of Phenanthrene and Benzo-a-pyrene binding to Dissolved Organic Carbon from Lake Michigan Sediments

3.1 Introduction

A number of researchers have shown that hydrophobic organic compounds (HOCs) exist in "bound" forms associated with either dissolved or colloidal organic matter. Chiou et al. (19) showed that the water solubility of HOC's was enhanced by humic and fulvic acid addition. Compounds with high water solubility exhibited no detectable solubility enhancement, however, more hydrophobic compounds such as DDT showed significant solubility enhancement. Other researchers have demonstrated the ability of organic colloids to alter the subsurface transport of contaminants (Schwarzenbach et. al., 1981; McCarthy et. al., 1989; Magee et. al., 1991, Bertsch, et. al., 1993) The role of particulate organic matter in decreasing accumulation of polynuclear aromatic hydrocarbons in aquatic biota has also been shown (McCarthy, 1983). Other researchers have identified the binding of HOC's as a reason for decreasing bio-availability of HOC's (Geisey, 1981).

In order to evaluate the extent of binding of PAH's to dissolved organic carbon, it is necessary to measure the "free" and "bound" distribution of the compound as well as the amount of binding material in solution. The objective of this chapter is to describe two experimental techniques, fluorescence quenching and reverse phase separation, which have been developed by researchers for measuring PAH binding to dissolved organic carbon. Additionally, the chapter

describes the experiments which were used to measure phenanthrene and benzo-a-pyrene binding to dissolved organic carbon from Lake Michigan Sediments.

Fluorescence quenching is a technique originally presented by Gauthier (1986) for measuring the equilibrium constant which describes the interaction that hydrophobic fluorescent compounds have with dissolved organic carbon. The procedure is based on the observation that the fluorescence of the hydrophobic compound decreases proportionally to its association with organic carbon. The organic carbon inhibits the fluorescence of PAH's when it is present in solution. It is believed that this is due to binding with the PAH molecules. One researcher describes the process as a cage-like structure around the PAH which absorbs the energy normally dissipated as fluorescence (Morra, 1990).

Fluorescence quenching has continued to be developed through other researchers including Gschwend and Backhus (1990), Morra, et. al. (1990), and Slautman (1992). The binding of hydrophobic chemicals to organic carbon is important in assessing the fate and transport of pollutants in environmental systems. The fluorescence quenching technique has been used to describe binding of PAH to organic carbon to assess the colloidal transport of PAH's in groundwater (Backhus and Gschwend, 1990; Magee, 1991)

Reverse-phase separation was used by Landrum, et. al., (1984) to measure pollutant binding to dissolved organic carbon by physically separating the organic carbon bound and free phase of

pollutants at equilibrium. It was developed from the observation that humic-bound benzo-a-pyrene and other PAHs could be separated from the "freely dissolved" benzo-a-pyrene using XAD-4 resins (Landrum and Giesy, 1981).

3.2 Quantifying DOC Released from Lake MI Sediments

In order to quantify PAH distribution in the aqueous phase, it is necessary to quantify the sorbent transfer of solute binding material (in our case DOC) to solution. Voice (1983) noted the difficulties associated with defining the components of the aqueous phase. Experimental techniques are hindered by the fact that complete phase separation is difficult if not impossible to achieve. Under these conditions, operational definitions for "free" and "bound" compound must be set forth in experimental techniques.

Eadie (1990) conducted a study of HOC distribution between particle bound, dissolved organic matter bound and freely dissolved constituents. Operational definitions were achieved by glass fiber filtration and reverse phase separation using SepPak^{r} cartridges. His results indicated that for most compounds including benzo-a-pyrene, the free fraction was dominate. However, these studies were undertaken for natural water column conditions 1-5 ppm TOC and 0.2 to 5 ppm of total suspended matter.

In our experiments it was necessary to correlate TOC to some other measurable parameter since radiolabelled chemicals were used in the sorption experiments. The following experiments describe the correlation which was developed to quantify the aqueous DOC.

3.2.1 Materials and Methods

Batch bottle point experiments were set up for the DOC transfer measurement similar to the experiments used for PAH sorption in chapter 1. A known quantity of sediment was placed in a 25 ml centrifuge tube and combined with a known quantity of deionized, reverse osmosis, and filtered water. The mixture was shaken on a wrist action shaker for 24 hours to allow equilibrium to be achieved. Initially, a kinetic study was performed by adding the same amount of sediment to several tubes and equilibrating for varying amounts of time.

For the purposes of this study, the sediment was separated from solution by centrifugation at 12,000 RCF for 2 hours. Residual organic matter in solution both in the form of micro-particulates and dissolved material was defined as the sorbing phase resulting from sediment transfer. The instrument specifications which were used for this study are included in Appendix II.

The quantification of the amount of total organic matter transferred from the sediment to the solution was accomplished

through a series of experiments. After solid separation by centrifugation, a portion of the supernatant was used to measure absorbance at 255 nm. Additional portions of the supernatant were used to evaluate the total organic carbon, TOC, by using a Shimadzu TOC analyzer. A separate experiment was conducted to evaluate turbidity in several of the samples by removing a 15 ml portion of the water from the tube and measuring on a turbidity meter.

3.2.2 Results and Discussion

Kinetics of TOC desorption from freeze dried Lake Michigan Sediments were determined to be relatively fast. As shown in figure 3.1, greater than 80 % of the material desorbed in less than 5 hours. The remainder of the DOC slowly entered solution over an extended period (30 hours in this study). These kinetics, however, are slower than the time required for binding of PAH's to dissolved organic material as modeled by humic and fulvic acids using fluorescence quenching (Gschwend and Backhus 1990, Gauthier 1986, Slautman 1992).

As shown in figure 3.2, the absorbance values correlated to the sediment concentration using a logarithmic regression. The regression equation, $y = a * X^b$, found to provide the best fit for the data, was the same form of equation used by Voice relating TOC to sediment concentration. Approximately 94 % of the scatter in the data is described by the logarithmic regression. The deviation from

Figure 3.1: Release of Organic Carbon from **10 g/l**

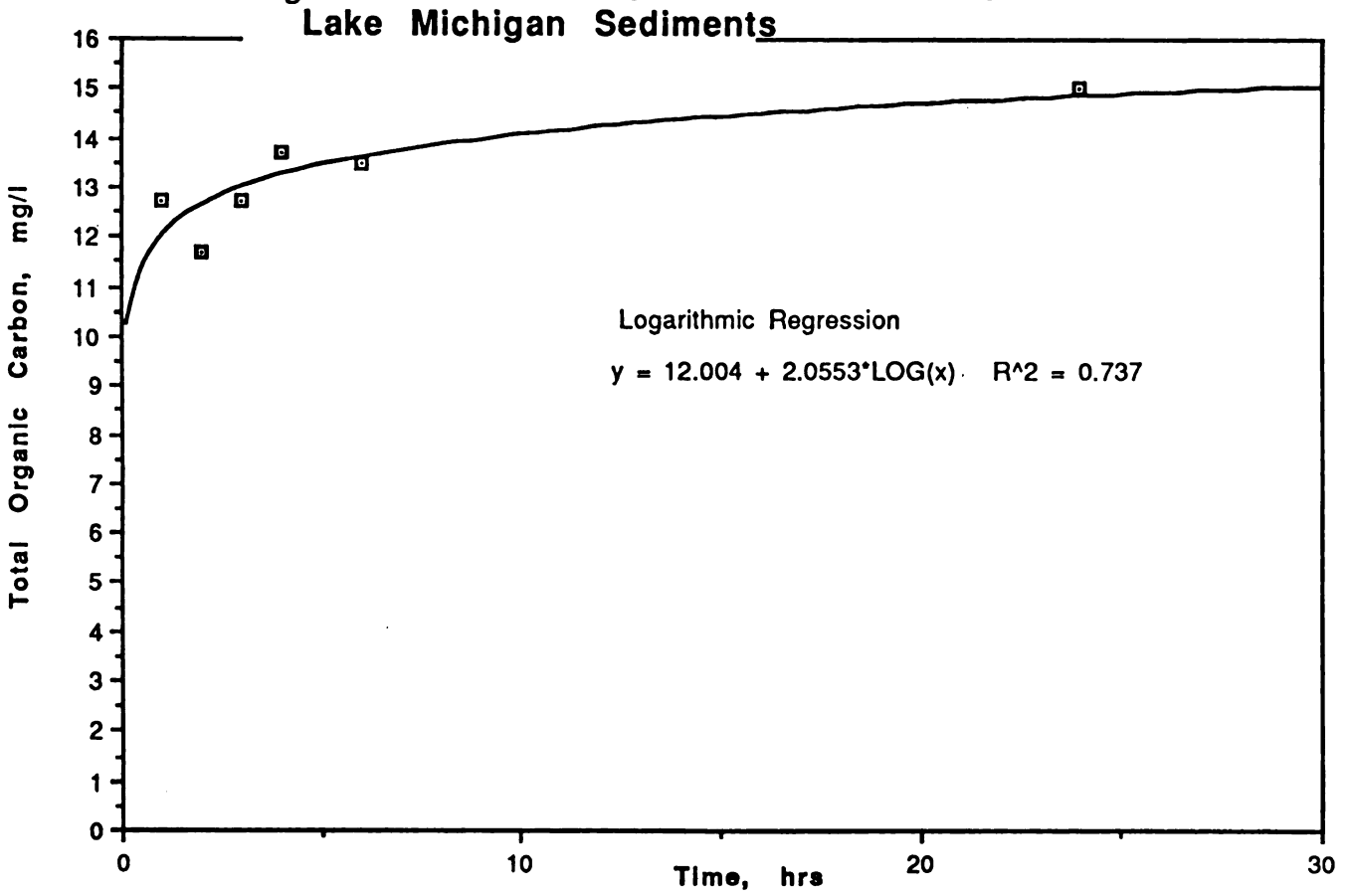

Figure 3.2: Absorbance at 255 vs Sediment Concentration

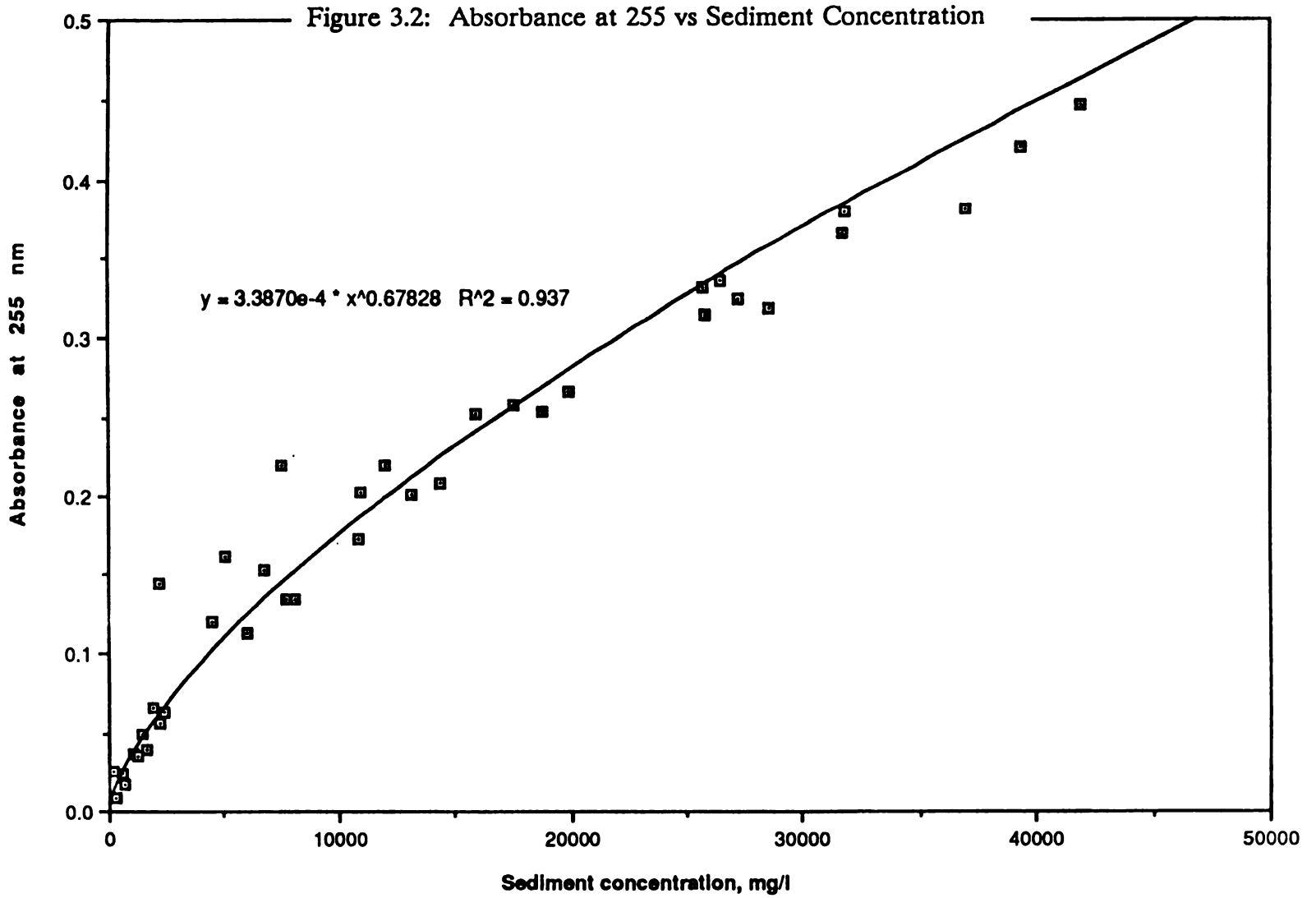

linearity is possibly the result of readsorption by organic material at the higher solids concentration or alternately, an approach to solubility limits of the organics.

Figure 3.3 shows that TOC can be determined as a function of absorbance. The correlation that we found was subsequently used in the DOC binding experiments to evaluate the amount of solute binding material in solution at equilibrium as TOC.

An additional measurement was made to determine solution turbidity. This was done since other researchers have identified that incomplete phase separation of dissolved and particulate material can affect the measurement of K_{doc} values for HOC's (Gschwend and Wu 1985, Voice 1985).

Figure 3.4 shows the results obtained by correlating TOC and turbidity to absorbance. Under ideal assumptions, turbidity, defined as a measure of the light scattering properties of a solution, measures particulate material. Absorbance, however, is a measure of the absorption of light at specific wavelengths and relates to dissolved material. The absorbance readings in our data from about 0.05 to 0.5 relate to a range in TOC of about 5 to 45 mg/l. This range in absorbance allows much more measurement ability than the 15 to 25 NTU range on a turbidity instrument.

Figure 3.3: TOC vs Absorbance at 255 nm

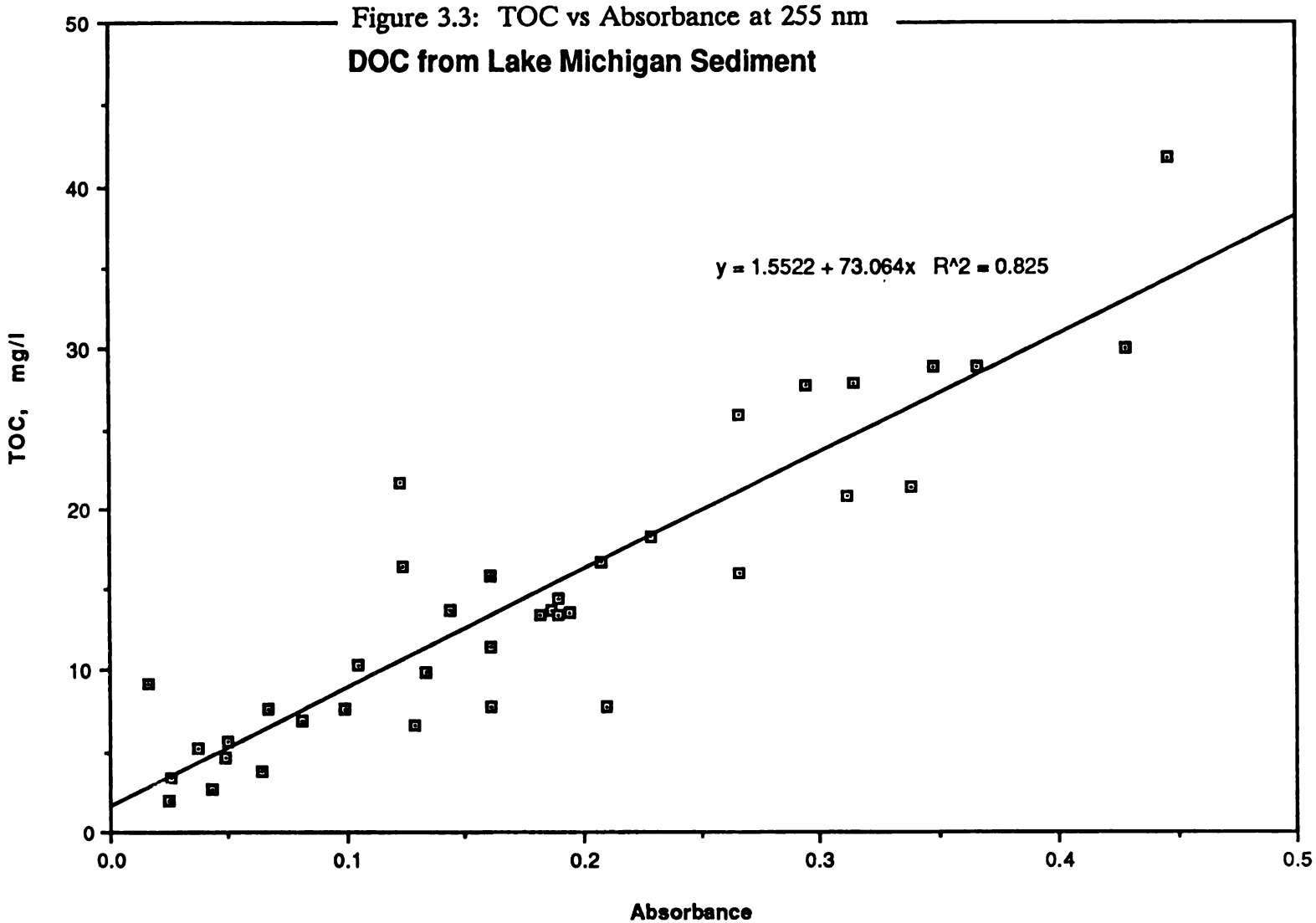

Figure 3.4: TOC and Turbidity vs Absorbance

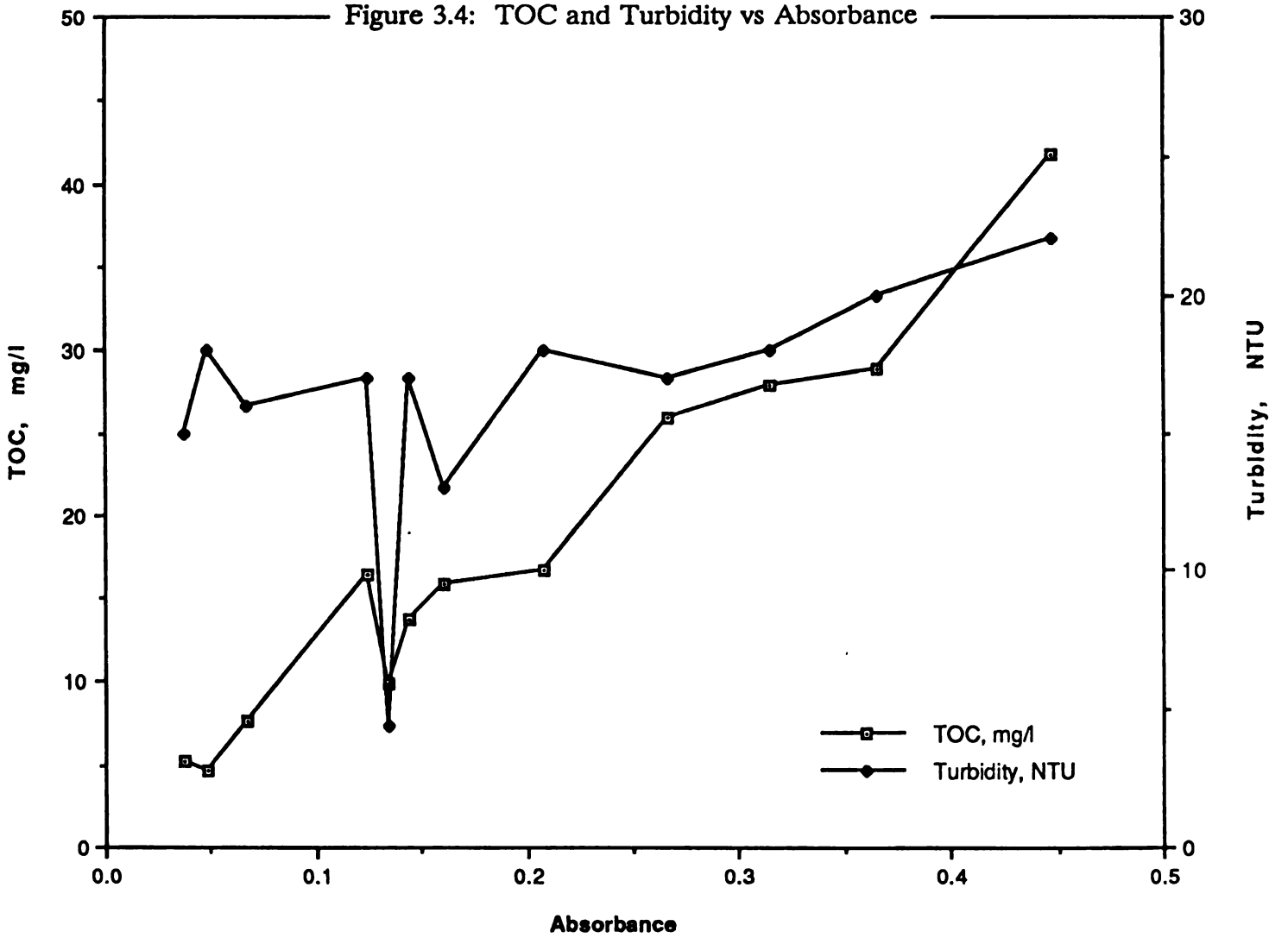

The regression:

$$TOC\ (mg/l) = 1.5522 + 73.064 * Abs \qquad R^2 = 0.825$$

was subsequently used in the study to estimate DOC values from absorbance.

3.3 Fluorescence Quenching

Fluorescence quenching has been used by many researchers to study PAH partitioning to aqueous-phase organic material (Gschwend and Backhus, 1990; Gauthier, 1986; Slautman, 1992). Its advantage is that a physical separation of "free" and organic carbon "bound" components in solution is not necessary. Hence recovery and separation efficiencies do not hinder its use. Fluorescence quenching is founded on the assumption that the measured fluorescence intensity is decreased in proportion to the fluorescent compound's binding to a quencher (Gauthier, 1986). In natural waters, the principal quencher is believed to be dissolved organic carbon.

Three mechanisms of fluorescence quenching are defined in the literature. Apparent quenching, referred to as the inner filter effect is due to attenuation of light at the excitation wavelength and absorption of light at the emission wavelength during a fluorescence measurement. Additionally, the fluorescent molecule can interact with a quencher by either association or collision mechanisms. The first is referred to as static quenching and the latter as dynamic

quenching (Gauthier 1986). All of the mechanisms may be present when measuring the decrease in fluorescence associated with a quencher. The mechanisms involved in binding of organic carbon with PAH's is static and dynamic quenching.

Gauthier's method makes use of a fluorescence correction coefficient which defines the proportion of exciting and emitting light which is lost through absorption. Any remaining losses in the presence of the quencher are assumed to result from interactions with the quencher, either by binding deactivation (static quenching) or by collisional de-excitation (dynamic quenching) of the fluorescent molecule.

The procedure relies on the assumption that the decreases in fluorescence which are observed in the presence of organic material are directly proportional to the extent of binding. A simple derivation of this interaction as a conditional equilibrium equation is included in Appendix 1. The Stern-Volmer equation is an expression which relates the ratio of fluorescence in the presence to fluorescence in the absence of a quencher with the partitioning coefficient, K_{doc}, and the concentration of quencher (DOC) in the sample.

$$F_o/F = 1 + K_{doc} * DOC$$

Corrections for absorption of the excitation and emission radiation are obtained by measuring absorption at the fluorescence

excitation and emission wavelengths. Miller, 1981, has derived the correction factor for perpendicular cell geometry. A summary of this derivation is also included in Appendix I. The decrease in fluorescence intensity after the correction has been applied is due to interaction with a quencher. Miller reports that for a correction factor greater than 1.8, the correction is increasingly inaccurate. Due to the relatively low absorbance values for the DOC used in our experiments, this value was not exceeded.

Gschwend and Backhus (1990) identified two possible problems to the Gauthier procedure. The first suggested that the DOM-PAH complex may fluoresce. The second identified the need to correct for glassware sorption when compounds with high hydrophobicity are used. Slautman (1992), experimented with these ideas for a number of PAH compounds absorbing to humic and fulvic acids. He noted that the quantum efficiency of the PAH-DOM complex approached zero for all the PAH's that were studied. Additionally, he found that the technique of Gauthier was satisfactory for PAH's of moderate hydrophobicity.

In order to correct for the fluorescence of the DOM-PAH complex, the following equation can be developed (Gschwend and Backhus, 1990):

$$F_o/F = (1 + o*K_{doc}*DOC)/(1 + K_{doc}*DOC)$$

where, o = quantum yield of PAH-DOM complex

This equation is essentially a modified Stern-Volmer expression with the F_o/F ratio defined as follows:

$$F_o/F = [PAH]_{total}/\{[PAH]_{free}+o*[PAH]_{bound}\}$$

Additionally, Gschwend and Backhus, (1990) note that by measuring the fluorescence of a sample over time, glassware sorption can be eliminated by extrapolating to time zero.

3.3.1 Methods and Materials for Fluorescence Quenching Measurements of Phenanthrene and Benzo-a-pyrene

For the purposes of this study, the phenanthrene binding coefficients to dissolved organic carbon from Lake Michigan sediments were estimated using Gauthier's technique. It was assumed that little or no glassware sorption took place. Slautman (1992) indicates that this approach is valid for the moderately hydrophobic PAH's. The technique for benzo-a-pyrene, however, implemented the procedure developed by Backhus and Gschwend (1990) to correct for glassware sorption.

The instrument specifications and settings are included in appendix II. For measurement of phenanthrene, a Perkin Elmer LS 50 spectrafluorimeter with a xenon arc lamp for the source was used. Excitation and emission wavelengths were set at 255 nm and 365 nm respectively since a high intensity peak occurred at these wavelengths. The excitation and emission slits were both set at 5 nm

in order to maintain the resolution of the peak while allowing maximum intensity readings. Activity of ^{14}C in the samples was measured on a Beckman liquid scintillation counter. Absorbances were measured on a Shimadzu UV spectrophotometer.

The samples which were measured in this portion of the study came from the sediment sorption studies which were completed in chapter 1. The initial step in the procedure was to estimate the ^{14}C activity and the fluorescence intensity of the blank sample in order to relate the two measurements. This procedure was necessary to estimate the total PAH in solution by fluorescence in the absence of the quencher. Accordingly, the disintegrations per minute of ^{14}C activity and the fluorescence of each sample was measured on a small portion of aqueous sample which had been separated from the sediments by centrifuging.

The sample was withdrawn from the centrifuge tubes by disposable glass pipettes and placed in a quartz cuvette. Initial experiments were conducted to identify the appropriate excitation and emission wavelengths for the fluorescence measurements. The goal was to choose wavelengths which resulted in an intensity peak from the PAH fluorescence. Figure 3.5 demonstrates the fluorescence

Figure 3.5: Phenanthrene Fluorescence Spectra

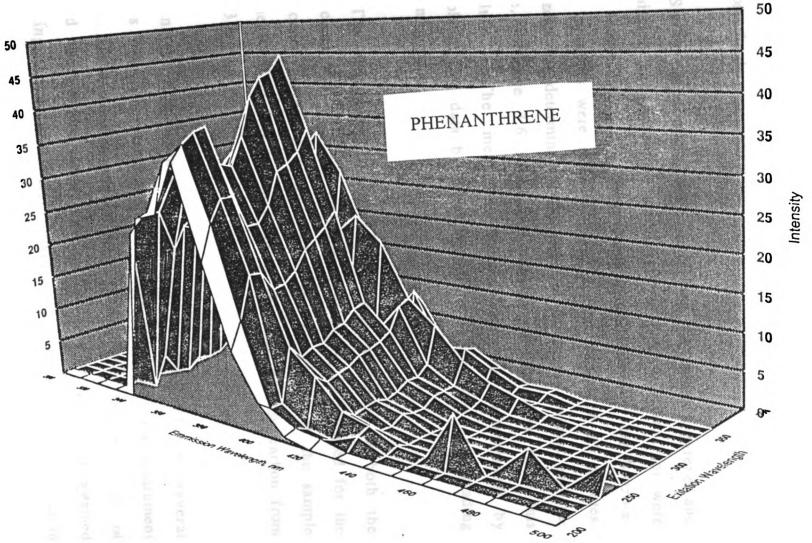

intensity of phenanthrene over a range of excitation wavelengths from 200 to 350 nm and emission wavelengths from 300 to 500 nm. The phenanthrene peak at 250 nm excitation and 365 nm emission was chosen for the measurement.

Similar experiments were conducted for benzo-a-pyrene and an emission and excitation wavelength of 380 and 445 nm were chosen respectively. The fluorescence measurements of the benzo-a-pyrene solutions were measured over a time period of 15 minutes. Time zero was determined at the point of filling the cuvette with the sample. Figure 3.6 shows an example of the data from this procedure. The measured fluorescence was determined by extrapolating the data by linear regression to time zero and reading the intensity value.

The absorbance of each sample was measured at both the fluorescence excitation and emission wavelengths to be used for the fluorescence correction factor. Also, the absorbance of the sample was measured at 255 nm to correlate the total organic carbon from Figure 3.3.

In the fluorescence measurement of phenanthrene, several samples had concentrations high enough to exceed the instrument range. These samples were diluted by adding a known amount of distilled water to the sample cuvette. A dilution factor was obtained by taking the sample weight divided by the sample plus dilution water weight.

Figure 3.6: Benzo-a-pyrene Fluorescence Extrapolation

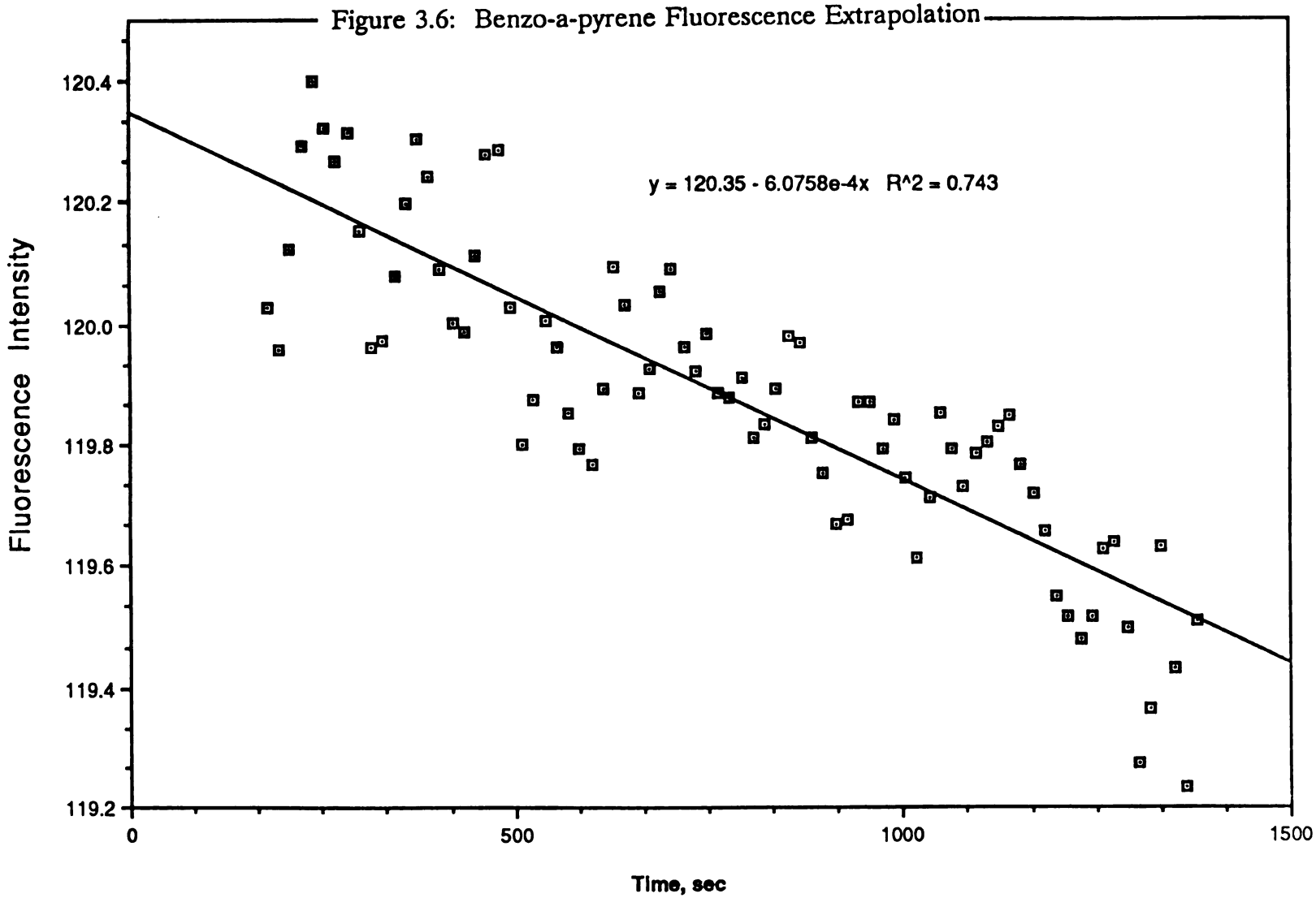

About five ml of additional sample was taken from each tube and placed in liquid scintillation vials. The weight of each sample was determined to the nearest tenth of a gram by tarring the vial and measuring the sample weight. Ten ml of high performance liquid scintillation cocktail was then added to each vial. The vials were capped, shaken and counted for three ten-minute repetitions on the Beckman liquid scintillation counter.

3.3.2 Results and Discussion: Calculation of K_{doc}

Table 3.1 shows the data reduction and calculations which were used for the K_{doc} of phenanthrene. The ^{14}C activity of the aqueous sample is shown in column 2. The fluorescence intensity in the absence of a quencher was estimated by multiplying the ^{14}C aqueous activity by the equivalent fluorescence intensity shown at the top of the table. This calculation was necessary to determine Fo. The fluorescence intensity estimating the amount of free compound in the samples is shown in column four. The free fluorescence was multiplied by the dilution factor where necessary to determine the actual sample fluorescence. The value for the actual fluorescence was entered as F total.

The absorbances at the emission and excitation wavelengths were then used to estimate the factor which corrects for the inner filter effect. The full derivation of this equation is included in Appendix 1. As shown, the corrected "free" fluorescence is obtained

Table 3.1: **Fluorescence Quenching, Phenanthrene**

Table 3.1: Fluorescence Quenching, Phenanthrene

Fluorescence quenching												
Fo= 30000 intensity units/(138967 dpm/5.02 ml *1000 ml/l)=					0.00108371							
sample	DPM/l	Fo	F	Dilution	F total	Abs @ 250	Abs @ 365	Correction	F, corrected	Fo/F	TOC, mg/l	Koc. kg/l
1	7.60E+06	8.24E+03	210.06	1.25	262.58	0.10	0.05	1.17	307.58	26.79	10.10	2.55E+03
2	9.23E+06	1.00E+04	950.26	1.00	950.26	0.14	0.03	1.21	1149.09	8.70	9.60	8.02E+02
3	1.06E+07	1.15E+04	658.78	2.17	1432.42	0.09	0.02	1.12	1610.04	7.15	11.13	5.52E+02
4	1.47E+07	1.59E+04	777.98	2.49	1933.58	0.08	0.01	1.10	2136.08	7.43	9.50	6.77E+02
5	1.53E+07	1.66E+04	122.16	9.98	1218.76	0.01	0.00	1.00	1218.76	13.63	12.10	1.04E+03
6	2.77E+07	3.00E+04	591.46	6.47	3827.09	0.01	0.00	1.00	3827.09	7.84	5.20	1.32E+03
7	1.86E+07	2.02E+04	509.76	1.25	637.20	0.01	0.00	1.00	637.20	31.64	7.50	4.09E+03
8	1.37E+07	1.48E+04	831.72	1.46	1212.10	0.10	0.03	1.15	1392.36	10.63	7.70	1.25E+03
9	5.26E+06	5.70E+03	416.66	1.78	743.32	0.08	0.02	1.11	828.46	6.88	9.60	6.13E+02
10	1.60E+06	1.73E+03	491.48	1.00	491.48	0.28	0.06	1.43	705.08	2.45	17.30	8.40E+01
11	1.00E+06	1.09E+03	474.96	1.00	474.96	0.06	0.01	1.08	512.09	2.13	25.60	4.39E+01

be multiplying the correction factor by F total. Knowing F_o and the corrected fluorescence, F, the Stern Volmer equation could be evaluated.

The procedure for determining the Stern-Volmer constant is also included in appendix 1. In our experiments, this constant is equal to the binding constant when the dissolved organic carbon concentration is substituted in the Stern-Volmer expression. For these experiments, the dissolved organic carbon content is estimated by substituting the absorbance measured at 255 nm into the regression equation shown in Figure 3.3.

Table 3.2 shows the data reduction for benzo-a-pyrene. The procedure was similar to phenanthrene except that the fluorescence at time zero was extrapolated from fluorescence measurements taken over fifteen minutes. The benzo-a-pyrene timed fluorescence data is included in appendix 1.

Referring to Table 3.1, the measured ^{14}C activity for the 11 phenanthrene spiked samples is consistent with the varying and constant sediment isotherm procedures discussed in Chapter 1. The first five samples represent constant sediment trials with varying phenanthrene spike. Accordingly, the measured disintegrations per minute per liter of sample increased with increasing spike. F_{total} after adjustment for dilution also increases over the five samples with increasing spike. Column 12 demonstrates that the estimated

Table 3.2: Fluorescence Quenching, Benzo-a-pyrene

Fluorescence quenching/ BAP data													
Fo= 800 intensity units/(300000 dpm)=						0.0027							
sample	Free	DPM/l	Fo	F	Dilution	F total	Abs @ 380	Abs @ 445	Correction	F, corrected	Fo/F	TOC, mg/l	Koc. kg/l
	dpm/l												
1	45131.25	2.93E+05	7.82E+02	120.35	1.00	120.35	0.00	0.00	1.00	120.35	6.49	5.02	1.09E+06
2	73537.50	2.01E+05	5.35E+02	196.10	1.00	196.10	0.00	0.00	1.00	196.10	2.73	7.59	2.28E+05
3	107711.25	1.91E+05	5.09E+02	287.23	1.00	287.23	0.00	0.00	1.00	287.23	1.77	11.84	6.51E+04
4	151800.00	1.64E+05	4.37E+02	404.80	1.00	404.80	0.00	0.00	1.00	404.80	1.08	17.08	4.67E+03
5		9.85E+04	2.63E+02	607.84	1.00	607.84	0.00	0.00	1.00	607.84	0.43	25.74	
6	131992.50	1.49E+05	3.98E+02	351.98	1.00	351.98	0.00	0.00	1.00	351.98	1.13	14.37	9.04E+03
7	122516.25	2.98E+05	7.95E+02	326.71	1.00	326.71	0.00	0.00	1.00	326.71	2.43	14.23	1.01E+05
8	137021.25	4.39E+05	1.17E+03	365.39	1.00	365.39	0.00	0.00	1.00	365.39	3.20	14.20	1.55E+05
9	133125.00	4.64E+05	1.24E+03	355.00	1.00	355.00	0.00	0.00	1.00	355.00	3.48	14.40	1.72E+05
10	63671.25	8.32E+05	2.22E+03	169.79	1.00	169.79	0.00	0.00	1.00	169.79	13.07	14.29	8.44E+05
11	135281.25	9.65E+05	2.57E+03	360.75	1.00	360.75	0.00	0.00	1.00	360.75	7.14	14.26	4.30E+05
12	78990.00	1.67E+05	4.45E+02	210.64	1.00	210.64	0.00	0.00	1.00	210.64	2.11	8.54	1.30E+05
13	76725.00	3.29E+05	8.78E+02	204.60	1.00	204.60	0.00	0.00	1.00	204.60	4.29	8.44	3.90E+05
14	84195.00	5.08E+05	1.35E+03	224.52	1.00	224.52	0.00	0.00	1.00	224.52	6.03	8.58	5.87E+05
15		6.28E+05	1.67E+03		1.00	0.00	0.00	0.00	1.00				
16		6.98E+05	1.86E+03		1.00	0.00	0.00	0.00	1.00				
17		1.36E+05	3.63E+02	514.41	1.00	514.41	0.00	0.00	1.00	514.41	0.71	22.48	
18	205725.00	4.38E+05	1.17E+03	548.60	1.00	548.60	0.00	0.00	1.00	548.60	2.13	22.33	5.06E+04
19	188782.50	7.67E+05	2.05E+03	503.42	1.00	503.42	0.00	0.00	1.00	503.42	4.06	22.15	1.38E+05

TOC values for the constant sediment procedure ranged from 9.5 to 12.1, indicating a range of variability of 2.6 mg/l of TOC

Similarly for the varying sediment procedure, the estimated TOC increased with increasing sediment concentration. Accordingly, the measured fluorescence of the constant phenanthrene spike decreased for samples 6 through 11. This decrease was due to the three mechanisms described previously, including apparent, static and dynamic quenching. After the correction for absorbance measurements at 250 and 365 nm (apparent quenching), column 10 shows the corrected fluorescence representing the concentration of free phenanthrene in each sample.

Referring to Table 3.2, the measured ^{14}C activity of the benzo-a-pyrene and the fluorescence values were consistent with the constant and varying sediment experiments. Column 5 shows the ^{14}C activity in the aqueous portion of the sediment water mix. Samples 1 through 5 are varying sediment experiments with constant benzo-a-pyrene spike. The TOC values estimated in column 15 increased with increasing sediment concentration and Fo decreased. Samples 6 through 11, 12 through 14, and 17 through 19 represent constant sediment procedures which resulted in TOC values on average of 14, 8.5 and 22.3 mg/l TOC respectively.

For the benzo-a-pyrene experiments, the dilution factor and correction factor were both one for all samples. This occurred because the undiluted samples were within the measurement range of the fluorimeter (less than 1000 intensity units). Additionally, the absorbance at the emission and excitation wavelengths of 380 nm and 445 nm respectively, was negligible, indicating that all quenching was either static or dynamic and not apparent quenching.

As shown by Backhus and Gschwend (1990), the fluorescence measurement for extensively hydrophobic compounds must be corrected for glass absorption. A linear regression was applied to extrapolate the measured fluorescence to time zero. The fluorescence at time zero was the value tabulated in the spreadsheet, Table 3.2. Apparent from the Figure 3.6 is the fact that the measured fluorescence changed little over the 15 minute time period indicating little absorption to the glassware on that time scale.

3.3.3 Conclusions: Fluorescence Quenching

In both the phenanthrene and benzo-a-pyrene data, using the results for Fo/F, K_{doc} was calculated from the Stern-Volmer expression by the formula:

$$Fo/F = 1 + K_{doc}*TOC$$

The K_{doc} values which were calculated for phenanthrene and benzo-a-pyrene varied widely with sediment concentration. This

variation is demonstrated in Figure 3.7 and 3.8. The range of K_{doc} values obtained using the fluorescence technique is shown below.

PAH	DOC concentration, (mg/l)	Log K_{doc}
Phenanthrene	5.20 - 25.60	1.6 - 3.6
Benzo-a-pyrene	5.02 - 25.74	3.7 - 6.0

For both phenanthrene and benzo-a-pyrene, the K_{doc} calculated by fluorescence quenching shows a decrease with increasing sorbent concentration. Although the dependence of K_{oc} on sorbent concentration has been shown by a variety of researchers, the relationship of K_{doc} with changing sorbent concentration has not been well documented. This apparent dependence on solids concentration or dissolved organic matter concentration has been noted by other researchers. McCarthy and Jimenez, 1985, found that the binding affinity of benzo-a-pyrene, anthracene and

Figure 3.7: Phenanthrene Reverse Phase and Fluorescence, K_{doc}

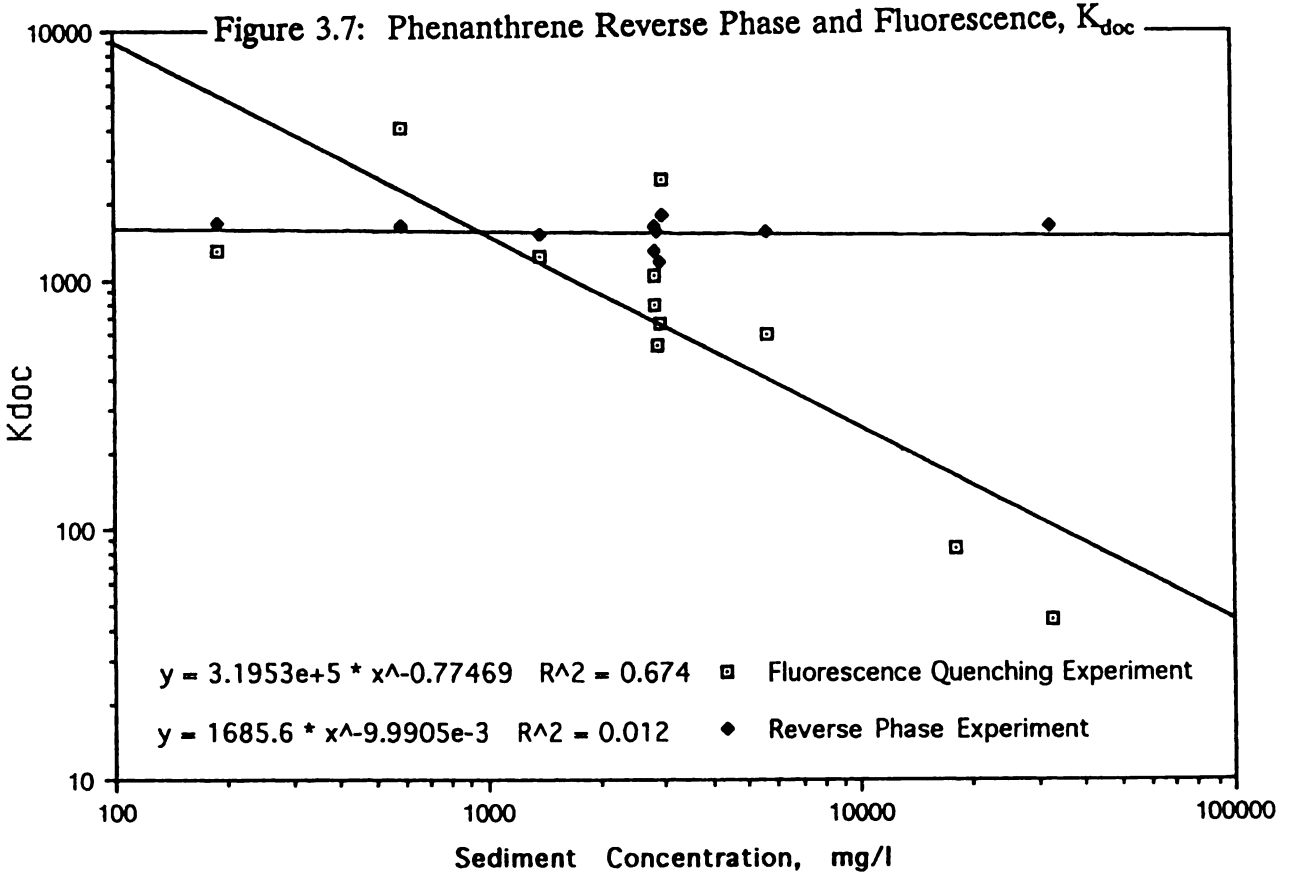

Figure 3.8: Benzo-a-pyrene Reverse Phase and Fluorescence, K_{doc}

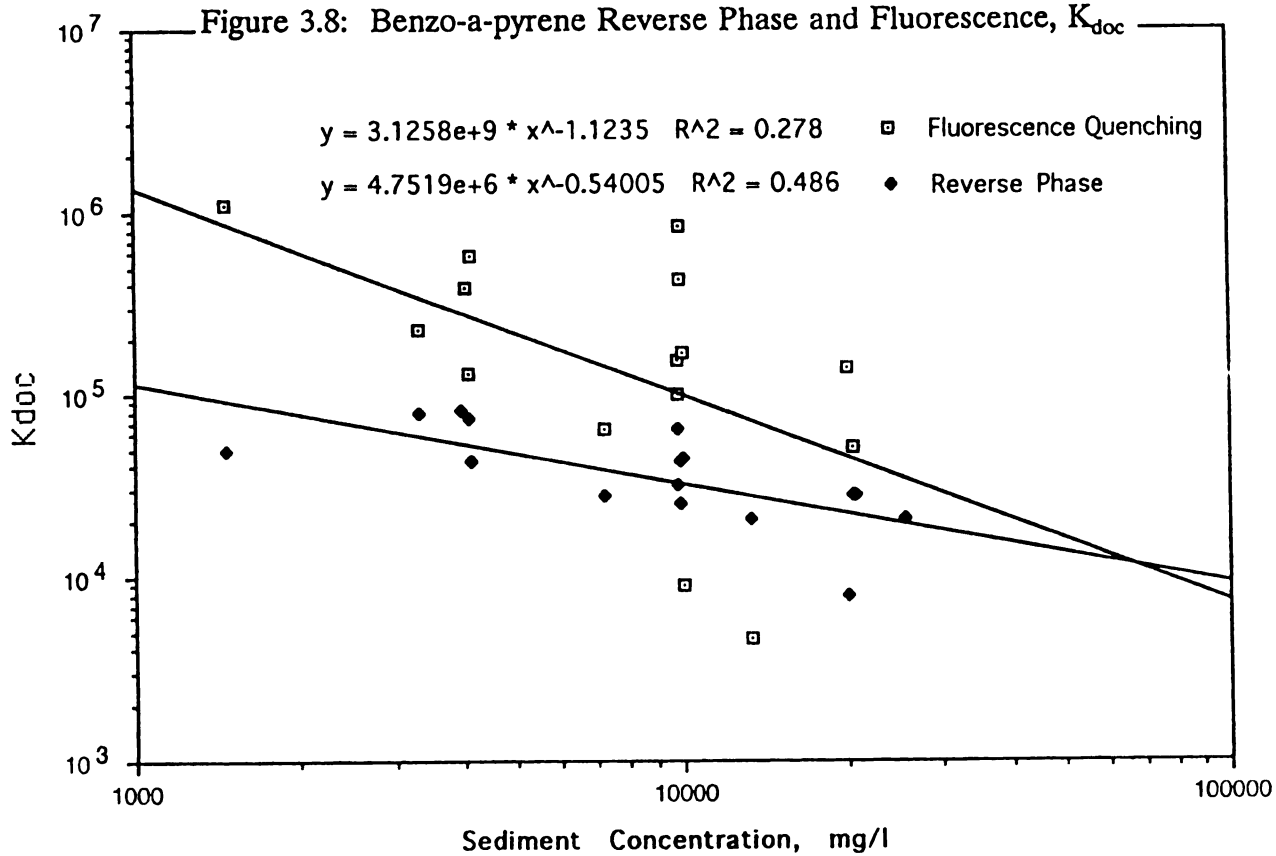

benzanthracene decreased with increasing dissolved humic material. Landrum, 1984, found similar results for benzo-a-pyrene and anthracene.

3.4 Reverse Phase Separation

The reverse phase separation method for determining pollutant binding to dissolved organic carbon was developed by Landrum et. al. (1984). The organic carbon bound pollutant was separated from "freely dissolved" pollutant by using a Sep-Pak C-18 cartridge. Organic carbon bound pollutant passed through, while the unbound pollutants were retained by the column. The partition coefficient was calculated as (grams of pollutant bound/grams of organic carbon)/(grams of pollutant freely dissolved/milliliter).

This technique was developed from the observation that an anomalous breakthrough of benzo a pyrene occurred during concentration with Amberlite XAD-4 resin from aqueous solution (Landrum and Giesy, 1981). These resins among many absorbing materials were used to concentrate pollutants at trace concentrations within environmental samples. The breakthrough of the pollutants was determined to be the result of binding to dissolved minerals and organics.

In the experiments with benzo-a-pyrene using the reverse phase column (Landrum, 1984), it was noted that minimal contact

time between the column and humic-pollutant complex minimized the potential for pollutant-DOC complex dissociation because of column interactions. The procedure used a flow-rate of about 12 ml/min. Where breakthrough of free compound occurred in the absence of DOC, an empirical correction was used. It is thought that pollutants bound to dissolved organic matter pass through the cartridge at pH sufficiently high (greater than 5) to polarize the humic substances.

In the following experiments, we have used Empore^R extraction disks as an alternate sorbent to study reverse phase separation of free and bound phenanthrene and benzo-a-pyrene. The filter disks, enmeshed in special fibrils, are made of C-18 moiety bonded particles. A filtration apparatus, consisting of a vacuum flask stoppered with a glass frit and filter clamp and attached to a vacuum meter and pump were then used to perform the extractions.

It is suspected that the C-18 coated disk will eliminate the potential for erroneous data due to short circuiting. Short circuiting was noted to be a problem for some pollutants using the Sep-Pak column even at low flow conditions. As previously noted a correction was applied to the "bound" concentration to adjust for the amount of "free" compound passing through the column (Landrum, 1984). Additionally, the enhanced contact provided by the even particle distribution within the Empore^R disk should permit much higher flow rates and reduce the potential desorption of the "bound"

contaminant. This condition of increasing bound contaminant with increasing flow was also noted by Landrum, 1984.

3.4.1 Materials and Methods: Empore^R Disk Extraction

The initial experiment was designed to determine whether breakthrough of a solution of ^{14}C labelled pyrene would occur at high flow rates. The vacuum filter apparatus described above was connected to a vacuum source metered by a Vacu-trol pressure gauge. A range of pressures from 200 to 600 mm of Hg were supplied to filter 10 ml of sample prepared at about 10,000 dpm. The disks were pre-conditioned using the following procedure as described by the manufacturer:

1. Flush with 10 ml MeCl2
2. Flush with 10 ml MeOH
3. Flush with 10 ml DI

The elution solvent was MeCl2 and it was used initially to flush contaminants from the disk. Methanol was then flushed through to remove the MeCl2 and prepare the disk for a DI water flush. After rinsing the disk with DI water in the final step, the disk was not allowed to dry prior to extracting the samples. For each sample, the procedure was repeated with a new disk.

Immediately following the preconditioning step while a meniscus of DI water was still visible, 10 ml of sample were filtered

through the Empore^R disk at varying flow rates, corresponding to varying pressure. The disks were filtered until dry, and the supernatant was combined with 5 ml of LSC cocktail and counted using the method described in Appendix II. Subsequently, 10 ml of a MeCl2/MeOH mixture in a 80/20 ratio was used to extract the disk. The extractant was transferred to a scintillation vial, combined with 5 ml of LSC cocktail and counted for ^{14}C activity.. After the extraction, the disk itself was also transferred to an LSC vial, combined with 5 ml of LSC cocktail and counted.

Figure 3.9 identifies the flowrate/pressure calibration curve determined for the Empore^R disks using DI water. This curve was completed to approximate the flow rate which corresponded to a given pressure.

For the breakthrough experiment, the flow rates were varied between 6 to 20 ml/minute by adjusting the pressure in order to determine if breakthrough would occur. Over this pressure range, however, no significant change occurred. Greater than 99% of the pyrene was absorbed to the disk at all pressures which were tested.

With these results, a pressure of 400 mm Hg was chosen to extract the DOM complexed samples using the procedure described above. The "bound" constituent was determined by counting the 14C activity of the filtrate, while the "free" constituent was determined by extraction absorbed PAH from the disk and counting the 14C

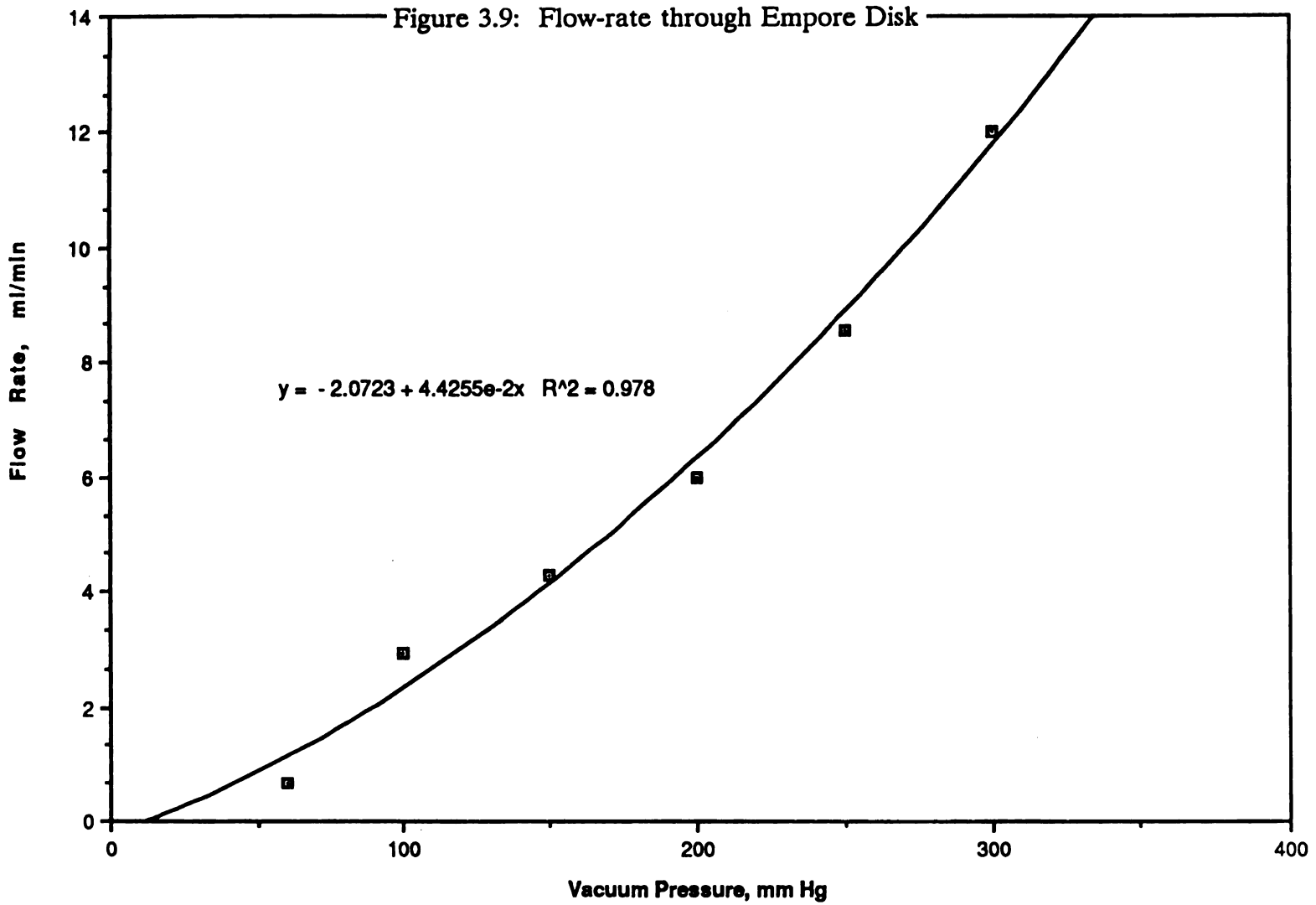
Figure 3.9: Flow-rate through Empore Disk
y = - 2.0723 + 4.4255e-2x R^2 = 0.978
Flow Rate, ml/min
Vacuum Pressure, mm Hg
0
2
4
6
8
10
12
14
0
100
200
300
400

activity. The following equation was used to determine the partitioning coefficient to aqueous DOM:

$$K_{doc} = C_{bound}/(C_{free}*DOC)$$

Where DOC was estimated using the correlation shown in Figure 14. Extraction efficiencies were necessary to adjust the concentration of the "free" compound because not all of the absorbed PAH could be removed from the disk.

The following steps detail our laboratory experiments:

1. Ten ml of water sample was removed from the PAH batch sorption experiments and filtered through the Empore^R disk at 15 ml/min, 400 mm Hg.
2. The filtrate was combined with 5 ml of LSC cocktail and counted using the method described in appendix II.
3. After filtering the disk to dryness, the disk was extracted using 10 ml of 80/20, MeCl2/MeOH mixture. The extractant was combined with 5 ml of LSC cocktail and counted.
4. The disk was then combined with 5 ml of LSC cocktail and counted.
5. The "free" measurement obtained from the disk extraction was then adjusted to reflect the extraction efficiency.
6. DOC was estimated using absorbance at 255 and C_{bound} was normalized to the organic carbon.
7. $K_{doc} = C_{bound}/C_{free}$

3.4.2 Results and Discussion: Empore^r Disk Extraction

Tables 3.3 and 3.4 show the data reduction which was used for the Empore^R disk extraction method. The supernatant was the material passing through the disk. It represented the organic carbon bound PAH. The elution of the disk itself using MeCl2 was counted for the free compound measurement. Additionally, the disk itself was placed in scintillation cocktail and counted because the extraction was not fully efficient.

Since the total aqueous ^{14}C activity was previously measured in the PAH sorption studies, a recovery estimate was calculated by adding the activity from the supernatant, the eluant, and the disk, and dividing the sum by the total activity. The recovery percentage is shown in the tables. It was assumed the estimated "free" activity determined from the disk extraction should be adjusted by the recovery efficiency since its value was measured directly by the Empore^r extraction. The value was entered as adjusted "free" concentration in the tables.

Knowing the activity of the "bound" portion which passed through the disk and the "free" concentration which was extracted from the disk, a partitioning coefficient was calculated from the following expression:

$$K_{doc} = [PAH]_{bound}/\{[PAH]_{free}*DOC\}$$

Table 3.3: Reverse Phase Seperation, Phenanthrene

Sample #	Estimated DOC, mg/l	Sed, mg/l	Empore Supernatant DPM	Empore Elution DPM	Free, dpm/l 10 ml sample	Bound dpm/kg TOC	Recovery	Adjusted Free	Kdoc Recovery adj
1	7.19	2989.77	956	2.51E+04	2.51E+06	1.33E+10	34.25	7.32E+06	1.82E+03
2	7.00	2842.94	1030	3.21E+04	3.21E+06	1.47E+10	35.91	8.94E+06	1.65E+03
3	7.04	2876.87	1160	6.26E+04	6.26E+06	1.65E+10	60.04	1.04E+07	1.58E+03
4	7.14	2952.76	1235	7.71E+04	7.71E+06	1.73E+10	53.44	1.44E+07	1.20E+03
5	7.02	2856.58	1407	9.03E+04	9.03E+06	2.01E+10	59.82	1.51E+07	1.33E+03
6	2.42	190.04	1139	1.74E+05	1.74E+07	4.70E+10	63.39	2.75E+07	1.71E+03
7	3.43	591.95	1044.53	8.33E+04	8.33E+06	3.04E+10	45.32	1.84E+07	1.66E+03
8	4.93	1402.89	1011	9.27E+04	9.27E+06	2.05E+10	68.61	1.35E+07	1.52E+03
9	10.25	5671.88	818	2.92E+04	2.92E+06	7.98E+09	57.05	5.12E+06	1.56E+03
10	20.56	17944.99			0.00E+00	0.00E+00	0.00	#NUM!	#NUM!
11	30.15	32779.11	456	4.22E+03	4.22E+05	1.51E+09	46.58	9.06E+05	1.67E+03

Table 3.4: Reverse Phase Seperation, Benzo-a-pyrene

Sample #	Estimated DOC, mg/l	Sed, mg/l	Empore Supernatant DPM	Empore Elution DPM	Empore Disk DPM	Free, dpm/l 10 ml sample	Bound dpm/kg TOC	Recovery	Adjusted Free	Kdoc
1	5.02	1462.45	572.91	1192.50	762.74	1.96E+05	1.14E+10	86.26	2.27E+05	5.03E+04
2	7.59	3308.03	708.29	541.43	459.40	1.00E+05	9.33E+09	85.20	1.17E+05	7.95E+04
3	11.84	7255.37	420.49	514.35	331.67	8.46E+04	3.55E+09	66.40	1.27E+05	2.79E+04
4	17.08	13324.04	359.26	295.36	305.27	6.01E+04	2.10E+09	58.56	1.03E+05	2.05E+04
5	25.74	25608.78	307.47	188.14	236.02	4.24E+04	1.19E+09	74.31	5.71E+04	2.09E+04
6	14.37	10035.86	518.25	311.99	285.35	5.97E+04	3.61E+09	74.80	7.99E+04	4.52E+04
7	14.23	9875.92	1334.29	694.96	578.02	1.27E+05	9.38E+09	87.40	1.46E+05	6.44E+04
8	14.20	9843.08	1237.58	986.18	1056.28	2.04E+05	8.72E+09	74.75	2.73E+05	3.19E+04
9	14.40	10075.94	0.00	0.00	0.00	0.00E+00	0.00E+00	0.00	#NUM!	#NUM!
10	14.29	9952.48	1834.21	1517.25	1355.51	2.87E+05	1.28E+10	56.57	5.08E+05	2.53E+04
11	14.26	9909.31	3084.67	1500.15	1711.32	3.21E+05	2.16E+10	65.22	4.92E+05	4.39E+04
12	8.54	4102.36	618.82	425.45	438.47	8.64E+04	7.25E+09	88.93	9.71E+04	7.46E+04
13	8.44	4017.36	0.00	0.00	0.00	0.00E+00	0.00E+00	0.00	#NUM!	#NUM!
14	8.58	4136.69	1222.86	1252.05	999.54	2.25E+05	1.43E+10	68.40	3.29E+05	4.33E+04
15	8.43	4009.47	0.00	0.00	0.00	0.00E+00	0.00E+00	0.00	#NUM!	#NUM!
16	8.38	3969.32	2519.00	1588.74	1187.60	2.78E+05	3.00E+10	75.85	3.66E+05	8.21E+04
17	22.48	20684.44	405.72	182.62	181.78	3.64E+04	1.80E+09	56.61	6.44E+04	2.80E+04
18	22.33	20468.19	1308.58	572.28	623.53	1.20E+05	5.86E+09	57.15	2.09E+05	2.80E+04
19	22.15	20198.73	876.42	1010.30	699.72	1.71E+05	3.96E+09	33.72	5.07E+05	7.80E+03

Figures 3.7 and 3.8 show the K_{doc} values determined from the above expression and plotted as a function of solids concentration. As apparent in these figures, the K_{doc} for phenanthrene did not exhibit a dependence on solid concentration while the K_{doc} for benzo-a-pyrene decreased with increasing solids in the system. This apparent dependence on solids concentration or dissolved organic matter concentration has been noted by other researchers. McCarthy and Jimenez, 1985, found that the binding affinity of benzo-a-pyrene, anthracene and benzanthracene decreased with increasing dissolved humic material. Landrum, 1984, found similar results for benzo-a-pyrene and anthracene.

3.4.3 Conclusions: Empore^R Disk Extraction

A summary of the K_{doc} values obtained using the Empore Extraction technique appears in the following table:

PAH	DOC concentration, (mg/l)	log K_{doc}
Phenanthrene	2.42 - 30.15	3.1 - 3.3
Benzo-a-pyrene	5.02 - 25.74	3.9 - 4.9

To demonstrate a correction technique for the solid phase K_{oc} values which were obtained in Chapter 1, the K_{doc} values which were measured by reverse phase were applied to the benzo-a-pyrene sorption data using the following equation:

$$K_{oc} = (C_s + C_{"bound"})/C_{"free"}$$

This correction includes the amount bound in solution as part of the total amount bound to the sediments and includes only the "free" concentration in the aqueous term. Figure 3.10 shows that the corrected K_{oc} value is higher because of the correction, however, the corrected K_{oc} still shows a decreasing trend with increasing solids concentration.

The significance of this data is that we have demonstrated the range of K_{doc} values which may be obtained by the fluorescence quenching technique and the reverse technique. It also demonstrates that measured values of K_{doc} using current techniques are not sufficient to describe the dependence that K_{doc} has on solid concentration by correcting for the amount bound in solution.

Figure 3.10: Benzo-a-pyrene, Corrected K_{oc}

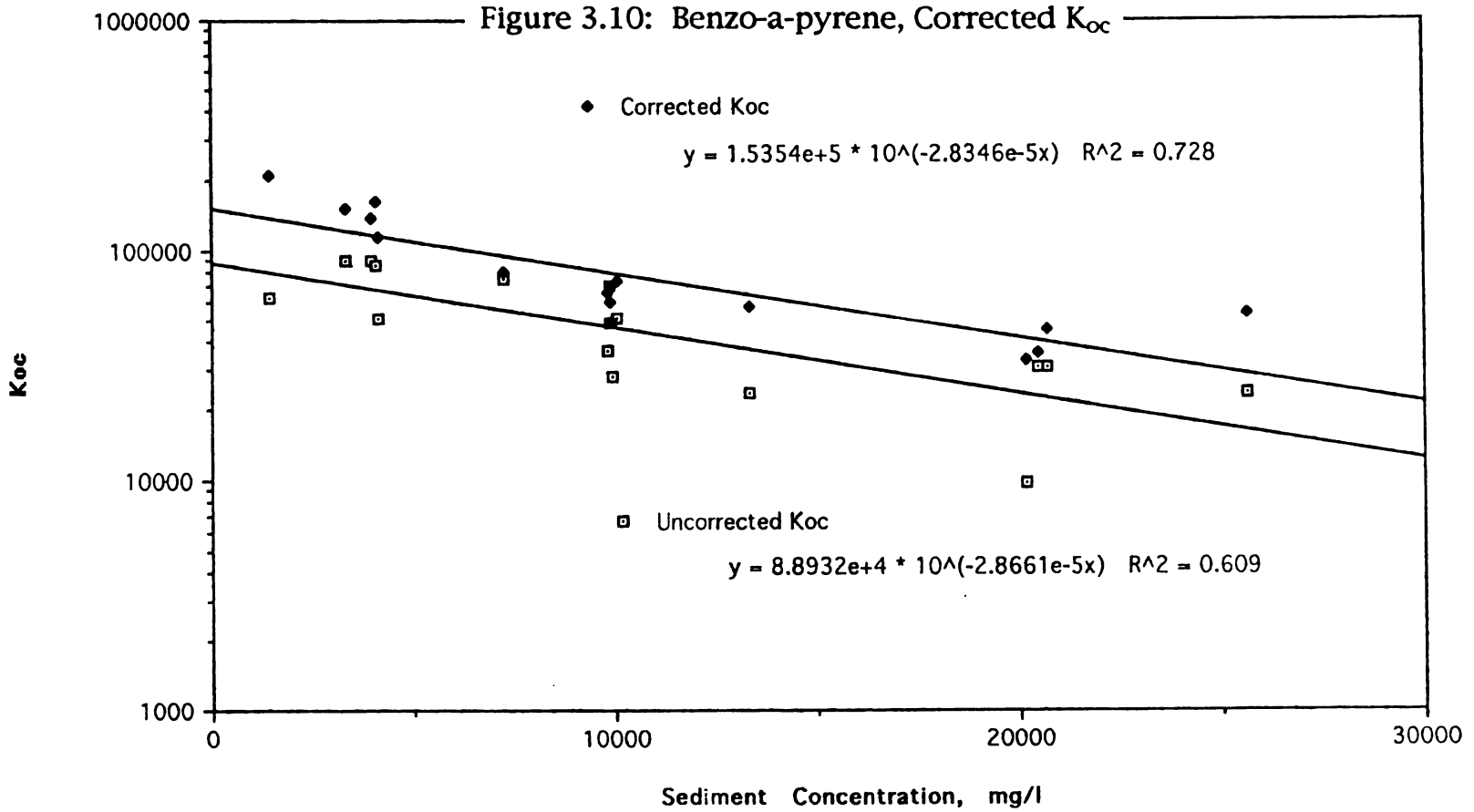

Chapter IV: Modeling Benzo-a-pyrene Sorption to Lake Michigan Sediments by the Solute Complexation Model

4.1 Introduction

The first three chapters of this Thesis have sought to develop the idea that the interaction of HOC's with sediments and dissolved organic matter is not simple. Typical techniques like linear partitioning models and simplified corrections for binding to DOM are not sufficient to describe what is happening when a system of water, solids, and HOC's is mixed. Rigorous analytical technique for experimental data and reasonable models which describe both experimental and natural observations under simplifying assumptions are necessary to evaluate some of the observations which were described in chapters one through three.

For HOC's, the primary process which controls the distribution within environmental systems is absorption to soils and sediments. Consequently, models which describe the fate and transport of HOC's rely on experimental techniques to provide sorption data which can be extrapolated to environmental systems. The variation in partitioning data which is obtained by using constant and varying solid isotherm techniques is currently of interest in its relationship to actual environmental partitioning. The concept of a heterogeneous solute was developed by Voice to explain these observations. This model is applied to the benzo-a-pyrene data obtained in this study.

4.2 Results and Discussion:

4.2.1 Model Calibration

A model was developed by Voice, 1985, to describe three phase partitioning of HOC's between solid, aqueous free and aqueous bound sinks. The model conceptualizes a phase transfer of HOC binding material from organic solids and a distribution of the aqueous phase between "free" and "bound" constituents. A schematic of the model system is shown in Figure 4.1. Concentrations of HOC's within each compartment can be predicted by using equilibrium partitioning coefficients.

The aqueous HOC species within Voice's model are defined by a partition coefficient between the dissolved organic carbon (DOC) and water. Each constituent in the liquid phase is in turn distributed to the solid phase by distinct partition coefficients, K1 and K2. The overall partition coefficient or apparent Kp determined experimentally is then defined as:

$$Kp = (Csf + Csb)/(Cwf + Cwb)$$

Where,

Csf = mass fraction of free compound in solid

Csb = mass fraction of bound compound in solid

Cwf = mass fraction of free compound in solution

Cwb = mass fraction of bound compound in solution

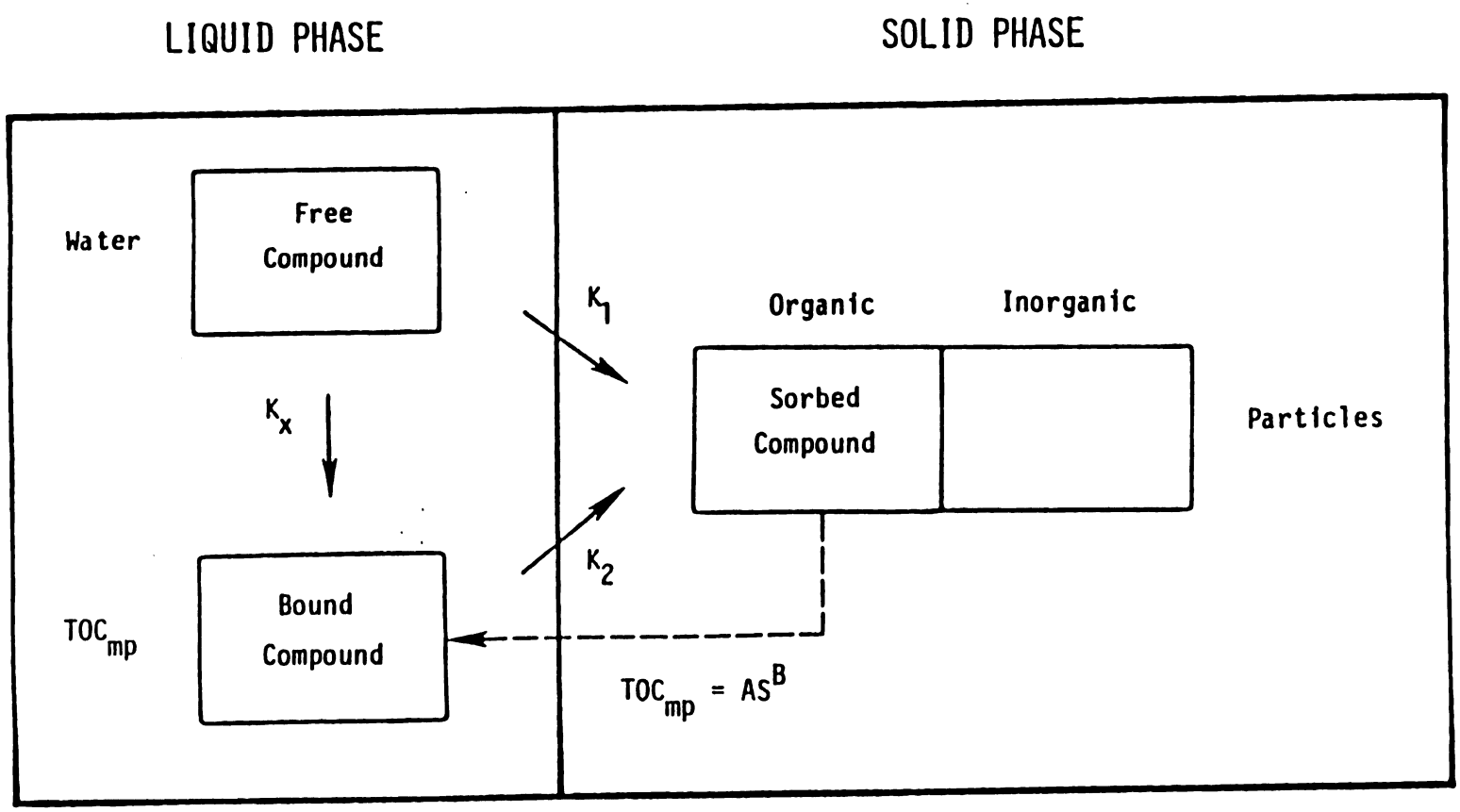

4.1 Schematic of Solute Complexation Model

Although Voice did not propose a distinction between Csf and Csb, we have developed it in this way since K_1 and K_2 are equilibrium coefficients and as such define two separate and distinct compartments. Voice proposed that the observed decrease in the partitioning coefficient with changes in solids concentration be attributed to transfer of a sorbing, or solute binding material from the solid to the liquid phases. The amount of the binding material released to solution would increase with increasing solids, resulting in values of Koc which decrease as a logarithmic function of solids concentration. In order to evaluate the amount of a contaminant at equilibrium within each phase, the solid phase partitioning coefficient as well as the free/bound distribution within the aqueous phase must be measured.

The solute complexation approach also incorporates solute heterogeneity in its development by allowing for different equilibrium sorption coefficients for the "bound" and "free" phase in solution. Figure 4.2, adapted from Voice, shows a hypothetical chart indicating the effect of the isotherm procedure on observed partitioning for a heterogeneous solute. The curves represent a system with two compounds having partition coefficients of 10^4 and 10^2. Each initially comprises 50 % of the mixture. The curves are developed assuming both the constant and varying solids experimental techniques. As can be seen, the varying procedures result in different isotherms. The constant sediment isotherm is linear while the constant concentration isotherm is non-linear even on the log-log plot. Voice 1983, experimented with humic and fulvic

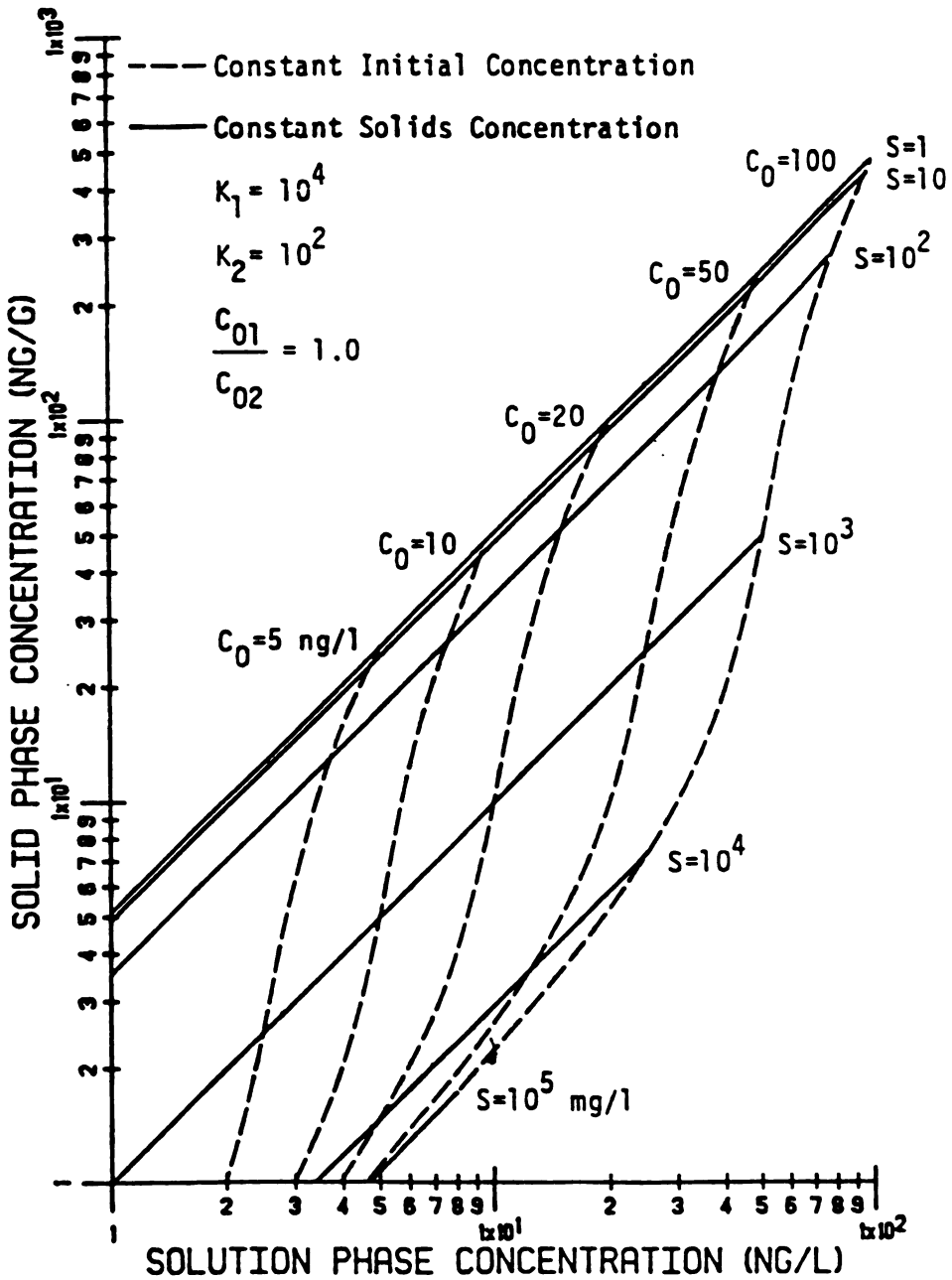

Figure 4.2: Effect of Isotherm Procedure for Heterogeneous Solute

acid sorption to activated carbon and showed data trends similar to the hypothesized heterogeneous solute curves. He interpreted the results as examples of heterogeneous solute sorption.

The equations developed by Voice for the solute complexation model were used to analyze the data obtained for benzo-a-pyrene. The idea was to describe the partition coefficient in terms of the solid concentration and three distribution coefficients. K_p, the apparent partitioning coefficient, was evaluated by the following expression:

$$K_p = \frac{1/(S + 1/K_1) + K_x*TOC/(S + 1/K_2)}{1/(K_1*S + 1) + K_x*TOC/(K_2*S + 1)}$$

Where S = solids concentration in kg/l

K_1, K_2, K_x = unitless partitioning coefficients

TOC = total organic carbon in kg/l

Under the proposed modeling scheme, K_1 represents the solid phase partition coefficient of the "free" contaminant; whereas, K_2 represents the solid phase partition coefficient of the "bound" contaminant. The coefficients K_1 and K_2 represent partitioning at equilibrium. By definition, however, K_x, is the initial distribution of the free and bound contaminant in the aqueous phase. K_x is not, therefore, defined by K_{doc}.

Voice presented a sensitivity analysis which demonstrated the effects that each distribution coefficient had on K_p, the observed overall partition coefficient. As indicated in Figures 4.3, 4.4, and 4.5,

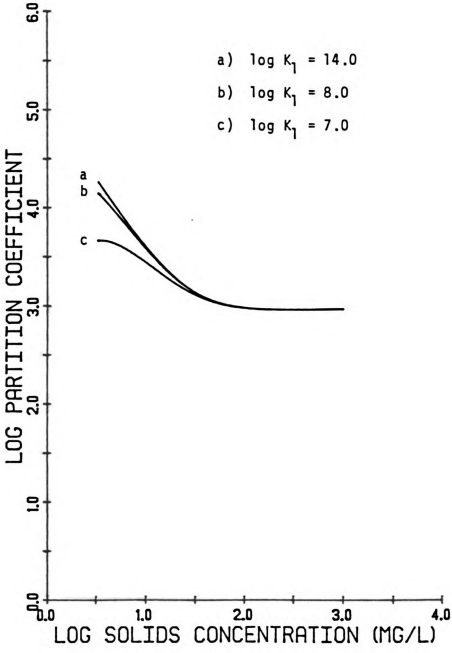

Figure 4.3: Sensitivity of Solute Complexation Model to K1

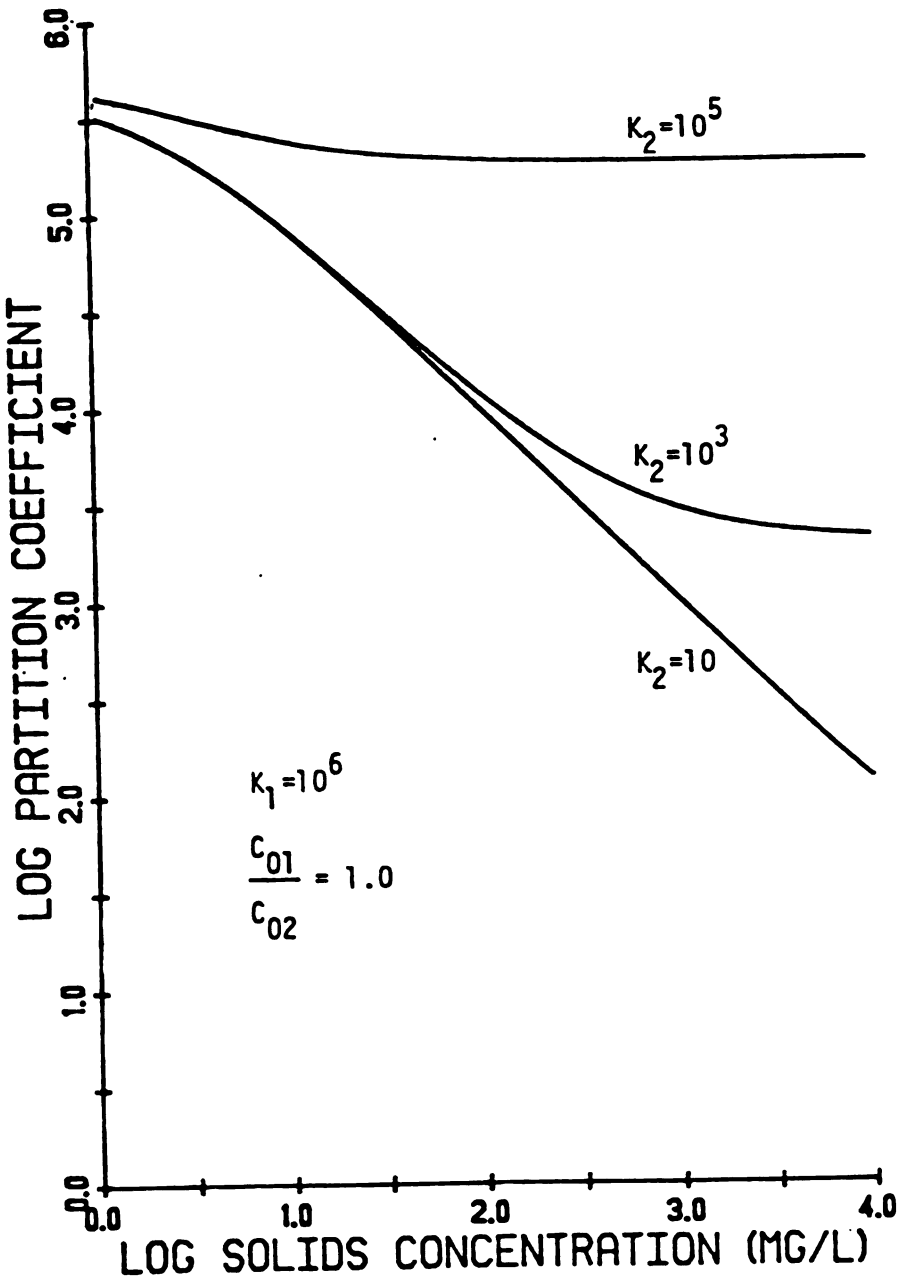

Figure 4.4: Sensitivity of Solute Complexation Model to K2

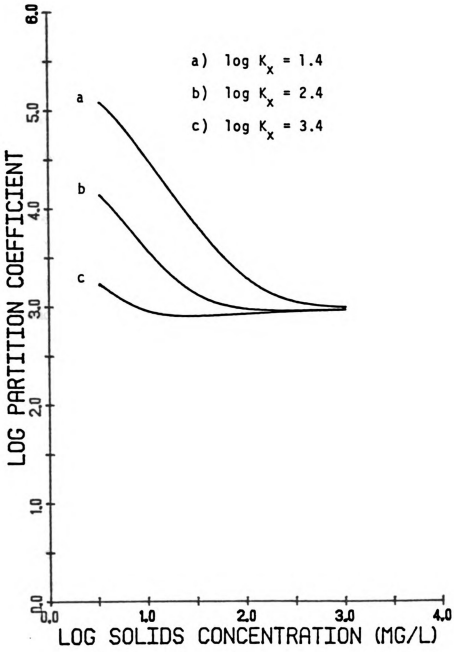

Figure 4.5: Sensitivity of Solute Complexation Model to K_x

increasing K_x decreased the apparent partition coefficient at low solids concentration, whereas increases in K_2 increased the apparent coefficient at high solids concentration. Additionally, increases in K_1 also increased the partition coefficient at low solids concentration, however, it was not as sensitive as the other parameters, K_1 and K_2.

The first step in our procedure was to model the observed data using the equations developed by Voice. Accordingly, values of K_x, K_1, and K_2 were chosen and altered to see whether the model could be calibrated to predict results which were obtained for benzo-a-pyrene. The model and experimentally determined K_p values are plotted vs. solids concentration in Figure 4.6. The values which were chosen for each coefficient are as follows:

$$K_x = 1.61 \times 10^4$$

$$K_1 = 2.51 \times 10^6$$

$$K_2 = 1.35 \times 10^4$$

As indicated, the model can be calibrated for the results obtained using benzo-a-pyrene over the experimental range of solid concentrations.

Figure 4.7 shows the experimental data overlain on the model data obtained using the terms for C_{sb}, C_{wf}, C_{wb}, and C_{wf} which

Figure 4.6: Model and Experimental K_{oc} Data, Benzo-a-pyrene

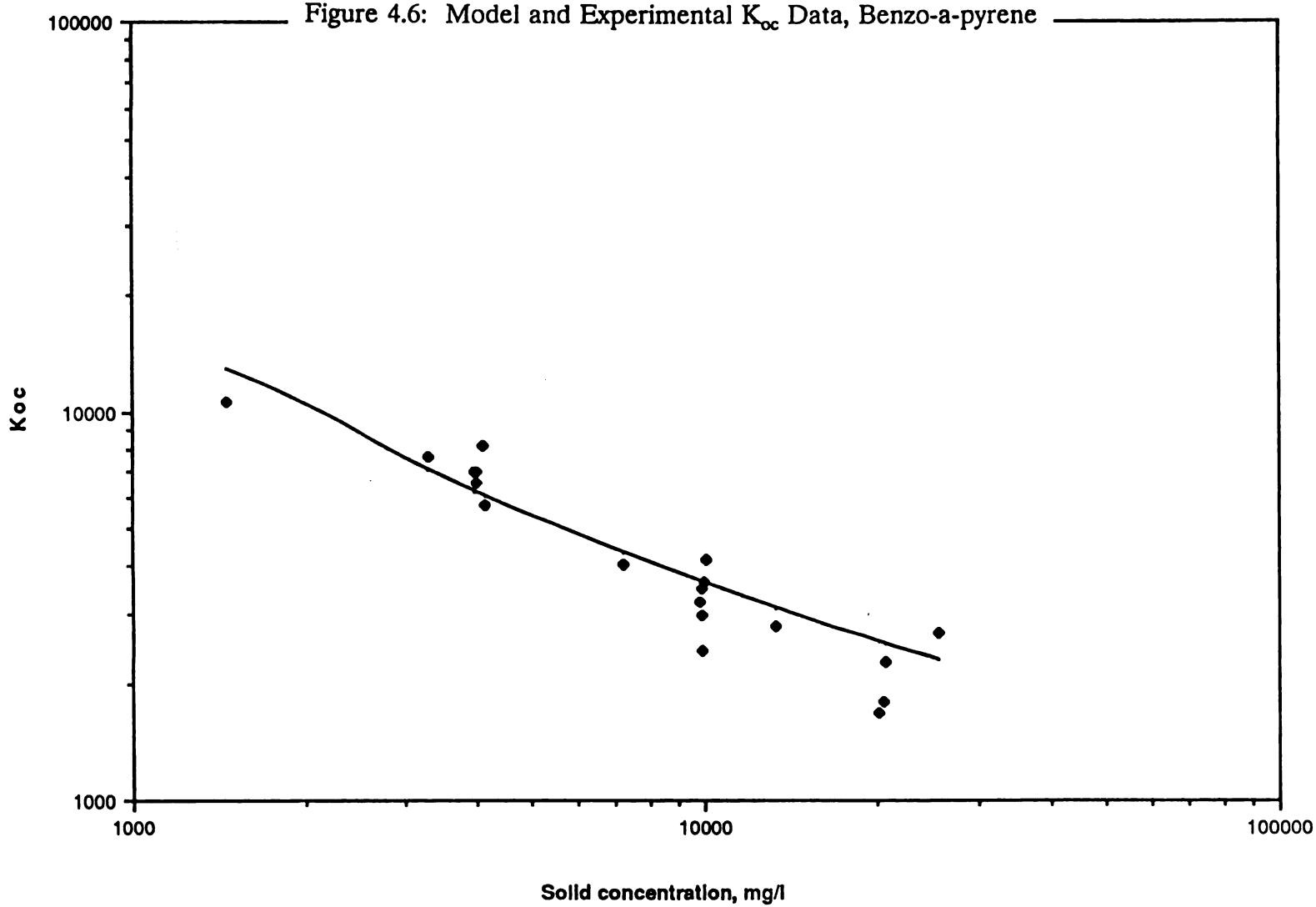

Figure 4.6: Model and Experimental K_{oc} Data, Benzo-a-pyrene

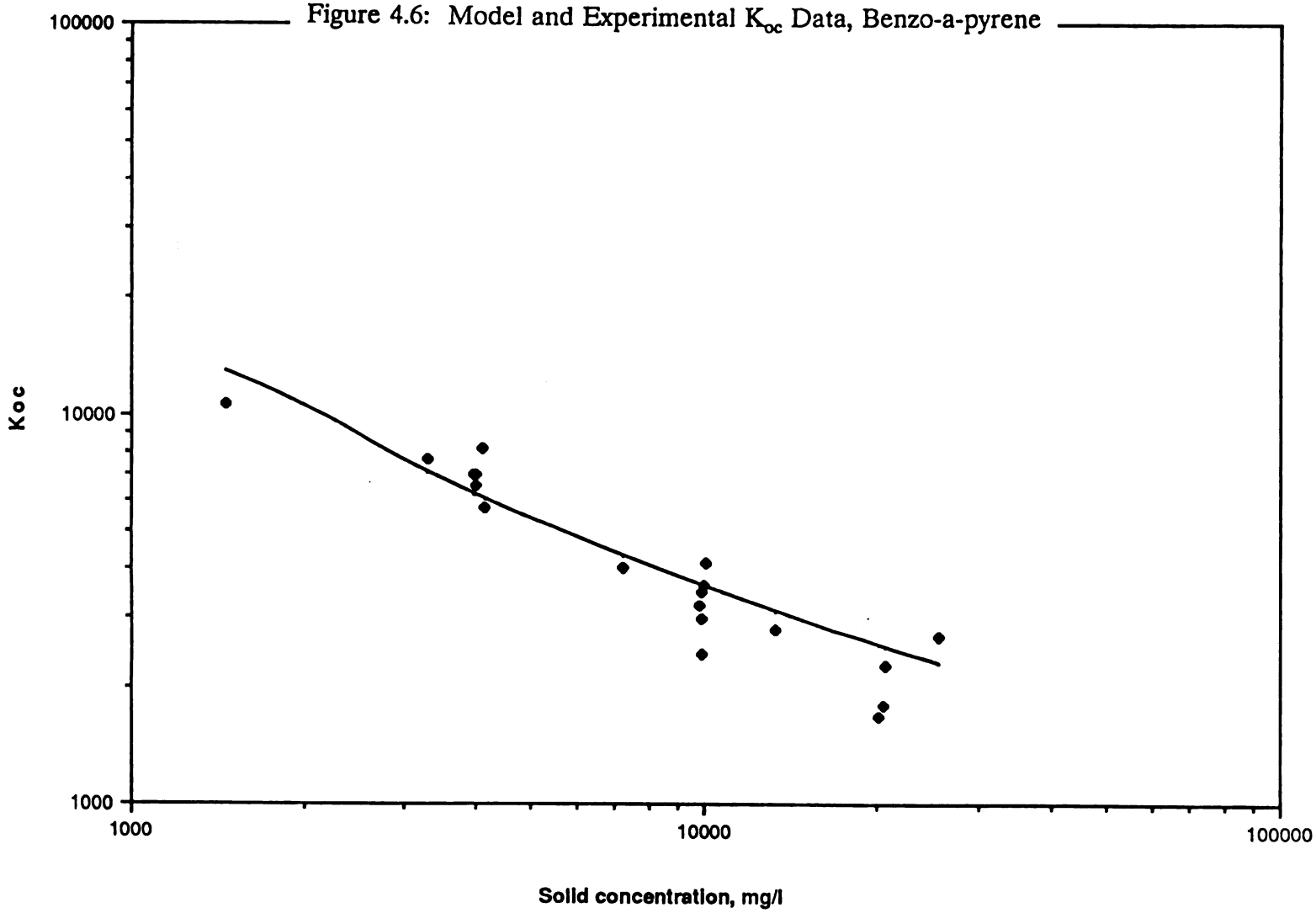

Figure 4.7: Benzo-a-pyrene Sorption Isotherm, Model and Experimental Data

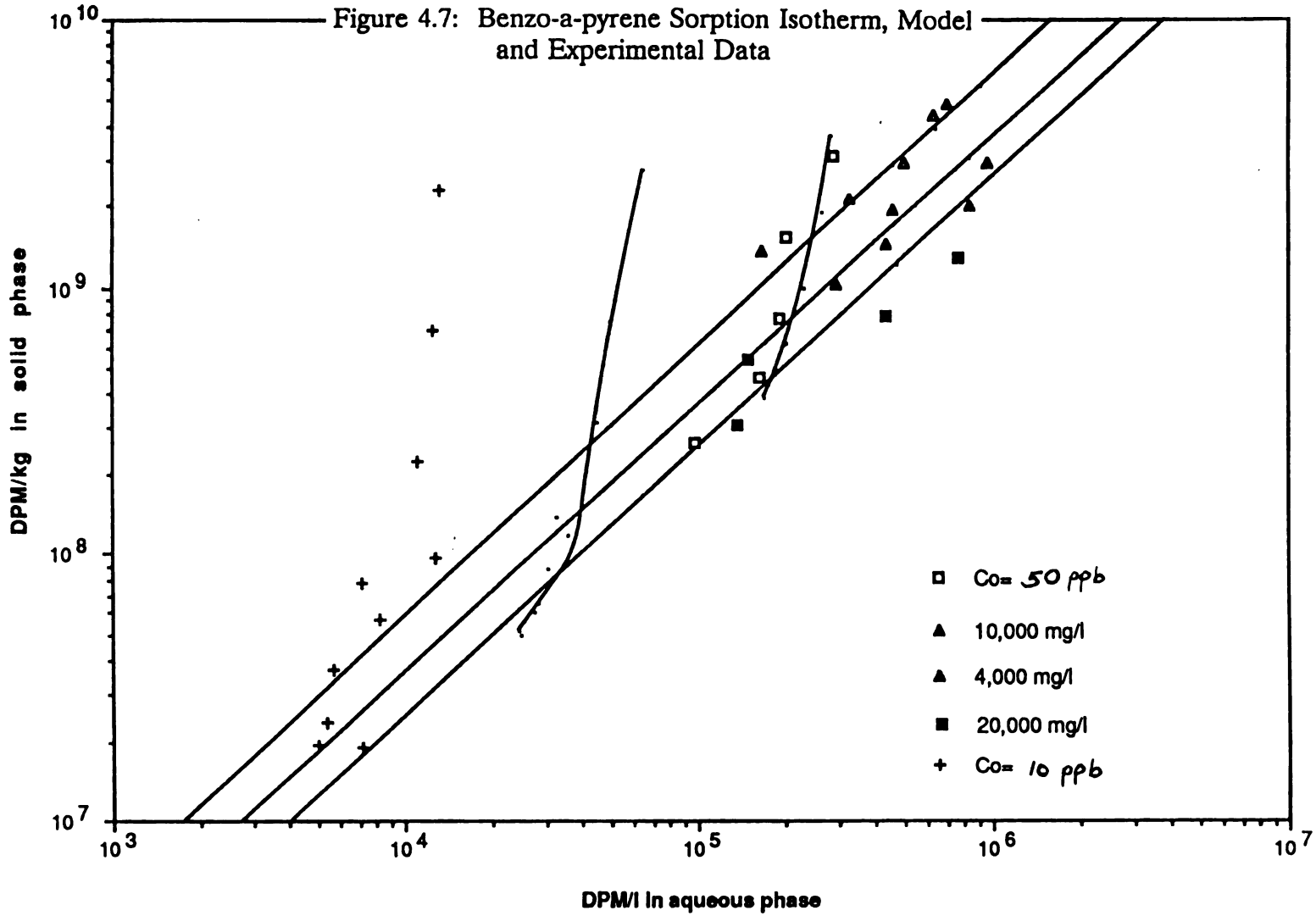

Figure 4.7: Benzo-a-pyrene Sorption Isotherm, Model and Experimental Data

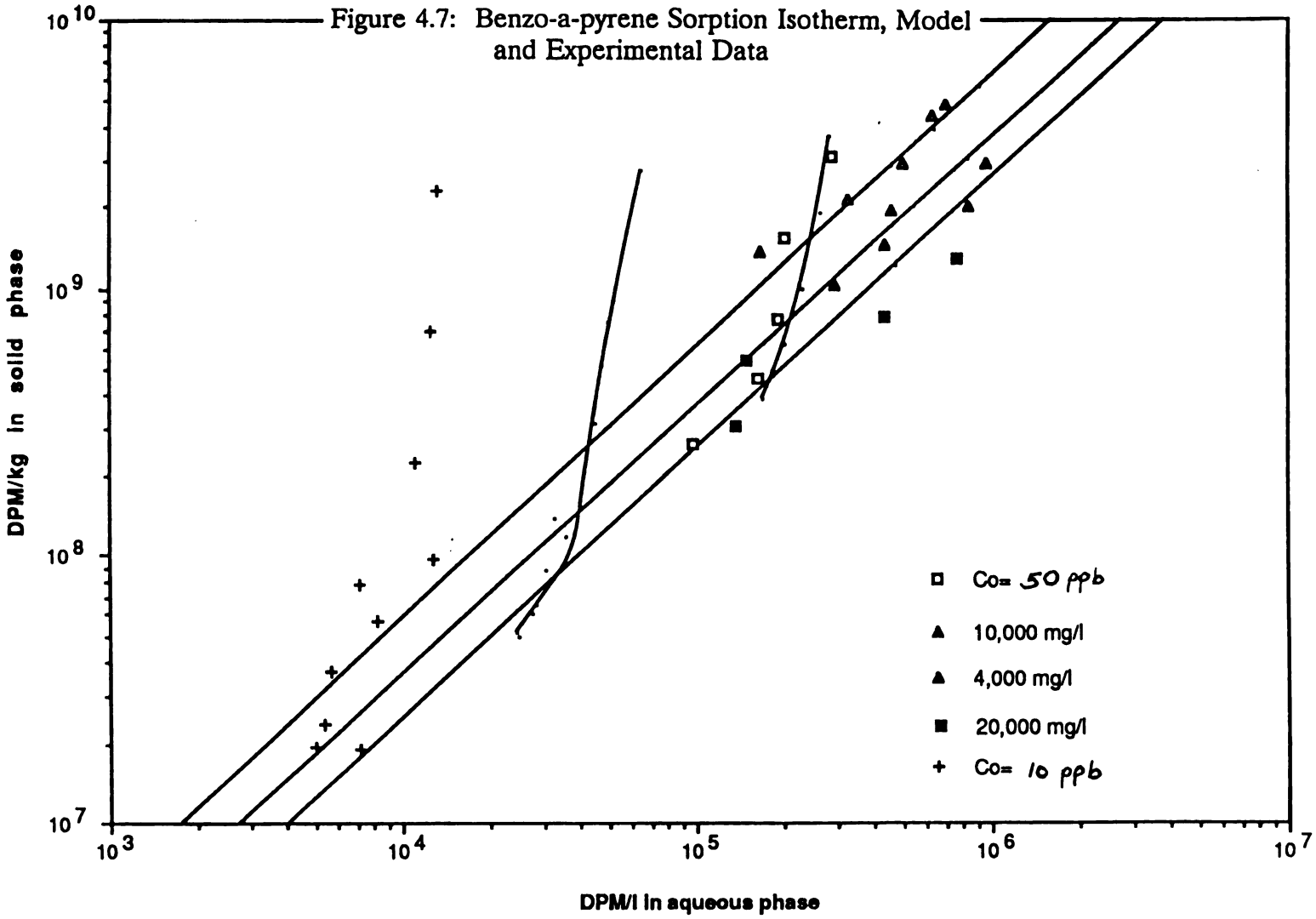

represent each term in the K_p equation. The values figure 4.7 were calculated from the following equations:

$$C_o = C_{wf} + C_{wb}$$

$$C_{wb} = K_x * C_{wf}$$

Substituting, $$C_{wf} = C_o/(1 + K_x)$$

$$C_{sf} = K_2 * C_o/(1 + K_x)$$

$$C_{wb} = K_x * C_o/[S * (1 + K_x)]$$

$$C_{sb} = K_1 * K_x * C_o/[S * (1 + K_x)]$$

The graph is a plot of (C_{sf} +C_{sb}) vs (C_{wf} + C_{wb}) showing both variable and constant solid isotherm data. As shown, the experimental results are reasonably described by the model equations over the solids range and initial concentration values used in our experiment. Deviations at low solid concentrations may be the result of estimates for organic carbon transfer from the solid phase and the difficulty in fully separating particulate material from solution.

Since the value of K_x used in Voice's model does not correspond to the equilibrium K_{doc}, the model values for C_{free} and C_{bound} were evaluated using each term in the numerator of the K_p equation with the intent of ultimately identifying how the model predicts equilibrium K_{doc}. The results are graphed in Figure 4.8. As indicated, the model predicts that the amount of bound compound will decrease only slightly over the experimental range of solid

Figure 4.8: Model Free and Bound Concentration, Benzo-a-pyrene

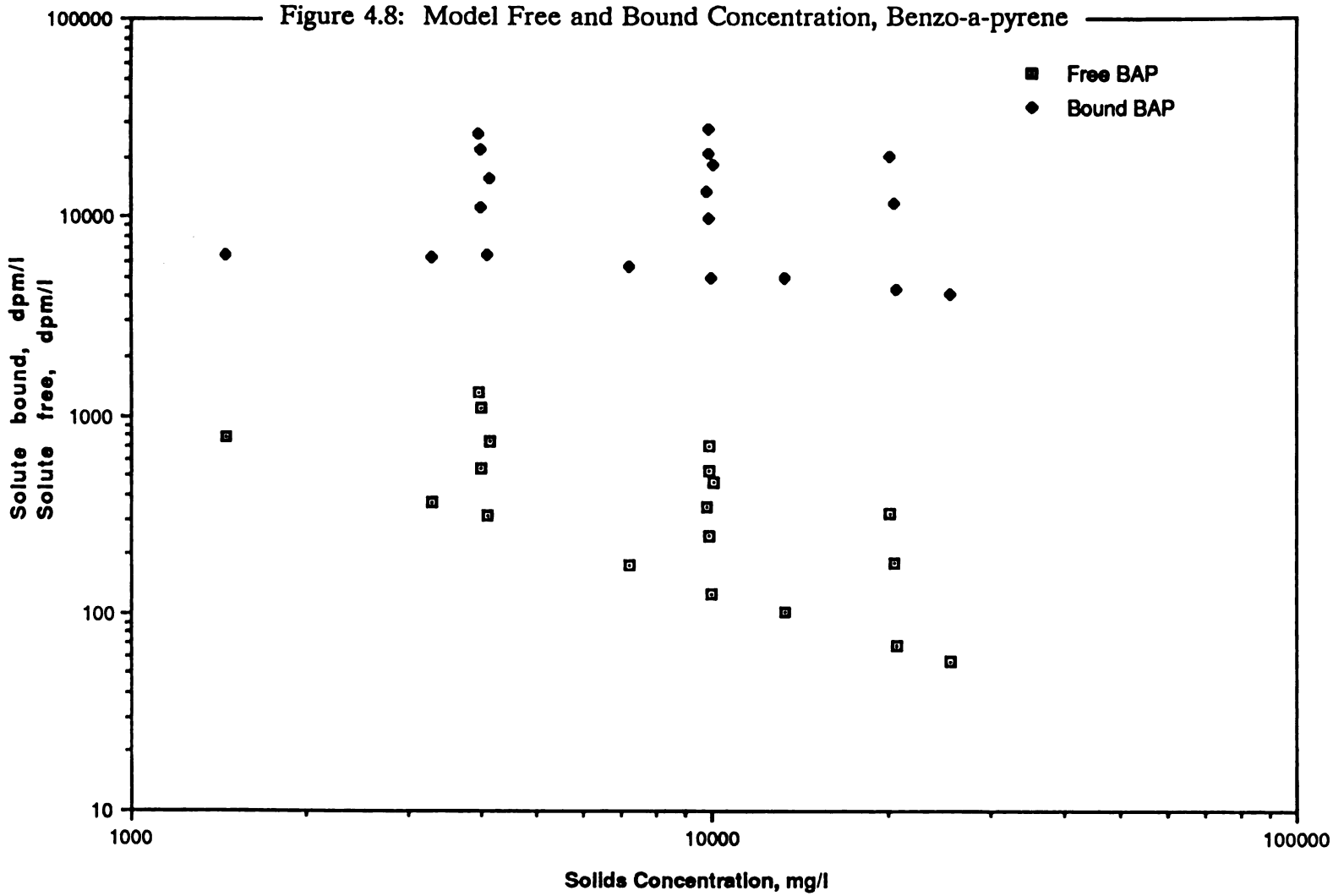

concentrations. The solution phase of the free compound however, decreases significantly over the solids range. Also seen on the curve are the points which form a vertical line above a constant solid value. These are the varying solute/constant solid model predicted points.

From these results the K_{doc} value which is "hidden" within the model can be determined. Figure 4.9 shows that the model predicts an increasing distribution of HOC in the bound form with increasing solid concentration. This observation suggests that the binding constant of solution phase HOC to dissolved organic mater increases with increasing solid concentration. It appears from a log-log plot of the data that the constant is most affected at low solid concentrations and reaches a plateau at high solids concentrations. The results are obviously dependent on chosen values for K_x, K_1 and K_2, however as more data becomes available on solution phase partitioning to DOM, this prediction can be tested.

Model prediction and experimental results for K_{doc} of benzo-a-pyrene are shown in Figure 4.10. The model predicted results are the same as shown in Figure 4.9, and they are shown again in Figure 4.10 so that we can compare them to the experimental data. The experimental results were obtained from the fluorescence quenching and reverse phase techniques. The model predicts K_{doc} results which are generally higher than the experimental data.

Figure 4.9: Model K_{doc}, Benzo-a-pyrene

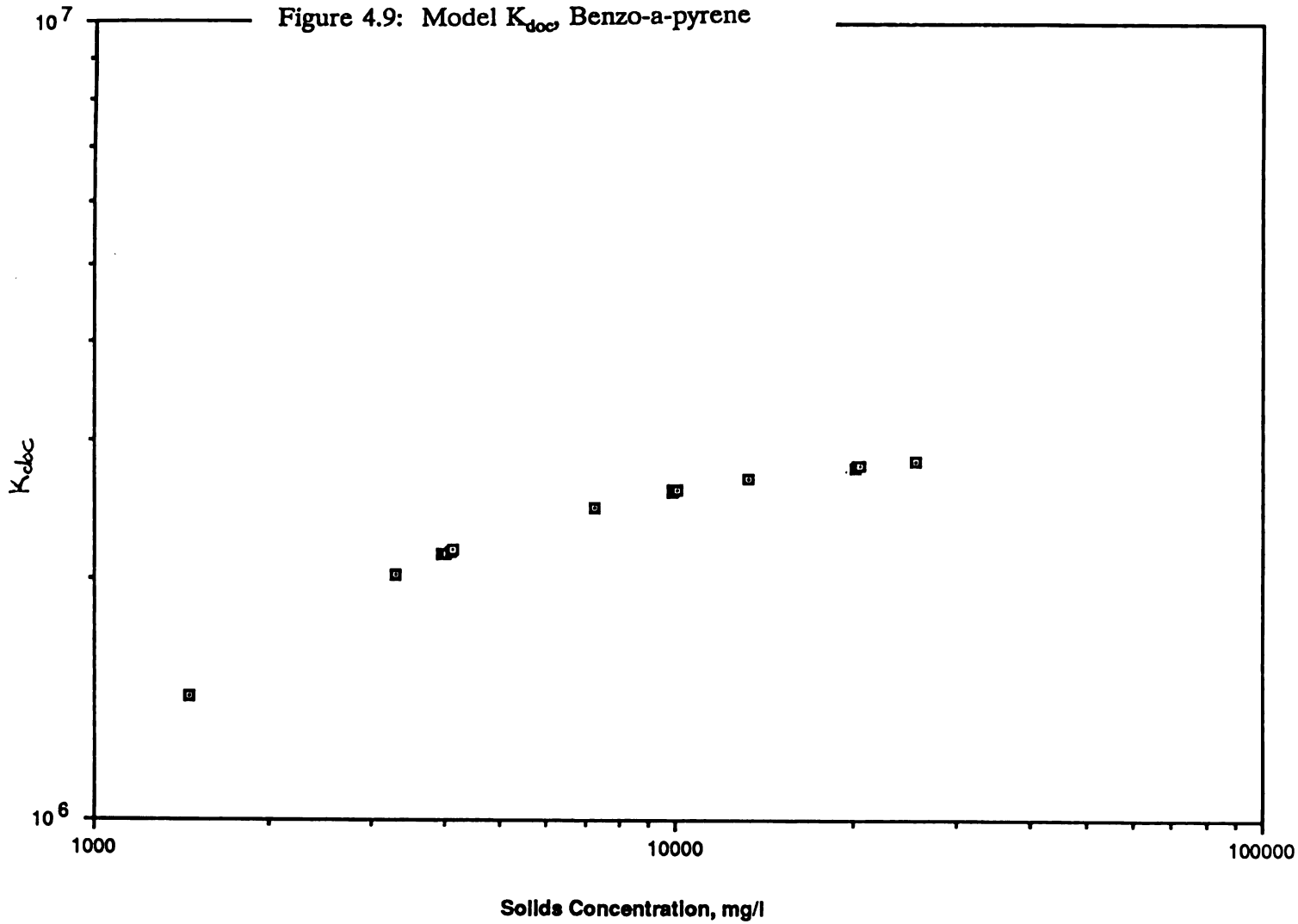

Figure 4.10: Model and Experimental K_{doc}, Benzo-a-pyrene

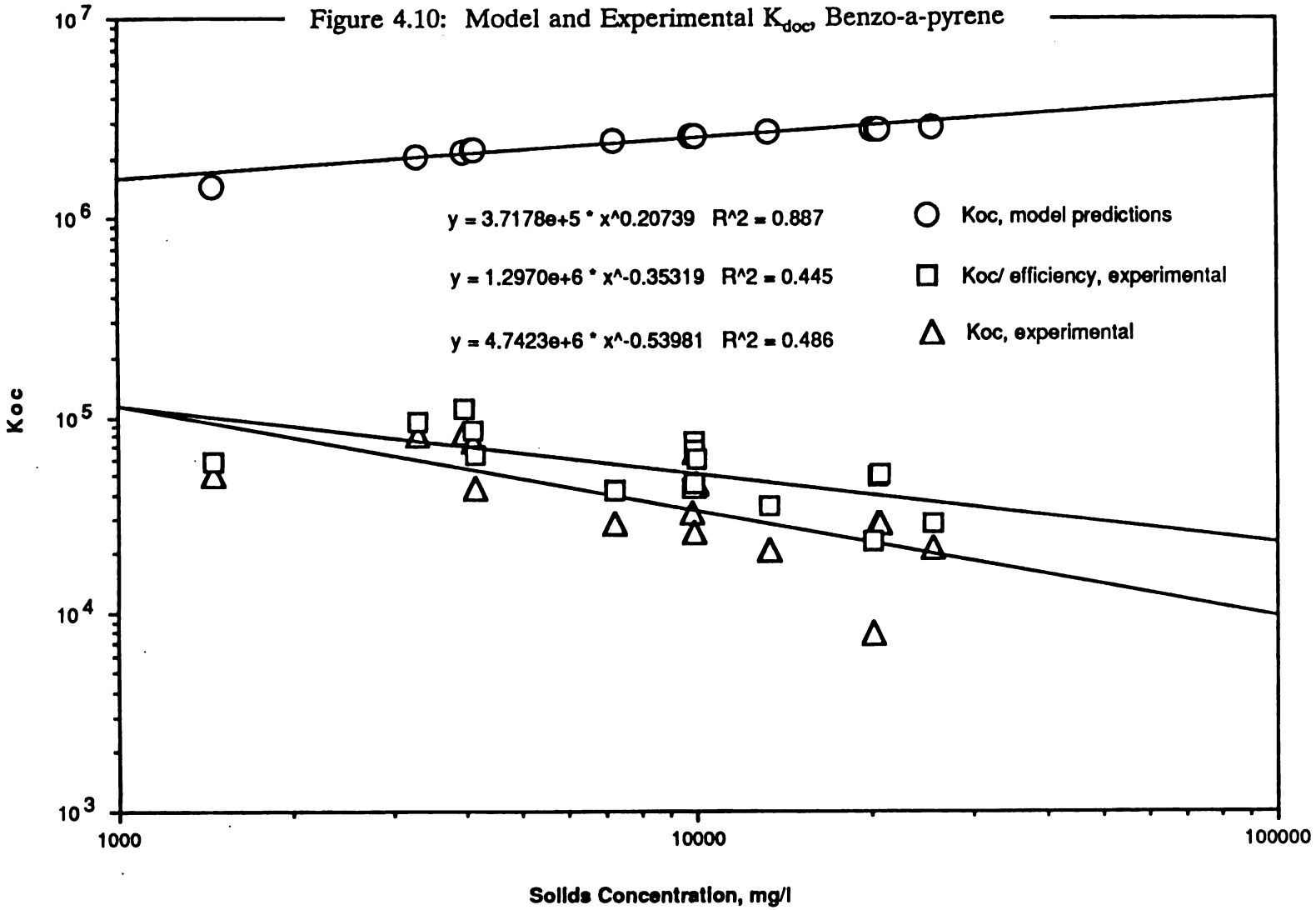

4.2.2 Non-Linear Parameter Estimation

The final procedure in modeling the benzo-a-pyrene data was to develop an expression for observed K_p which eliminated the non-equilibrium K_x present in Voice's model and allowed a regression to estimate K_1 and K_2. In order to accomplish this, the equation was intended to be written in terms of the C_{free} which was determined experimentally in our system. The expression for K_p is then:

$$K_p = (C_{free}*K_1 + C_{free}*K_{doc}*DOC*K_2)/(C_{free} + C_{free}*K_{doc}*DOC)$$

Where: C_{free} = "free" benzo-a-pyrene in solution

K_{doc} = aqueous distribution coefficient

DOC = dissolved organic carbon

K_1, K_2= model parameters

This expression describes the same sink model which was developed by Voice, however, it is written in terms of the experimentally determined C_{free} value.

The equation for K_p was then applied to the SYSTAT Non-linear Parameter Estimation technique to determine K_1 and K_2. The residuals and regression information are included in Appendix V. K_1 and K_2 were determined to be:

$$K_1 = 5.9 \times 10^3$$

$$K_2 = 3.6 \times 10^3$$

Using the K_1 and K_2 estimations, the values for K_{oc} at each C_{free} measurement were then calculated with the intent of showing how model predicted K_{oc} values varied with solid concentration. Experimental and calculated K_{oc} values are shown in Figure 4.11 as a function of solid concentration. The experimental values are shown as graph points and the model values are shown as a line. As can be seen, the heterogeneous solute model with the modification for the C_{free} term does not describe a decrease in K_{oc} which approximates that which is observed experimentally. The presence of the non-equilibrium K_x value in Voice's model appears to make a significant contribution in describing the observed data. The additional degree of freedom provided by the term K_x allows the data to be fit better.

Figure 4.11: Model and Experimental K_{oc}, Benzo-a-pyrene

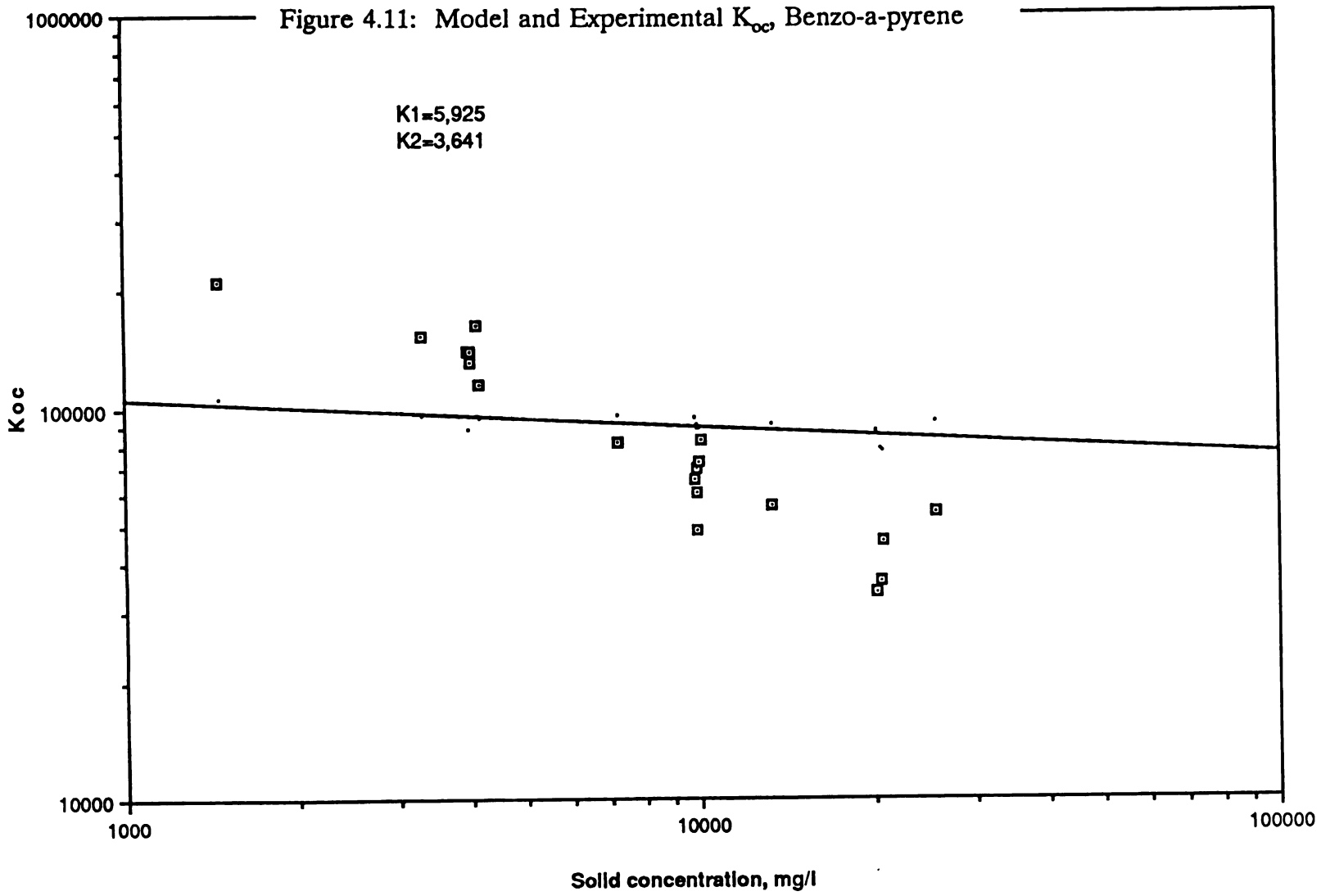

Conclusions

An understanding of the distribution of PAH compounds in sediment/water systems is a complex process. Laboratory sorptionstudies provide at best only a partial view of actual field phenomena. Interpretations of experimental results are obscured by inefficient compound recovery procedures, operational definitions for "free" and "bound" contaminant, and limits in defining particulate as opposed to freely dissolved organic material.

Within this study, an attempt was made to evaluate sediment sorption of four PAH compounds exhibiting a range of hydrophobicities. We found that apparent K_{oc} values determined by a varying solid sorption technique showed a dependence on solid concentration. The observed value of apparent K_{oc} decreased with increasing solid concentration. Generally, this dependence appeared to increase for increasing compound hydrophobicity. A similar effect is noted in field data from a study undertaken within the Grand Calumet River (Hoke and Giesy 1992), however, the evaluation was based on f_{oc} as opposed to solid concentration.

An approach to adjust the apparent K_{oc} by subtracting the amount of "bound" compound from the aqueous phase did not correct for the solid dependence observed in the phenanthrene and benzo-a-pyrene data. This procedure was completed using values of "free" compound which were determined by the fluorescence quenching and reverse phase techniques.

The varying solid and constant solid isotherm techniques for benzo-a-pyrene produced a series of curves which are similar to those produced for heterogeneous solute partitioning (Voice, 1984). Model data obtained using the solute complexation model developed by Voice 1985, was capable of describing the experimental data. When we introduced a term for C_{free} into the solute complexation model equations and applied a non-linear parameter estimation for the coefficients K_1 and K_2, however, the model failed to adequately describe the data. This observation suggests that either the non-equilibrium distribution coefficient which is incorporated in the derivation of Voice's model is a significant factor in the ability of the model to describe heterogeneous solute partitioning, or that experimentally determined values of "free" compound were not capable of calibrating the model to the observed solid phase partitioning data for benzo-a-pyrene.

Future Research

In terms of experimental techniques, future research to provide a more rigorous separation of particulate and aqueous dissolved organic material should continue. Additionally, techniques which are intended to estimate the "free" and "bound" contaminant in the aqueous phase should continue to be refined. Typically, these techniques provide operational definitions which need to be evaluated in order to define their limitations and applicability to different compounds and different sorbents.

With respect to modeling, many approaches and hypothesis have been suggested by different researchers. Our research used the solute complexation model to evaluate experimental partitioning data. Other models are available, however, and the applicability of these models needs to be evaluated.

Although the solute complexation model could be calibrated to the experimental sorption data for benzo-a-pyrene, it is not known how closely model data predict similar environmental systems. The variation in observed partitioning with f_{oc} which was apparent in data from the Grand Calumet may be a phenomena parallel to laboratory data. More field studies of this effect should be conducted.

REFERENCE LIST

Aquatic Surface Chemistry, Edited by Werner Stumm, John Wiley and Sons, New York 1987, pg 7-9.

Bertch, P.M., J.M. Novak, (1993), Pyrene sorption by Water Soluble Organic Carbon, Environ. Sci. Technol., 27, 398-402.

Booth P.N., M.A. Jacobson, (1992) Development of Cleanup Standards at Superfund Sites: An Evaluation of Consistency, J. Air Waste Manage. Assoc., 42, 762-766.

Briggs, G.G., (1973), A Simple relation Ship Between soil Sorption of Organic Chemicals and Their Octanol/Water Partition coefficients, Proc. 7th British Insecticide and Fungicide Conf. 11, 475-478.

Carter, C.W., I.H. Suffet, (1982) Binding of DDT to Dissolved Humic Materials, Environ. Sci. Technol., *16*, 735-740.

Chiou, C.T., V.H. Freed, R.L. Kohnert, (1977) Partition Coefficient and Bioaccumulation of Selected Organic Chemicals, Environ. Sci. technol., 11, 475-478.

Chiou, C.T.; P.E. Porter, D.W. Schmeddling, (1983), Partition Equilibria of Non-ionic Organic Compounds Between Soil Organic Matter and Water, Environ. Sci. Technol., 4, 227-230.

Curl, R.L.; G.A. Keolian, (1984) Implicit-Adsorbate Model for Apparent Anomalies with Organic Adsorption on Natural Adsorbents, Environ. Sci. Technol., 18, 916-922.

DiToro, D.M., (1991), Technical Basis for Establishing Sediment Quality Criteria for Nonionic Organic Chemicals Using Equilibrium Partitioning, Environ. Toxicol. Chem 10, 1541-1583

DiToro, D.M., J.D. mahoney, P.R. Kirchgraber, A.L. O'Byrne, L.R. Pasquale, D.C. Piccinilil, (1986) Effects of Non-reversibility, Partcle concentration, Ionic Strength on Heavy Metal Sorption, Environ. Sci. Technol., 20, 55-61.

Eadie, B.J. (1990), Three-phase Partitioning of Hydrophobic Organic Compounds In Great Lakes Waters, Chemosphere, ***20*** Nos 1-2 pp 161-178.

Gauthier, T.D., E.C. Shane, W.F. Guerin, W.R. Seitz, C.L. Grant (1987), Fluorescence Quenching Method for Determining Equilibrium Constants for PAH Binding to Dissolved Humic Materials, Environ. Sci Technol. ***20***, 1162-1166

Gschwend P.M., D.A. Backhus, (1990) Fluorescent Polycyclic Aromatic Hydrocarbons as Probes for Studying the Impact of Colloids on Pollutant Transport in Groundwater, Environ. Sci. Technol, ***24***, 1214-1223.

Gschwend, P.M. and S. Wu (1985), On the Constancy of Sediment Water Partition coefficients of Hydrophobic Organic Pollutants, Environ. Sci. Technol., ***19***, 90-96.

Handbook of Environmental Data on Organic Chemicals

Hoke, R.A., J.P. Giesy, M.J. Zabik, 1992(Prepublication), A Field Evaluation of Equilibrium Partitioning in the Grand Calumet River, and Indiana Harbor

Karickoff, S.W., D.S. Brown, T.A. Scott, "Sorption of Hydrophobic Pollutants on Natural Seidments", Water Research, ***13***, 1979, pp 241-248

Karickoff, S.W., "Semi-Emperical Estimation of Sorption of Hydrophobic Pollutants on Natural Sediments and Soils, Chemosphere, ***10*** 1981 pp 833-846

Karickoff, S.W., "Sorption Kinetics of Hydrophobic Pollutants in Natural Sediments", Contaminants and Sediments, Vol. 2, Ann Arbor Science Publishers, Inc., Ann Arbor MI, 1980, pp 193-205

Lake, J.L., N.I. rubinstein, H. Lee II, c.A. Lake, J. Heishe, Spavibnano,1990, Equilibrium Partitioning and Bioaccumulation of Sediment associated Contaminants by Infaunal Organisms, Environ. Toxicol. Chem ***9***: 1095-1106

Lambert, S.M., (1967), Functional Relationship Between Sorption in Soil and Chemical Structure, J. Agric. Fd. Chem., 15, 572-576.

Lambert, S.M., (1968), Omega, A Useful Index of Soil Sorption Equilibria, J. Agric. Fd. Chem., 16, 340-343.

Lambert, s.M., (1966) the influence of soil Moisture on Herbicidal Response, Weeds, 14, 273-275.

Landrum, P.F., Giesy, J.P., "Advances in Identification and Analysis of Organic Pollutants in Water", Keith L. H., Ed., Ann Arbor Science: Ann Arbor, MI, 1981, *1*, pp 345-355

Landrum, P.F., S.R. Nihart, B.J. Eadie, W.S. Gardner, 1984, Reverse Phase Seperation Method for Determing Pollutant Binding to Aldrich Humic Acid and Dissolved Organic Carbon of Natural Waters, Environ Sci. Technol, *18*, 187-192

Magee, B.R., L.W. Lion and A.T. Lemley (1991), Transport of Dissolved Organic Macromolecules and Their Effect on Transport of Phenanthrene in Porous Media, Environ. Sci. Technol., *25*, 323-331.

McCarthy, J.F., (1983), Role of Particulate Organic Matter in Decreasing Accumulation of Polynuclear Aromatic Hydrocarbons by Daphnia magna, Arch. Environ. Contam. Toxicol. *12*, 559-568 (1983).

McCarthy, J.F., J.M. Zachara, (1989), Subsurface Transport of Contaminants, Environ. Sci. Technol., *23*, 496-502.

McCarthy, J.G., B.D. Jimenez, (1985), Interactions between Polycyclic Aromatic Hydrocarbons and Dissolved Humic Material: Binding and Dissociation, Environ. Sci. Technol., *19*, 1072-1076.

McKay D., A. Bobra, W.Y. shiu, Relationships Between Aqueous Solubility and Octanol-Water Partitioning Coefficients, Chemosphere, *9* 1980 pp 701-711

Means, J.C., S.G. Wood, J.J. Hassett, W.L. Banwart, (1980), Sorption of Polynuclear Aromatic Hydrocarbons by Sediments and Soils, Environ. Sci. Technol., *14*, 1524-1528.

Morra, M. J.; M.O. Corapcioglu, P.M.A. von Wandruska, D.B. marshall, and K. Topper, (1990), Fluorescence Quenching and Polarization Studies of Naphthalene and 1 Napthol Interaction with Humic Acid, Soil. Sci. Soc. Am. J., 54, 1283-1288.

Murphy, E.M., J.M. Zachara, S.C. Smith, 1990, Influence of Mineral Bound Humic Substances on the Sorption of Hydrophobic Organic Compounds, Environ. Sci. Technol., ***24***, 1507-1516

O'Connor D.J. and J.P. Connolly, 1980, The effect of concentration of Absorbing Solids on the Partition Coefficient, Water Resources ***14***, 1517-1523.

Slautman, M., Mineral Surfaces and Humic Substances: Partitioning of Hydrophobic Organic Pollutants, PhD Thesis, 1992

Standards in Fluorescence Spectroscopy, 1981, J.N. Miller, Chapman Hall, New York

Standards Methods for The Analysis of Water and Wastewater, (1990)

Swarzenbach, R.P., J. Westall, Transport of Nonpolar Organic Compounds from Surface Water to Groundwater, Laboratory Sorption Studies, Environ. Sci. Technol., 15, # 11, 1360 - 1367.

Voice, T.C., C.P. Rice and W.J. Weber Jr. (1983), Effect of Solids Concentration on the Sorptive Partitioning of Hydrophobic Pollutants in Aquatic Systems, Environ. Sci. Technol., ***12***, 513-518.

Voice, T.C., W.J. Weber, Jr., (1985), Sorbent Concentration Effects in Liquid/Solid Partitioning, Environ. Sci. Technol., ***19***, 789-796.

Weber, W.J. Jr., T.C. Voice, A. Jodellah, (1983), Adsorption of Humic Substances: The Effects of Heterogeneity and System Characteristics, J.AWWA, Dec., 612-619.

APPENDICIES

APPENDIX A: Fluorescence Quenching

Appendix I: Fluorescence Quenching Stern-Volmer Equation and Correction Coefficient

Stern-Volmer Equation

$$PAH + DOM = [PAH\text{-}DOM]_{complex}$$

Defining, Fo = Fluorescence in absence of quencher
F = Fluorescence in presence of quencher

$$K_{doc} = [PAH\text{-}DOM]_{complex}/\{[PAH]*[DOM]\}$$

and assuming $[PAH]_{total}/[PAH]_{free} = Fo/F$

Mass balance on the PAH, $[PAH]_{total} = [PAH]_{free} + [PAH]_{bound}$

Dividing by $[PAH]_{free}$,

$$[PAH]_{total}/[PAH]_{free} = 1 + [PAH]_{bound}/[PAH]_{free}*[DOM]/[DOM]$$

$$[PAH]_{total}/[PAH]_{free} = 1 + K_{doc}[DOM]$$

Substituting to obtain the form of the Stern Volmer plot,

$$Fo/F = 1 + K_{doc}[DOM]$$

Correction Coefficient

$Fo = C*F$ $\qquad$ $I = Io*10^{-Ad}$ $\qquad$ Beer Lambert Law

Io = intensity of excitation at sample surface

A = Absorbance per cm pathlength at relative wavelength

d = depth in cm of nominal path length of excitation

If F = c*I

$F = Fo*10^{-Ad}$, $C = Fo/F = 10^{Ad}$

For emmission absorbance, $C=10^{(Ad+A'd')}$

The assumptions for this derivation include the following:

Optical pathlength can be defined

Finite widths of beams is ignored

Reflection is insignificant

Bandwidth of light is infinitely small

Since F is porportional to light absorbed between d1 and d2

$F = Ky(10^{-Ad1}-10^{-Ad2})$

As A approaches 0, F approaches Fo and d1 and d2 are approximated by the first term in series expansion.

$F_o = Ky*2.3*A*(d_2-d_1)$

$C = 2.3*A*(d_2-d_1)/(10^{-Ad1}-10^{-Ad2})$

Benzo-a-pyrene Timed Fluorescence Data

Technique: PE FLTD
Subtechnique: Subtech
Type: SPECTRUM
Sample ID: TIMEBEN1.TMP
Data Type: BINARY
Software ID: FLDM (V2.50)
Analyst:
Created: 00:07:47, 92/03/22
Last Modified: 00:07:47, 92/03/22

Data set 1

X (SEC)	Y (INT)
0	120.029
15	119.957
30	120.124
45	120.294
60	120.399
75	120.322
90	120.269
105	120.317
120	120.164
135	119.962
150	119.974
165	120.082
180	120.198
195	120.306
210	120.241
225	120.092
240	120.001
255	119.988
270	120.112
285	120.28
300	120.287
315	120.029
330	119.802
345	119.875
360	120.005
375	119.962
390	119.852
405	119.792
420	119.766
435	119.893
450	120.095
465	120.034
480	119.884
495	119.924
510	120.054
525	120.09
540	119.962
555	119.92
570	119.983
585	119.884
600	119.879
615	119.91
630	119.813
645	119.834
660	119.892
675	119.982
690	119.97
705	119.813
720	119.752
735	119.669
750	119.676
765	119.671
780	119.671
795	119.792
810	119.839
825	119.745
840	119.611
855	119.713
870	119.851
885	119.794
900	119.732
915	119.784
930	119.804
945	119.829
960	119.85
975	119.766
990	119.72
1005	119.658
1020	119.549
1035	119.516
1050	119.479
1065	119.517
1080	119.628
1095	119.639
1110	119.499
1125	119.272
1140	119.364
1155	119.63
1170	119.431
1185	119.234
1200	119.509

Technique: PE FLTD
Subtechnique: Subtech
Type: SPECTRUM
Sample ID: TIMEBEN1.TMP
Data Type: BINARY
Software ID: FLDM (V2.50)
Analyst:
Created: 00:07:47, 92/03/22
Last Modified: 00:07:47, 92/03/22

Data set 1

X (SEC)	Y (INT)
0	120.028
15	119.957
30	120.124
45	120.294
60	120.399
75	120.322
90	120.268
105	120.317
120	120.154
135	119.962
150	119.974
165	120.082
180	120.198
195	120.306
210	120.241
225	120.092
240	120.001
255	119.988
270	120.112
285	120.28
300	120.287
315	120.028
330	119.802
345	119.875
360	120.005
375	119.962
390	119.852
405	119.792
420	119.766
435	119.893
450	120.095
465	120.034
480	119.884
495	119.924
510	120.054
525	120.09
540	119.962
555	119.92
570	119.943
585	119.884
600	119.879
615	119.91
630	119.813
645	119.834
660	119.892
675	119.942
690	119.97
705	119.813
720	119.752
735	119.669
750	119.676
765	119.871
780	119.871
795	119.792
810	119.839
825	119.745
840	119.611
855	119.713
870	119.851
885	119.794
900	119.732
915	119.784
930	119.804
945	119.829
960	119.85
975	119.766
990	119.72
1005	119.658
1020	119.549
1035	119.516
1050	119.479
1065	119.517
1080	119.628
1095	119.639
1110	119.499
1125	119.272
1140	119.364
1155	119.63
1170	119.431
1185	119.234
1200	119.509

Technique: PE FLTD
Subtechnique: Subtech
Type: SPECTRUM
Sample ID: TIMEBEN2.TMP
Data Type: BINARY
Software ID: FLDM (V2.50)
Analyst:
Created: 00:40:18, 92/03/22
Last Modified: 00:40:18, 92/03/22

TIMEBEN2.WK1

Data set 1

X (SEC)	Y (INT)
0	196.067
15	195.218
30	194.536
45	194.384
60	194.278
75	194.663
90	195.278
105	195.605
120	195.818
135	196.033
150	195.656
165	194.727
180	194.154
195	194.208
210	193.970
225	193.647
240	193.856
255	193.678
270	192.882
285	192.298
300	192.208
315	192.488
330	192.528
345	192.331
360	192.39
375	192.437
390	192.363
405	192.326
420	192.555
435	192.999
450	193.199
465	193.135
480	193.14
495	193.211
510	193.215
525	193.199
540	193.281
555	193.349
570	193.13
585	192.635
600	192.583
615	192.391
630	192.269
645	192.122
660	192.049
675	191.953
690	191.799
705	191.732
720	191.393
735	191.113
750	190.984
765	190.679
780	190.431
795	190.396
810	190.313
825	190.096
840	190.191
855	190.556
870	190.492
885	190.195
900	190.239
915	190.532
930	190.57
945	190.228
960	189.992
975	189.931
990	190.001
1005	189.954
1020	189.647
1035	189.654
1050	189.907
1065	189.911
1080	189.595
1095	189.285
1110	189.514
1125	189.837
1140	189.58
1155	189.269
1170	189.356
1185	189.502
1200	189.426

Technique: PE FLTD
Subtechnique: Subtech
Type: SPECTRUM
Sample ID: TIMEBEN2.TMP
Data Type: BINARY
Software ID: FLDM (V2.50)
Analyst:
Created: 00:40:10, 92/03/22
Last Modified: 00:40:10, 92/03/22

Data set 1

X (SEC)	Y (µNT)
0	196.067
15	195.218
30	194.538
45	194.384
60	194.278
75	194.663
90	195.278
105	195.605
120	195.816
135	196.033
150	195.656
165	194.727
180	194.154
195	194.208
210	193.979
225	193.647
240	193.856
255	193.678
270	192.882
285	192.298
300	192.208
315	192.488
330	192.528
345	192.331
360	192.30
375	192.437
390	192.363
405	192.326
420	192.555
435	192.999
450	193.199
465	193.135
480	193.14
495	193.211
510	193.215
525	193.199
540	193.281
555	193.349
570	193.13
585	192.835
600	192.583
615	192.391
630	192.269
645	192.122
660	192.049
675	191.953
690	191.799
705	191.732
720	191.393
735	191.113
750	190.984
765	190.679
780	190.431
795	190.398
810	190.313
825	190.086
840	190.191
855	190.556
870	190.492
885	190.195
900	190.239
915	190.532
930	190.57
945	190.228
960	189.992
975	189.931
990	190.001
1005	189.954
1020	189.647
1035	189.854
1050	189.907
1065	189.911
1080	189.595
1095	189.285
1110	189.514
1125	189.837
1140	189.58
1155	189.269
1170	189.356
1185	189.502
1200	189.426

Technique: PE FLTD
Subtechnique: Subtech
Type: SPECTRUM
Sample ID: TIMEBEND.TMP
Data Type: BINARY
Software ID: FLDM (V2.50)
Analyst: Ian Rowles
Created: 02:13:36, 92/03/22
Last Modified: 02:13:36, 92/03/22

Data set 1

X (SEC)	Y (INT)
0	288.093
15	285.845
30	284.886
45	284.988
60	285.031
75	284.876
90	284.571
105	284.301
120	284.183
135	284.108
150	283.966
165	283.872
180	283.741
195	283.511
210	283.423
225	283.592
240	283.444
255	283.213
270	283.207
285	282.902
300	282.561
315	282.468
330	282.528
345	282.491
360	282.151
375	281.94
390	282.219
405	282.336
420	281.756
435	281.15
450	280.940
465	280.697
480	280.211
495	279.894
510	279.883
525	279.934
540	279.898
555	279.559
570	278.956
585	278.631
600	278.424
615	278.232
630	278.106
645	277.765
660	277.416
675	277.322
690	277.385
705	277.353
720	277.307
735	277.188
750	277.066
765	276.883
780	276.573
795	276.286
810	276.043
825	276.151
840	276.288
855	276.201
870	276.221
885	276.227
900	276.042
915	275.886
930	275.731
945	275.543
960	275.432
975	275.258
990	275.376
1005	275.802
1020	275.98
1035	275.817
1050	275.482
1065	275.257
1080	275.186
1095	275.133
1110	274.957
1125	274.749
1140	274.863
1155	275.047
1170	275.084
1185	274.994
1200	274.854

Technique: PE FLTD
Subtechnique: Subtech
Type: SPECTRUM
Sample ID: TIMEBENM.TMP
Data Type: BINARY
Software ID: FLDM (V2.50)
Analyst:
Created: 02:49:04, 92/03/22
Last Modified: 02:49:04, 92/03/22

Data set 1

X (SEC)	Y (INT)
0	401.882
15	402.244
30	402.806
45	403.337
60	403.329
75	403.344
90	403.455
105	403.558
120	404.124
135	404.633
150	404.764
165	404.733
180	404.262
195	403.881
210	404.135
225	404.517
240	404.695
255	405.042
270	405.184
285	404.776
300	404.517
315	404.651
330	404.85
345	404.777
360	404.629
375	404.618
390	404.611
405	404.407
420	404.325
435	404.54
450	404.419
465	404.235
480	404.49
495	404.809
510	404.913
525	404.876
540	404.875
555	404.416
570	404.062
585	404.454
600	404.931
615	404.517
630	404.089
645	404.199
660	404.241
675	404.098
690	404.152
705	404.362
720	404.147
735	403.828
750	403.943
765	404.048
780	404.006
795	404.199
810	404.48
825	404.534
840	404.5
855	404.473
870	404.299
885	404.148
900	404.231
915	404.385
930	404.304
945	404.263
960	404.124
975	404.118
990	404.32
1005	404.412
1020	404.325
1035	404.388
1050	404.17
1065	403.725
1080	403.821
1095	403.856
1110	403.713
1125	404.082
1140	404.26
1155	404.038
1170	404.05
1185	404.038
1200	403.869

Technique: PE FLTD
Subtechnique: Subtech
Type: SPECTRUM
Sample ID: TIMEBENS.TMP
Data Type: BINARY
Software ID: FLDM (V2.50)
Analyst:
Created: 03:21:06, 92/03/22
Last Modified: 03:21:06, 92/03/22

Data set 1

X (SEC)	Y (INT)
0	605.815
15	605.947
30	605.775
45	605.14
60	605.323
75	606.271
90	606.913
105	607.479
120	608.152
135	608.143
150	607.29
165	606.24
180	605.774
195	606.091
210	606.416
225	605.951
240	605.055
255	604.794
270	605.195
285	605.468
300	605.58
315	605.942
330	606.106
345	605.827
360	605.508
375	604.916
390	604.325
405	604.591
420	605.201
435	605.453
450	605.348
465	604.964
480	604.706
495	604.972
510	604.762
525	604.423
540	604.322
555	603.846
570	603.509
585	603.69
600	604.096
615	604.476
630	604.39
645	604.192
660	603.79
675	603.456
690	603.666
705	603.311
720	602.776
735	602.822
750	603.019
765	603.271
780	603.386
795	603.401
810	603.273
825	603.02
840	602.961
855	603.078
870	603.104
885	603.034
900	602.908
915	602.57
930	602.075
945	601.904
960	602.011
975	602.028
990	601.885
1005	601.603
1020	601.66
1035	601.766
1050	601.505
1065	601.482
1080	601.663
1095	601.614
1110	601.427
1125	601.35
1140	601.28
1155	601.349
1170	601.487
1185	601.267
1200	600.866

Technique: PE FLTD
Subtechnique: Subtech
Type: SPECTRUM
Sample ID: TIMEBEN6.TMP
Data Type: BINARY
Software ID: FLDM (V2.50)
Analyst:
Created: 03.47:18, 92/03/22
Last Modified: 03.47:18, 92/03/22

Data set 1

X (SEC)	Y (INT)
0	351.938
15	351.855
30	351.945
45	351.851
60	351.393
75	350.725
90	350.516
105	350.631
120	350.796
135	350.901
150	350.752
165	350.64
180	350.605
195	350.516
210	350.453
225	350.622
240	350.623
255	350.542
270	350.034
285	349.862
300	349.788
315	349.671
330	349.836
345	350.116
360	350.197
375	350.061
390	349.910
405	350.024
420	350.247
435	350.310
450	350.085
465	349.772
480	350.063
495	350.325
510	349.958
525	349.761
540	349.716
555	349.650
570	349.576
585	349.535
600	349.645
615	349.6
630	349.447
645	349.18
660	348.975
675	348.93
690	348.754
705	348.85
720	349.074
735	349.214
750	349.26
765	349.077
780	349.096
795	349.012
810	348.751
825	348.593
840	348.446
855	348.588
870	348.691
885	348.471
900	348.294
915	348.073
930	347.706
945	347.583
960	347.776
975	348.121
990	348.297
1005	347.922
1020	347.488
1035	347.598
1050	348.031
1065	348.085
1080	347.705
1095	347.53
1110	347.362
1125	347.159
1140	347.42
1155	347.772
1170	347.941
1185	347.901
1200	347.649

Technique: PE FLTD
Subtechnique: Subtech
Type: SPECTRUM
Sample ID: TIMEBEN7.TMP
Data Type: BINARY
Software ID: FLDM (V2.50)
Analyst:
Created: 04:12:03, 92/03/22
Last Modified: 04:12:03, 92/03/22

Data set 1

X (SEC)	Y (INT)
0	326.7
15	326.514
30	326.57
45	326.483
60	326.324
75	326.118
90	325.887
105	325.533
120	325.645
135	325.605
150	325.654
165	325.720
180	325.508
195	325.46
210	325.652
225	325.625
240	325.717
255	325.606
270	325.689
285	325.643
300	325.666
315	325.614
330	325.249
345	324.733
360	324.484
375	324.44
390	324.462
405	324.644
420	325.03
435	325.14
450	324.721
465	324.381
480	324.367
495	324.403
510	324.291
525	324.441
540	324.666
555	324.429
570	324.379
585	324.536
600	324.352
615	324.16
630	323.971
645	323.723
660	323.968
675	324.255
690	324.118
705	323.994
720	323.854
735	323.763
750	323.991
765	323.991
780	323.521
795	323.318
810	323.519
825	323.564
840	323.669
855	323.963
870	323.938
885	323.766
900	323.626
915	323.226
930	322.901
945	323.021
960	323.242
975	323.438
990	323.56
1005	323.163
1020	322.667
1035	322.931
1050	323.223
1065	323.13
1080	323.177
1095	323.062
1110	322.896
1125	322.942
1140	322.839
1155	323.031
1170	323.15
1185	322.843
1200	322.835

Technique: PE FLTD
Subtechnique: Subtech
Type: SPECTRUM
Sample ID: TIMEBEN&.TMP
Data Type: BINARY
Software ID: FLDM (V2.50)
Analyst:
Created: 04:34:01, 92/03/22
Last Modified: 04:34:01, 92/03/22

Data set 1

X (SEC)	Y (INT)
0	366.477
15	365.899
30	365.966
45	366.131
60	365.536
75	364.714
90	364.383
105	363.887
120	363.403
135	363.451
150	363.28
165	362.585
180	362.063
195	361.943
210	362.139
225	362.683
240	363.031
255	363.031
270	362.935
285	362.578
300	362.479
315	362.647
330	362.684
345	362.746
360	362.813
375	363.054
390	363.219
405	362.972
420	362.856
435	363.069
450	363.026
465	363.126
480	363.294
495	362.731
510	362.323
525	362.452
540	362.535
555	362.722
570	362.761
585	362.3
600	362.036
615	362.052
630	361.856
645	361.518
660	361.17
675	361.086
690	361.015
705	360.735
720	360.617
735	360.881
750	361.27
765	361.212
780	360.951
795	361.037
810	361.208
825	360.81
840	360.186
855	360.274
870	360.722
885	360.711
900	360.546
915	360.379
930	360.022
945	359.888
960	359.941
975	359.993
990	360.136
1005	360.218
1020	360.048
1035	359.906
1050	360.106
1065	360.129
1080	359.898
1095	359.866
1110	359.859
1125	359.571
1140	359.227
1155	359.358
1170	359.716
1185	359.668
1200	359.356

Technique: PE FLTD
Subtechnique: Subtech
Type: SPECTRUM
Sample ID: TIMEBEND.TMP
Data Type: BINARY
Software ID: FLDM (V2.50)
Analyst:
Created: 05:06:02, 92/03/22
Last Modified: 05:06:02, 92/03/22

Data set 1

X (SEC)	Y (INT)
0	345.942
15	345.496
30	345.001
45	344.38
60	344.274
75	344.522
90	344.583
105	344.23
120	343.821
135	343.652
150	343.634
165	343.799
180	343.673
195	343.509
210	343.707
225	343.52
240	343.2
255	343.182
270	343.118
285	342.824
300	342.705
315	342.904
330	343.197
345	343.067
360	342.713
375	342.518
390	342.304
405	342.048
420	342.191
435	342.275
450	341.979
465	341.803
480	342.079
495	342.492
510	342.83
525	342.54
540	342.396
555	342.184
570	342.198
585	342.191
600	341.788
615	341.676
630	341.923
645	342.045
660	342.078
675	341.945
690	341.81
705	341.982
720	342.139
735	342.037
750	341.796
765	341.69
780	341.799
795	341.864
810	341.847
825	341.906
840	341.923
855	342.006
870	342.233
885	342.121
900	341.629
915	341.233
930	341.266
945	341.548
960	341.851
975	342.099
990	342.022
1005	341.466
1020	341.006
1035	341.222
1050	341.471
1065	341.348
1080	341.415
1095	341.737
1110	341.658
1125	341.165
1140	341.085
1155	341.165
1170	340.995
1185	341.096
1200	341.244

Technique: PE FLTD
Subtechnique: Subtech
Type: SPECTRUM
Sample ID: TIMBEN10.TMP
Data Type: BINARY
Software ID: FLDM (V2.50)
Analyst:
Created: 04:18:58, 92/03/22
Last Modified: 04:18:58, 92/03/22

Data set 1

X (SEC)	Y (INT)
0	151.622
15	151.847
30	152.041
45	152.147
60	152.293
75	152.404
90	152.591
105	152.686
120	152.794
135	153.031
150	153.279
165	153.589
180	153.762
195	153.701
210	153.421
225	153.017
240	152.743
255	152.57
270	152.327
285	152.102
300	151.989
315	152.032
330	152.124
345	152.197
360	152.389
375	152.506
390	152.651
405	152.649
420	152.209
435	151.941
450	152.134
465	152.287
480	152.239
495	152.311
510	152.294
525	152.182
540	152.057
555	151.905
570	151.932
585	151.803
600	151.594
615	151.769
630	152.018
645	151.857
660	151.621
675	151.721
690	151.918
705	151.951
720	151.839
735	151.713
750	151.656
765	151.672
780	151.581
795	151.458
810	151.51
825	151.567
840	151.575
855	151.56
870	151.477
885	151.541
900	151.751
915	151.707
930	151.592
945	151.704
960	151.655
975	151.535
990	151.748
1005	152.064
1020	152.137
1035	151.856
1050	151.561
1065	151.576
1080	151.705
1095	151.887
1110	152.011
1125	151.954
1140	151.941
1155	151.934
1170	151.947
1185	151.978
1200	151.852

Technique: PE FLTD
Subtechnique: Subtech
Type: SPECTRUM
Sample ID: TIMBEN11.TMP
Data Type: BINARY
Software ID: FLDM (V2.50)
Analyst:
Created: 06:43:55, 92/03/22
Last Modified: 06:43:55, 92/03/22

Data set 1

X (SEC)	Y (INT)
0	349.641
15	349.429
30	349.438
45	349.431
60	349.591
75	349.632
90	349.169
105	348.811
120	348.719
135	348.448
150	348.379
165	348.568
180	348.434
195	348.054
210	347.8
225	347.891
240	347.819
255	347.35
270	347.352
285	347.74
300	347.664
315	347.293
330	347.272
345	347.315
360	347.162
375	346.956
390	346.704
405	346.574
420	346.459
435	346.326
450	346.51
465	346.76
480	346.666
495	346.635
510	346.585
525	346.307
540	346.286
555	346.521
570	346.72
585	346.771
600	346.846
615	347.043
630	346.848
645	346.55
660	346.554
675	346.469
690	346.433
705	346.484
720	346.569
735	346.468
750	346.018
765	346.08
780	346.49
795	346.4
810	346.239
825	346.115
840	346.107
855	346.386
870	346.296
885	346.119
900	346.125
915	346.207
930	346.366
945	346.156
960	345.957
975	345.979
990	345.912
1005	346.006
1020	345.91
1035	345.686
1050	345.82
1065	345.933
1080	345.864
1095	345.585
1110	345.419
1125	345.434
1140	345.316
1155	345.125
1170	344.954
1185	344.855
1200	344.876

Technique: PE FLTD
Subtechnique: Subtech
Type: SPECTRUM
Sample ID: TIMBEN12.TMP
Data Type: BINARY
Software ID: FLDM (V2.50)
Analyst:
Created: 07:13:07, 92/03/22
Last Modified: 07:13:07, 92/03/22

Data set 1

X (SEC)	Y (INT)
0	200.506
15	199.871
30	200.307
45	200.768
60	200.019
75	199.397
90	199.536
105	199.707
120	200.106
135	200.181
150	199.297
165	198.782
180	199.077
195	199.49
210	200.038
225	200.655
240	200.747
255	199.811
270	198.869
285	198.6
300	198.826
315	198.485
330	198.012
345	198.175
360	198.285
375	198.094
390	198.016
405	198.25
420	198.455
435	198.123
450	197.773
465	197.667
480	197.551
495	197.557
510	197.567
525	197.542
540	197.461
555	197.505
570	197.786
585	197.878
600	197.843
615	197.968
630	198.12
645	198.21
660	198.127
675	198.028
690	198.021
705	197.679
720	197.744
735	197.59
750	197.397
765	197.296
780	197.307
795	197.351
810	197.311
825	197.231
840	197.299
855	197.598
870	197.601
885	197.346
900	197.211
915	197.086
930	197.095
945	197.241
960	197.25
975	197.069
990	197.02
1005	197.092
1020	197.102
1035	197.12
1050	197.067
1065	197.02
1080	197.06
1095	197.054
1110	197.144
1125	197.35
1140	197.091
1155	196.726
1170	196.846
1185	196.941
1200	196.796

Technique: PE FLTD
Subtechnique: Subtech
Type: SPECTRUM
Sample ID: TIMBEN13.TMP
Data Type: BINARY
Software ID: FLDM (V2.50)
Analyst:
Created: 07:35:11, 92/03/22
Last Modified: 07:35:11, 92/03/22

Data set 1

X (SEC)	Y (INT)
0	198.336
15	197.863
30	197.531
45	197.307
60	197.049
75	197.067
90	197.328
105	197.175
120	196.749
135	196.816
150	197.14
165	197.077
180	196.839
195	196.822
210	197.039
225	197.16
240	197.057
255	197.13
270	197.299
285	197.275
300	196.962
315	196.406
330	196.253
345	196.163
360	196.201
375	196.435
390	197.189
405	198.74
420	199.603
435	198.631
450	197.351
465	196.734
480	196.304
495	196.018
510	195.966
525	196.082
540	196.173
555	196.059
570	195.956
585	195.831
600	195.581
615	195.449
630	195.849
645	195.948
660	195.899
675	195.695
690	195.610
705	195.653
720	195.842
735	195.946
750	195.827
765	195.715
780	195.624
795	195.745
810	196.025
825	195.865
840	195.827
855	196.15
870	196.024
885	195.695
900	195.623
915	195.521
930	195.457
945	195.645
960	195.688
975	195.554
990	195.558
1005	195.533
1020	195.58
1035	195.601
1050	195.429
1065	195.409
1080	195.491
1095	195.483
1110	195.515
1125	195.421
1140	195.345
1155	195.487
1170	195.421
1185	195.406
1200	195.587

Technique: PE FLTD
Subtechnique: Subtech
Type: SPECTRUM
Sample ID: TIMBEN14.TMP
Data Type: BINARY
Software ID: FLDM (V2.50)
Analyst:
Created: 08:00:53, 92/03/22
Last Modified: 08:00:53, 92/03/22

TIMBEN14.WK1

Data set 1

X (SEC)	Y (INT)
0	214.05
15	213.579
30	212.911
45	212.67
60	212.706
75	212.695
90	212.885
105	213.21
120	213.352
135	213.23
150	213.089
165	213.248
180	213.121
195	212.626
210	212.321
225	212.106
240	211.905
255	211.844
270	211.782
285	211.494
300	211.269
315	211.084
330	210.862
345	211.066
360	211.492
375	211.29
390	211.106
405	211.536
420	211.573
435	211.167
450	210.893
465	210.648
480	210.472
495	210.508
510	210.473
525	210.137
540	209.86
555	209.912
570	210.167
585	210.476
600	210.595
615	210.618
630	210.773
645	210.839
660	210.94
675	211.145
690	211.073
705	210.634
720	210.402
735	210.487
750	210.296
765	210.014
780	210.056
795	210.169
810	210.03
825	209.831
840	209.854
855	210.02
870	209.867
885	209.718
900	209.944
915	209.911
930	209.688
945	209.683
960	209.754
975	209.882
990	210.035
1005	209.981
1020	209.963
1035	210.159
1050	210.342
1065	210.334
1080	210.012
1095	209.727
1110	209.804
1125	209.873
1140	209.796
1155	210.04
1170	210.32
1185	210.004
1200	209.788

Technique: PE FLTD
Subtechnique: Subtech
Type: SPECTRUM
Sample ID: TIMBEN17.TMP
Data Type: BINARY
Software ID: FLDM (V2.50)
Analyst:
Created: 08:23:17, 92/03/22
Last Modified: 08:23:17, 92/03/22

Data set 1

X (SEC)	Y (INT)
0	500.36
15	499.64
30	499.294
45	499.568
60	499.427
75	498.993
90	498.550
105	498.075
120	497.524
135	497.316
150	497.497
165	497.666
180	497.778
195	497.481
210	496.680
225	496.347
240	496.546
255	496.54
270	496.213
285	496.020
300	495.997
315	495.772
330	495.837
345	495.923
360	495.721
375	495.973
390	496.202
405	495.957
420	495.731
435	495.846
450	495.448
465	495.313
480	495.465
495	495.846
510	496.2
525	496.024
540	495.632
555	495.323
570	495.216
585	495.337
600	495.243
615	495.281
630	495.407
645	494.935
660	494.492
675	494.823
690	495.179
705	495.284
720	495.337
735	495.034
750	494.915
765	495.133
780	494.775
795	494.248
810	494.495
825	495.074
840	495.456
855	495.242
870	494.745
885	494.568
900	494.38
915	494.431
930	494.86
945	494.833
960	494.32
975	494.056
990	494.136
1005	494.246
1020	494.355
1035	494.198
1050	494.025
1065	494.051
1080	493.972
1095	494.025
1110	493.991
1125	493.705
1140	493.517
1155	493.464
1170	493.447
1185	493.298
1200	493.11

Technique: PE FLTD
Subtechnique: Subtech
Type: SPECTRUM
Sample ID: TIMBEN18.TMP
Data Type: BINARY
Software ID: FLDM (V2.50)
Analyst:
Created: 08:45:43, 92/03/22
Last Modified: 08:45:43, 92/03/22

Data set 1

X (SEC)	Y (INT)
0	$38.868
15	$38.243
30	$37.321
45	$36.651
60	$35.75
75	$35.014
90	$34.685
105	$34.425
120	$34.181
135	$33.479
150	$32.925
165	$32.955
180	$32.816
195	$32.406
210	$32.102
225	$32.249
240	$32.39
255	$32.261
270	$31.899
285	$31.791
300	$32.15
315	$32.102
330	$31.286
345	$31.15
360	$31.643
375	$31.631
390	$31.178
405	$31.023
420	$31.276
435	$31.274
450	$30.974
465	$31.081
480	$31.244
495	$31.034
510	$31.306
525	$31.656
540	$31.432
555	$31.503
570	$31.48
585	$30.717
600	$30.283
615	$30.655
630	$30.793
645	$30.778
660	$31.023
675	$31.102
690	$30.948
705	$30.758
720	$30.846
735	$31.005
750	$31.059
765	$30.963
780	$30.605
795	$30.232
810	$30.374
825	$30.818
840	$30.948
855	$31.214
870	$31.526
885	$31.248
900	$30.768
915	$30.588
930	$30.543
945	$30.757
960	$31.226
975	$31.106
990	$30.953
1005	$31.581
1020	$31.943
1035	$31.575
1050	$31.22
1065	$31.312
1080	$31.534
1095	$31.538
1110	$31.104
1125	$30.768
1140	$31.156
1155	$31.35
1170	$31.074
1185	$31.268
1200	$31.931

Technique: PE FLTD
Subtechnique: Subtech
Type: SPECTRUM
Sample ID: TIMBEN10.TMP
Data Type: BINARY
Software ID: FLDM (V2.50)
Analyst:
Created: 09:08:16, 92/03/22
Last Modified: 09:08:16, 92/03/22

Data set 1

X (SEC)	Y (INT)
0	497.391
15	496.205
30	495.213
45	495.179
60	495.075
75	494.559
90	494.343
105	494.845
120	494.845
135	494.687
150	494.183
165	493.516
180	492.974
195	493.006
210	493.164
225	492.848
240	492.22
255	491.744
270	491.226
285	491.247
300	491.427
315	491.404
330	491.079
345	491.187
360	491.77
375	491.838
390	491.863
405	492.383
420	492.557
435	492.257
450	492.334
465	492.566
480	492.403
495	492.457
510	492.814
525	492.805
540	492.134
555	491.566
570	491.638
585	491.741
600	491.475
615	491.216
630	491.679
645	492.392
660	492.491
675	492.158
690	491.948
705	492.077
720	492.339
735	492.291
750	492.01
765	492.101
780	492.224
795	492.036
810	492.198
825	492.615
840	492.538
855	491.733
870	491
885	491.183
900	491.379
915	491.184
930	491.278
945	491.462
960	491.448
975	491.09
990	491.055
1005	491.811
1020	492.237
1035	492.093
1050	491.988
1065	491.93
1080	491.532
1095	491.822
1110	492.42
1125	492.457
1140	492.098
1155	492.14
1170	491.958
1185	492.086
1200	492.826

APPENDIX B: Instrument Specifications

APPENDIX B: Instrument Specifications

Instrument Specifications

I. Fluorimeter

Instrument: Perkin Elmer LS 50 Spectrafluorimeter

Source: Zenon Arc Lamp

	Phenanthrene	B-a-P
Excitation Wavelength	255 nm	380 nm
Emmission Wavelength	365 nm	445 nm
Excitation Slit	5 nm	15 nm
Emmission Slit	5 nm	15 nm
Time Drive	--	20 minutes
Frequency	--	15 seconds

II. Total Organic Carbon Analyzer

Instrument:	Shimadzu Total Organic Carbon Analyzer
Catalyst:	Low Sensitivity
Acid Purge:	5 minutes at pH of 3
Sensitivity:	10x

III. High Performance Liquid Chromatography

Instrument:	Gilson HPLC
Column:	C18, reverse phase
Mobile Phase:	1 minute, 50% acetonitrile, 50% water
	Ramp to 100% acetonitrile
	8 minutes, 100% acetonitrile
	15 minutes, 50% acetonitrile, 50% water
	16 minutes, end
Flow Rate:	2.5 ml/minute
Dectector:	UV 116, 0.01 AUFS
Injection Vol.:	20 ul

IV. Liquid Scintillation Counting

Instrument:	Beckman LS Counter
Time:	10 minutes
Region a: LL-UL	0.0-12.0
Region b: LL-UL	12.0-156.0
QIP :	tsie/AIC
Conventional DPM	

APPENDIX C: Key to Tables 2.2 through 2.6

APPENDIX C: Key to Tables 2.2 through 2.6

Key to Tables 2.2 through 2.6

Column	Definition
1	Sample identification
2	Grams of sediment (freeze dried) placed in 25 ml centrifuge tube
3	Grams of DI/RO water placed in 25 ml centrifuge tubes.
4	Concentration of sediment in 25 ml centrifuge tubes in mg/l. Calculated as (column 2/column 3) x 10^6
5	Amount of radiolabelled compound placed in the 25 ml centrifuge tube from stock solution, in discharge per minute (dpm).
6	Absorbance of supernatant in 25 ml centrifuge tube after equilibrium.
7	Grams of supernatant used for a liquid phase ^{14}C activity count.
8	^{14}C activity in liquid portion , in dpm.
9	14C activity in liquid phase, in dpm/l. (Column 8)/(Column 7)
10	ml of methylene chloride used to extract the ^{14}C activity in the sediments.
11	^{14}C activity in the sediments, in dpm.
12	^{14}C activity in the sediments in dpm/kg. (column 11)/(column2)x1000xTOTAL $MECL_2$/Sample Volume $MECL_2$.
13	^{14}C activity extracted from the glass tube, in dpm.
14	[(Column 8) x (Column 3)/(Column 7) + (Column 11) + (Column 13)]/(Column 5)
15	(Column 12)/(Column 14)
16	(Column 12)/(Column 9)/f_{OC}; where f_{OC}= 5%
17	(Column 15)/(Column 9)/f_{OC}; where f_{OC}= 5%

APPENDIX D: Modelling Data

BaP Nonlinear data

Non-linear Parameter Estimation						
		BAP	BAP	Total	Estimated Koc	
	BAP solutions	Reverse Phase	Reverse Phase	DPM/l	Using Nonlinear	
	Estimated	Adjusted		aqueous	K1, and K2 estimates	
Koc	DOC, mg/l	Free, dpm/l	Kdoc			
						Solids, mg/l
212626.358	5.02220355	226662.074	50328.4126	293076.923	105881.371	1462.45059
153634.694	7.5885197	117462.909	79460.8657	200591.716	95104.239	3308.03036
81193.0803	11.[illegible]353651	127411.169	27884.7344	190737.24	95210.7293	7255.36993
56240.7795	17.[illegible]823911	102566.539	20504.7512	163915.547	90109.0009	13324.0446
53643.4925	25.7424683	57082.7415	20924.1459	98461.5385	91439.7799	25608.7824
72894.3311	14.366444	79856.4314	45173.124	149139.579	88755.0017	10035.8566
69935.2324	14.2275727	145643.656	64391.3966	298301.887	90428.7712	9875.9209
65043.2205	14.1989641	273245.361	31898.0271	438811.881	94326.6002	9843.07572
83187.4284	14.4011358			463689.32		10075.9392
48374.2807	14.294134	507808.21	25269.1998	832035.398	88376.0358	9952.47525
60152.9608	14.2566202	492397.957	43941.6021	965354.331	83711.9825	9909.30599
163587.012	8.53721139	97145.6415	74614.8012	166730.402	96071.296	4102.35906
130418.497	8.43872069			329133.858		4017.36385
115003.546	8.57680758	329190.276	43311.5847	507976.654	94323.0636	4136.69065
140033.894	8.42954099			627800		4009.47119
139451.623	8.38274681	366038.183	82094.7582	698148.148	88403.7046	3969.3155
45399.6482	22.4804786	64370.2692	28037.258	136039.604	77788.597	20684.4409
35878.4849	22.3318182	209232.145	28005.7873	438195.777	78328.2052	20468.1873
33500.9646	22.1458734	507126.48	7803.74697	767039.106	86666.4786	20198.7281
			42102.7622			

Date: 24-AUG-92
Time: 14:13:13
File: SYSTAT Data Editor
has 5 variables and 19 cases.

OBS	KOC	DOC	FREE	KDOC	CT
1	212626.358	5.022	226662.074	50328.413	293076.923
2	153634.694	7.589	117462.909	79460.866	200591.716
3	81193.080	11.835	127411.169	27884.734	190737.240
4	56240.780	17.082	102566.539	20504.751	163915.547
5	53643.493	25.742	57082.742	20924.146	98461.539
6	72894.331	14.366	79856.431	45173.124	149139.579
7	69935.232	14.228	145643.656	64391.397	298301.887
8	65043.221	14.199	273245.361	31898.027	438811.881
9	48374.281	14.294	507808.210	25269.200	832035.398
10	60152.961	14.257	492397.957	43941.602	965354.331
11	163587.012	8.537	97145.641	74614.801	166730.402
12	115003.546	8.577	329190.276	43311.585	507976.654
13	139451.623	8.383	366038.183	82094.758	698148.148
14	45399.648	22.480	64370.269	28037.258	136039.604
15	35878.485	22.332	209232.145	28005.787	438195.777
16	33500.965	22.146	507126.480	7803.747	767039.106
17	.	.	.	.	.
18	.	.	.	.	.
19	.	.	.	.	.

19 cases printed out of 19 cases in the file.

ITERATION	LOSS	PARAMETER VALUES
0	0.1657391D+12	0.1000D+00 0.1000D+00
1	0.3457568D+11	0.6222D+04 0.3026D+04
2	0.3454619D+11	0.5925D+04 0.3641D+04
3	0.3454619D+11	0.5925D+04 0.3641D+04

DEPENDENT VARIABLE IS KOC

MISSING DATA OR ESTIMATES REDUCED DEGREES OF FREEDOM

SOURCE	SUM-OF-SQUARES	DF	MEAN-SQUARE
REGRESSION	.131198E+12	2	.655990E+11
RESIDUAL	.345462E+11	14	.246758E+10
TOTAL	.165744E+12	16	
CORRECTED	.420935E+11	15	

RAW R-SQUARED (1-RESIDUAL/TOTAL) = 0.792
CORRECTED R-SQUARED (1-RESIDUAL/CORRECTED) = 0.179

PARAMETER	ESTIMATE
K1	5924.718
K2	3640.774

constant let K_{DOC} vary with solids as $A \times b$

$$K_{oc} = \frac{C_F K_1 + C_F K_{DOC} DOC \cdot K_2}{C_{Total\ in\ aqueous\ phase} \cdot f_{oc}}$$

APPENDIX E: Dialysis Experiment

Appendix 6: Dialysis Experiment

Equilibrium dialysis was studied using the technique of Carter and Suffet, 1983, to physically seperate the free and bound forms of phenanthrene in solution. Phenanthrene at 0.5 mg/l, or about 50 % of its aqueous solubility was placed inside and outside of a 500 molecular weight cut-off bag (Millipore). A high concentration was required since we expected a significant portion of the phenanthrene to absorb to the bag. Varying concentrations of a humic acid solution (Aldrich^R) were introduced to the outside of the bag. Both the inside and outside concentrations of phenanthrene were measured over time as ^{14}C activity. The concentration of humic acid was measured using absorbance at 255 nm.

As demonstrated in Figures 1 and 2, we found that both the inside and outside concentration of phenanthrene decreased as the amount of humic acid in solution increased. The total amount of phenanthrene as determined by what is inside and outside of the bag should have remained the same. The inability to provide a complete material balance suggested that one of several things was happening:

1. A considerable amount of phenanthrene was absorbing to the dialysis bag over time and equilibrium was not achieved.

2. The measurement technique (^{14}C activity) was being hindered by the presence of humic acid both inside and outside of the bag.

The bag itself was not counted since it was not completely soluble in the scintillation fluid. Therefore the material balance could not be verified as in the other techniques which we tried (ie: fluorescence quenching and empore disk filtration).

The data for this failed experiment is provided in the following pages.

Phenanthrene Dialysis Experiment with Aldrich Humic Acid					
Date	DPM, outside	Volume	ABS @ 255	DPM, inside	Volume
28-Apr	3534	5	0.136	3408	4.96
30-Apr	3027	5.09	0.2	2811	5.02
4-May	2090	5.01	0.306	1873	4.98
11-May	1529	5.02	0.437	1396	5.08
12-May	1479	5.09	0.612	1240	5.06
14-May	1369	5.02	0.1088	1121	5.06
19-May	1329	5.04	1.78	1002	5.02

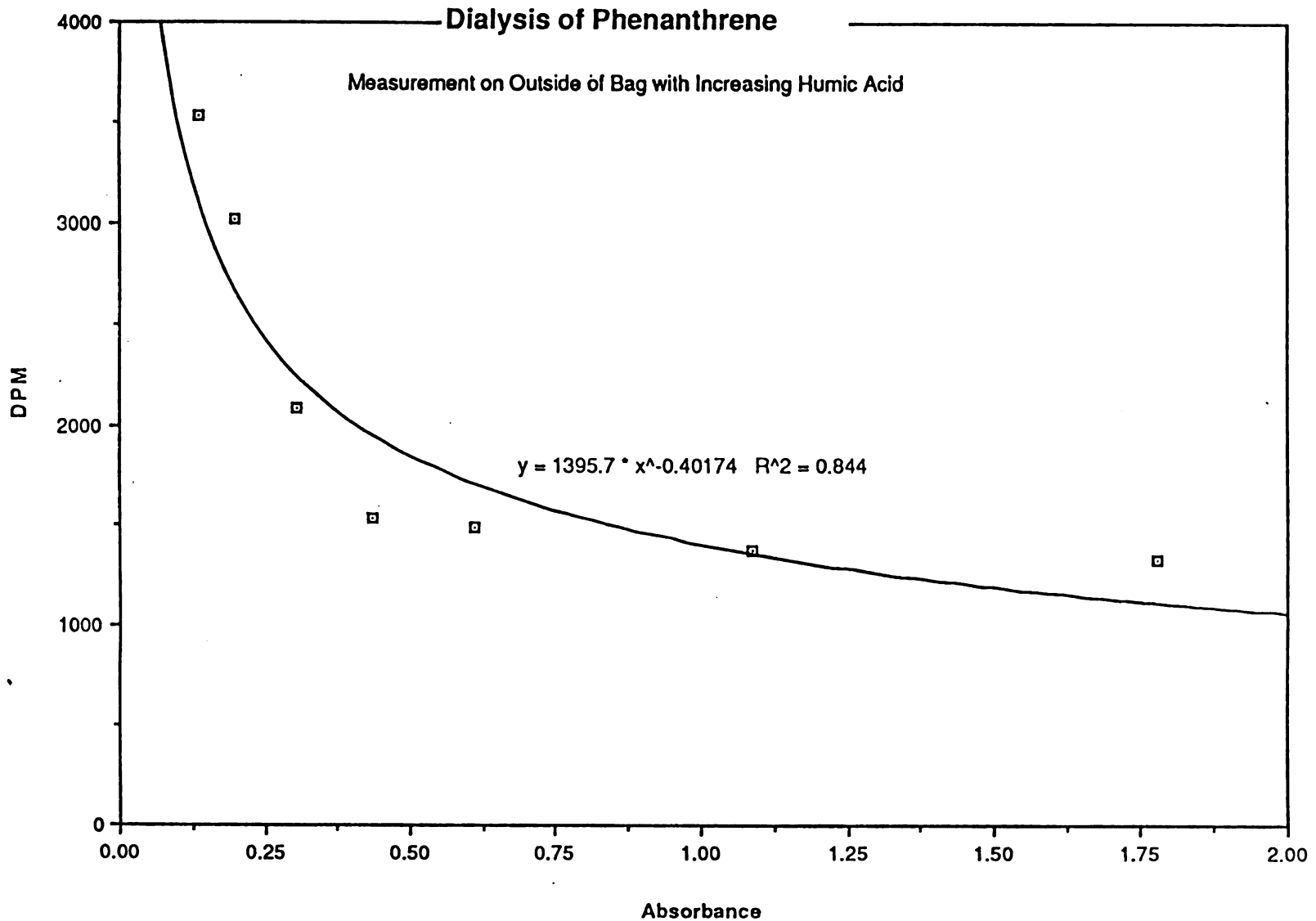
Dialysis of Phenanthrene
Measurement on Outside of Bag with Increasing Humic Acid
y = 1395.7 * x^-0.40174 R^2 = 0.844
DPM
4000
3000
2000
1000
0
0.00
0.25
0.50
0.75
1.00
1.25
1.50
1.75
2.00
Absorbance

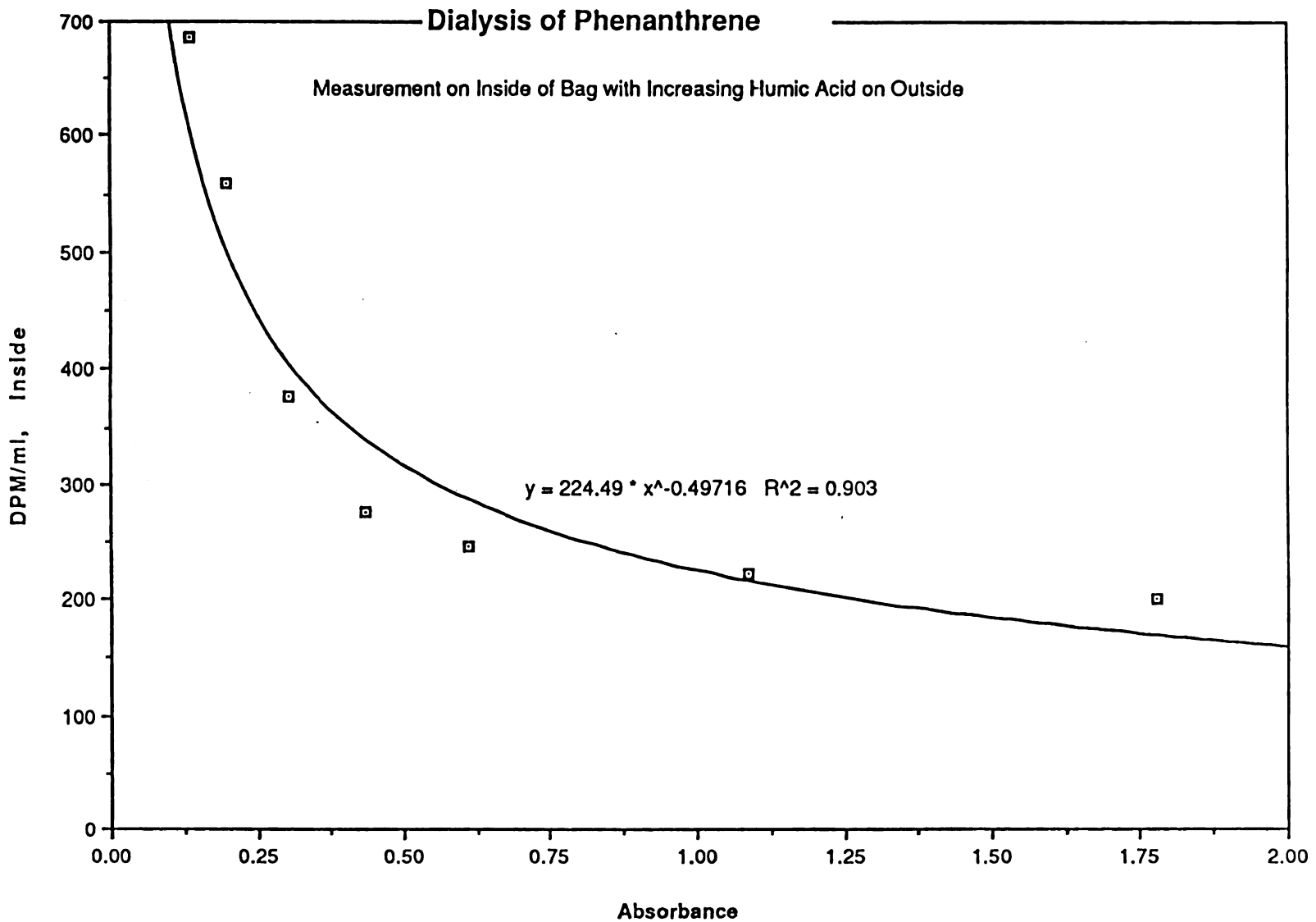
Dialysis of Phenanthrene
Measurement on Inside of Bag with Increasing Humic Acid on Outside
y = 224.49 * x^-0.49716 R^2 = 0.903
DPM/ml, Inside
Absorbance
700
600
500
400
300
200
100
0
0.00
0.25
0.50
0.75
1.00
1.25
1.50
1.75
2.00

*** PHOTOMETRIC ***

λ 255.0

A1

1	0.306	1st day
2	0.138	5/4
3	0.437	5/11
4	0.612	5/12
5	1.088	5/14
6	1.780	5/19

Protocol #: 9 19 MAY 92 20:32
Time = 10.00
Radionuclide: H3/C14
Region A: LL-UL= .0- 12.0 Bkg= .00 %2 Sigma= .00 Div(K)=1.00 Lcr= 0
Region B: LL-UL= 12.0-156.0 Bkg= .00 %2 Sigma= .00 Div(K)=1.00 Lcr= 0
Region C: LL-UL= .0- .0 Bkg= .00
QIP = tSIE/AEC
Conventional DPM
DPM1 = 200900
DPM2 = 106700

PID	S#	TIME	CPMA	2SIA	CPMB	2SIB	DPM1/K	DPM2/K	SIS	tSIE	FLAG		
(2 missing vials)													
8	3	10.00	426.40	3.06	2720.90	1.21	.00	3399.14	58.696	343			
8	3	10.00	426.90	3.06	2740.60	1.21	.00	3423.52	58.731	344			
8	3	10.00	425.60	3.07	2722.30	1.21	.00	3401.37	58.514	343			
			426.30	3.06	2727.93	1.21	.00	3408.04	58.647	343	A	4/28 out	5.00
8	4	10.00	387.30	3.21	2426.30	1.28	17.31	3031.77	58.091	341			
8	4	10.00	383.10	3.23	2455.80	1.28	.00	3068.40	58.562	343			
8	4	10.00	379.60	3.25	2385.70	1.29	14.08	2980.45	58.380	342			
			383.33	3.23	2422.60	1.29	8.36	3026.86	58.345	342	A		4.96
8	5	10.00	356.70	3.35	2249.70	1.33	11.16	2808.48	58.864	346			
8	5	10.00	354.50	3.36	2261.10	1.33	.93	2822.16	58.874	348			
8	5	10.00	358.60	3.34	2245.60	1.33	18.47	2802.43	59.291	348			
			356.60	3.35	2252.13	1.33	10.18	2811.02	59.010	347	A	4/30/out	5.09
8	6	10.00	259.60	3.93	1654.70	1.55	.00	2083.00	53.197	309			
8	6	10.00	262.40	3.90	1659.10	1.55	.00	2088.61	52.982	308			
8	6	10.00	266.90	3.87	1668.00	1.55	5.57	2099.83	52.999	308			
			262.97	3.90	1660.60	1.55	.00	2090.48	53.059	308	A		5.02
8	7	10.00	236.00	4.12	1502.00	1.63	1.21	1875.88	58.947	345			
8	7	10.00	240.80	4.08	1481.90	1.64	22.97	1849.92	58.774	345			
8	7	10.00	238.00	4.10	1515.00	1.62	1.24	1891.90	58.936	345			
			238.27	4.10	1499.63	1.63	8.47	1872.61	58.886	345	A	5/4 out	5.01
8	8	10.00	196.20	4.52	1203.30	1.82	14.34	1515.95	52.329	304			
8	8	10.00	194.10	4.54	1212.20	1.82	3.90	1527.15	52.412	305			
8	8	10.00	194.20	4.54	1224.30	1.81	.00	1543.10	52.267	304			
			194.83	4.53	1213.27	1.82	5.46	1528.74	52.336	304	A		4.98
8	9	10.00	180.60	4.71	1117.20	1.89	14.88	1394.49	58.834	346			
8	9	10.00	178.10	4.74	1119.80	1.89	7.19	1397.66	58.648	347			
8	9	10.00	177.10	4.75	1118.50	1.89	5.17	1395.89	59.307	348			
			178.60	4.73	1118.50	1.89	9.07	1396.01	58.930	347	A	5/11 out	5.02
8	10	10.00	194.90	4.53	1160.80	1.86	29.13	1467.97	49.563	289			
8	10	10.00	195.80	4.52	1178.50	1.84	22.66	1491.74	49.450	286			
8	10	10.00	193.20	4.55	1167.50	1.85	20.11	1477.55	49.205	287			
			194.63	4.53	1168.93	1.85	23.98	1479.08	49.406	287	A		5.08
8	11	10.00	159.10	5.01	1001.20	2.00	5.68	1250.24	58.850	345			
8	11	10.00	161.10	4.98	992.10	2.01	15.10	1238.45	58.276	345			
8	11	10.00	160.40	4.99	986.30	2.01	15.63	1231.27	58.503	345			
			160.20	5.00	993.20	2.01	12.14	1239.99	58.543	345	A	5/12 Out	5.09
8	12	10.00	167.10	4.89	1076.60	1.93	.00	1366.60	42.343	237			
8	12	10.00	159.90	5.00	1078.30	1.93	.00	1370.68	42.360	235			
8	12	10.00	163.70	4.94	1079.30	1.93	.00	1370.61	42.228	237			
			163.57	4.95	1078.07	1.93	.00	1369.28	42.311	236	A	5/12 IN	5.06
4	13	10.00	142.20	5.30	900.40	2.11	2.59	1124.64	58.340	344			
4	13	10.00	152.00	5.13	901.40	2.11	29.11	1124.64	58.115	345			
4	13	10.00	143.00	5.29	891.40	2.12	8.59	1113.27	58.761	343			
			145.73	5.24	897.73	2.11	13.44	1120.85	58.405	344	A	5/14 out	5.02

PID	S#	TIME	CPMA	2SIA	CPMB	2SIB	DPM1/K	DPM2/K	SIS	tSIE	FLAG	
4	14	10.00	140.20	5.34	1036.70	1.96	.00	1353.07	37.356	196		
4	14	10.00	145.50	5.24	1013.60	1.99	.00	1322.76	37.569	196		
4	14	10.00	136.10	5.42	1004.60	2.00	.00	1311.88	37.423	196		5/14 IN 5.06
			140.60	5.34	1018.30	1.98	.00	1329.24	37.449	196	A	
4	15	10.00	126.00	5.63	803.20	2.23	.13	1003.10	59.179	345		
4	15	10.00	123.40	5.69	805.70	2.23	.00	1006.85	59.314	343		
4	15	10.00	127.60	5.60	798.00	2.24	6.59	996.60	59.068	344		5/19 out 5.04
			125.67	5.64	802.30	2.23	.00	1002.18	59.187	344	A	
4	16	10.00	17213.6	.48	111067	.19	.00	133739	158.73	1000		
4	16	10.00	17333.6	.48	110890	.19	.00	133470	158.45	1003		
4	16	10.00	17263.7	.48	111022	.19	.00	133694	158.39	999		5/19 out 5.03
			17270.3	.48	110993	.19	.00	133634	158.52	1001	A	